INFLUENCE OF SURFACE CONDITIONING ON THE IONIZATION, BREAKDOWN, AND TRACKING OVER SOLID DIELECTRICS

by

Carl Paul Wiedow

A THESIS

submitted to

OREGON STATE COLLEGE

in partial fulfillment of
the requirements for the
degree of

DOCTOR OF PHILOSOPHY

June 1956

APPROVED:

[redacted]

Professor of Electrical Engineering

In Charge of Major

[redacted]

Head of Department of Electrical Engineering

[redacted]

Chairman of School Graduate Committee

[redacted]

Dean of Graduate School

Date thesis is presented May 8, 1956

Typed by Georgia McFarland

ACKNOWLEDGEMENTS

Professor Fred O. McMillan had proofread about ninety-five percent of the manuscript at the time of his sudden death on April 28, 1956. The author spent a year full time on the research during which Professor McMillan kept almost daily contact with the progress of the work. Professor McMillan was an outstanding teacher and his many unusual qualities may be best summed up in the word inspiration.

After the death of Professor F. O. McMillan, Professor Louis N. Stone assumed the responsibility of major professor to see the project completed.

At the suggestion of Professor McMillan, the author consulted Professors Wm. R. Varner and J. J. Brady of the physics department for their views on the problem. Doctor J. J. Brady granted permission to the author to sit in on his year sequence of lectures on the conduction of electricity through gases and solid state physics. Doctor Wm. R. Varner kept in constant touch with the progress of the entire research.

Professor R. R. Michael has been most generous in the use of many pieces of equipment from his measurements laboratory during the course of this research.

Mr. C. E. Boucher of Industrial X-Ray Engineers donated the ASTM arc tracking equipment, about 75 prepared test specimens, and assisted financially with the work.

TABLE OF CONTENTS

ILLUSTRATIONS

ILLUSTRATIONS Continued

ILLUSTRATIONS Continued

LIST OF TABLES

INFLUENCE OF SURFACE CONDITIONING ON THE IONIZATION, BREAKDOWN, AND TRACKING OVER SOLID DIELECTRICS

INTRODUCTION

Mr. C. E. Boucher of Industrial X-Ray Engineers observed that fewer failures occurred in his high voltage x-ray equipment when some of the components were coated with a suspension medium and small glass beads than when these components were untreated. An explanation of this behavior was sought in the understanding of the physical phenomena involved in order to have a sound basis upon which to write patent claims.

Several approaches were tried in order to find a mathematical theory as a solution to this problem. However, although a great deal of immediately related theory is available, no practical solution is apparent because of the large number of parameters involved and the unknown manner of their variation.

An experimental solution to the problem was found by the author and various physical phenomena were discovered in the process of the solution. In summary, the increased life of the dielectric is due to the suppression of surface ionization. The suppression of ionization decreases the ion bombardment of the dielectric and hence reduces its deterioration and disintegration.

CONDITIONING OF SPECIMENS

The various specimens prepared for this investigation were conditioned in accordance with the methods prescribed by the American Society For Testing Materials, Standard Methods of Conditioning Plastics and Electrical Insulating Materials for Testing (3, pp. 308-310). The conditioning procedure is necessary since the electrical and physical properties of electrical insulating materials are influenced by temperature, relative humidity, and contamination.

Because considerable time had elapsed between the preparation and use of the numerous specimens, the specimens were carefully washed and rinsed and their labels were removed. The labels were replaced by a system of code marks used to identify the specimens. The surface area of the code marks was very much less than that of the labels, and the code marks were not a disturbing influence electrically as were the labels. After cleaning, the specimens were placed in an electric oven designed and built to operate at the prescribed temperature of 50 $\pm$ 3 degrees centigrade. The oven is shown in Figure 1 and the heater elements and supporting racks in Figure 2. The performance of the oven was better than expected, because it is capable of holding the

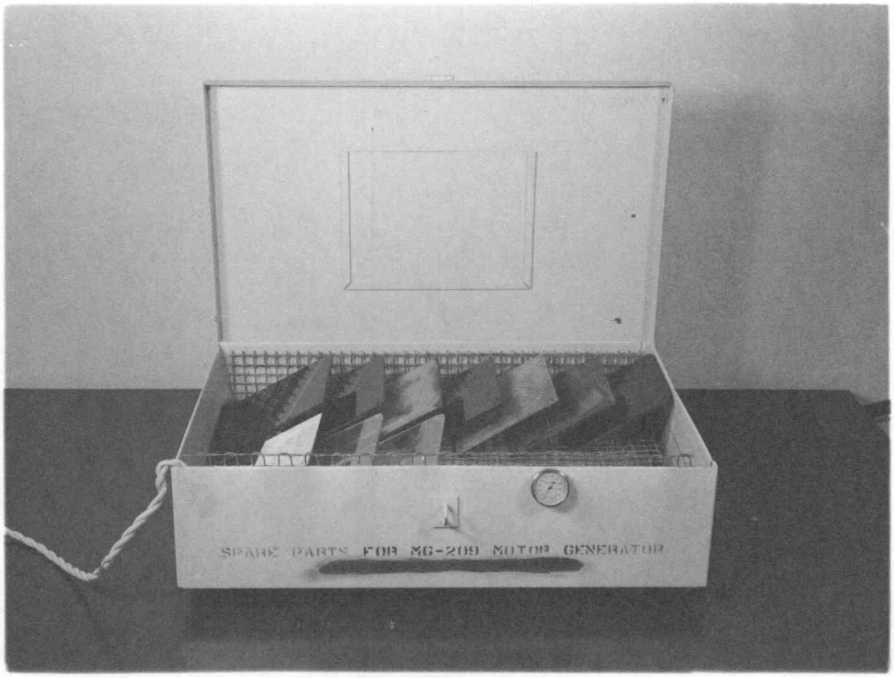

Figure 1.
Electric oven for drying specimens.

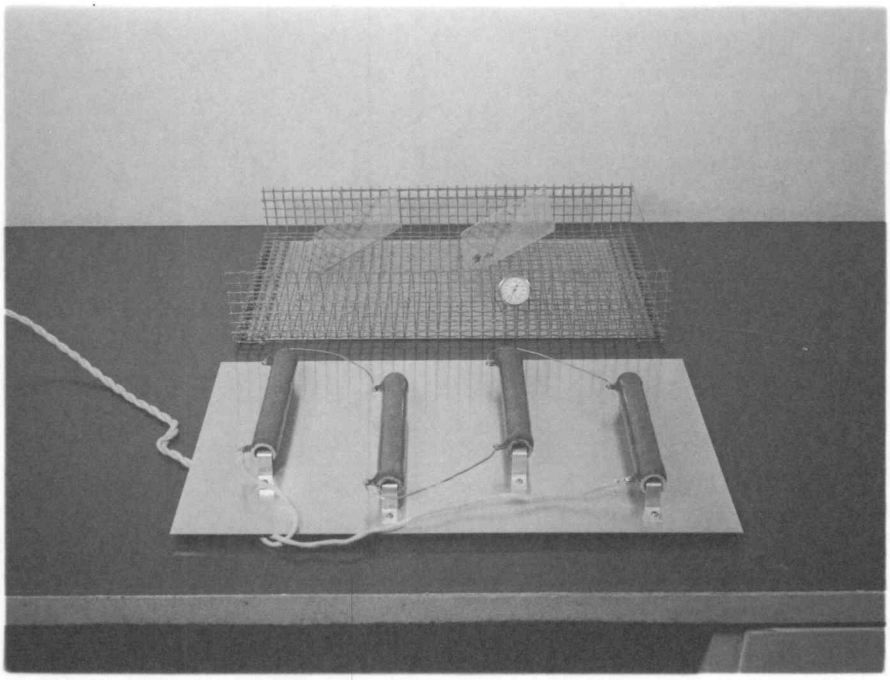

Figure 2.
Heater elements and supporting racks for electric oven.

temperature within one degree centigrade while the permissible tolerance was three degrees centigrade. The specimens were kept in the oven for the required 48 hours or longer.

After baking, the specimens were removed from the oven and cooled to room temperature in a desiccator over anhydrous calcium chloride. This desiccator, shown in Figure 3, also served as the permanent storage place for the approximately 100 specimens when not under test. The desiccator was equipped with a small blower to circulate the air and aid in the drying process. A small hole drilled in the corner of the various specimens enabled one to hang them on numbered hooks for filing purposes. Specimens of 0.25 inch in thickness or under must be kept in the desiccator at least five hours prior to test. All the specimens were less than 0.25 inch in thickness. The specimens were placed under test in less than one half hour after removal from the desiccator. To facilitate the handling of specimens a small wooden rack was made which is shown in the foreground of Figure 3. This rack also protects the prepared surfaces from unnecessary handling.

Room temperature is defined as an atmosphere in the temperature range of 20 to 30 degrees centigrade and

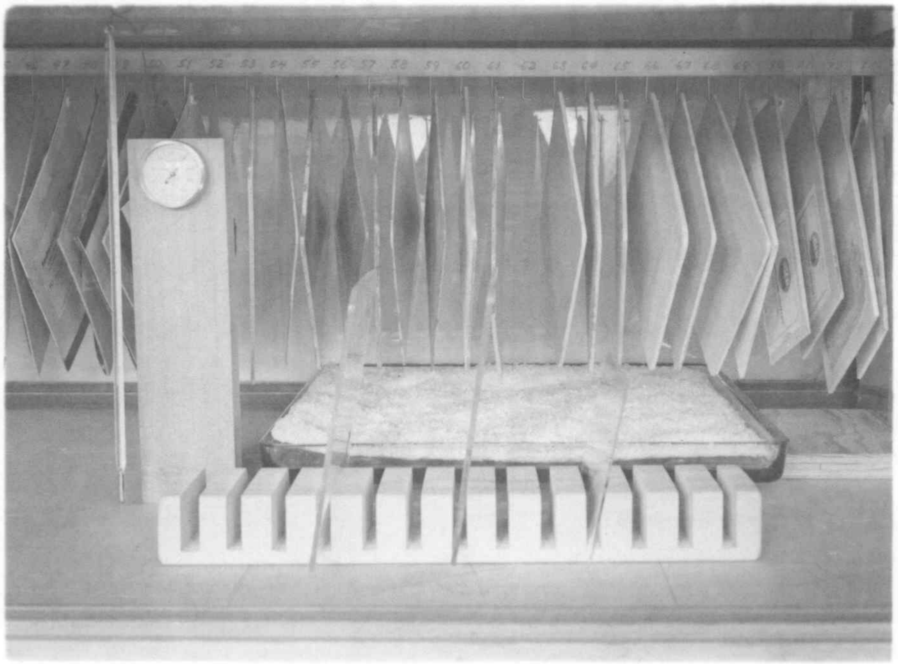

Figure 3.
Interior view of desiccator showing
specimens and desiccator tray.

an unspecified relative humidity. The extreme excursions of temperature experienced for the entire series of tests were within a much narrower range than that permitted by the ASTM standards. The extreme temperature limits for all tests were a maximum of 28.2 and a minimum of 23.3 degrees centigrade. This degree of temperature regulation was made possible by turning off the steam heat in the research room and replacing it with an electric heater of 2000-watt capacity. This heater operated 24 hours a day. The heater is equipped with a bi-metallic thermostat as a control element. The maximum, minimum, and average values of the atmospheric conditions experienced during the individual test series are given in Table I.

All voltage measurements were made with a 2.00 centimeter sphere gap. These measurements were corrected to standard conditions defined by a temperature of 25.0 degrees centigrade and a barometric pressure of 76.0 centimeters of mercury. These standards are set forth by the AIEE in their Measurement of Voltage in Dielectric Tests (1, pp. 3-7).

TABLE I

RANGE OF ATMOSPHERIC CONDITIONS EXPERIENCED DURING THE TESTS

	Maximum	Minimum	Average
IONIZATION CURRENT CHARACTERISTICS			
Barometric Pressure mm Hg	760.0	748.0	753.1
Temperature Centigrade	26.0	24.0	25.0
Vapor Pressure mm Hg	9.94	6.98	8.25
FLASHOVER CHARACTERISTICS			
Barometric Pressure mm Hg	763.3	740.2	752.2
Temperature Centigrade	28.2	23.3	25.7
Vapor Pressure mm Hg	8.56	6.79	7.35
RESISTANCE TO ARC TRACKING			
Barometric Pressure mm Hg	746.5	745.6	746.1
Temperature Centigrade	27.0	25.5	26.1
Vapor Pressure mm Hg	8.83	7.54	8.04

IONIZATION CHARACTERISTICS OF SURFACES AT ATMOSPHERIC PRESSURE

The High Voltage Bridge

High voltage gradients cause heavy ionization over the surface of materials and subsequent surface failure. The charged particles bombard the material and disintegrate it causing surface breakdown. Therefore, a method is needed to measure this surface ionization. Also, it is necessary to separate the ionization current from the charging current. This need led to the use of a bridge circuit as a means of separating these currents. This bridge circuit is used to balance out the 60 cycle charging current leaving the ionization current as the unbalanced portion of the current in one arm of the bridge.

Conventional methods used in balancing alternating current bridges were inadequate in this situation because of the high voltages used in making the measurements. High voltages give rise to a high electric field intensity, and a high field intensity does not permit a bridge to be constructed for simple lumped circuit parameters. All leads and components must be considered as distributed circuit parameters, and the bridge must have three dimensional symmetry in space or a balance cannot be achieved. This type of bridge proved to be very successful in researches conducted by Professor F. O. McMillan on insulator corona and conductor corona (6, p. 387, and 5, pp. 282-284). The source of excitation for the bridge was a 100 kv transformer for which the control circuit is given in Figure 4. The bridge circuit with the measured values of the components is shown in Figure 5. The symmetrical arrangement of the high voltage bridge is shown in Figure 6. A sheet of aluminum, 3 feet by 4 feet, serves as a ground plane for the bridge and the sphere gap. A general view which includes the apparatus used in this study except the arc tracking equipment (and the vacuum pump, which is hidden from view) is shown in Figure 7.

The parallel electrodes used on the test specimens are shown in Figure 8. This design of the electrodes was decided upon after a careful study of the various electrode shapes used by other research workers investigating the characteristics of solid dielectrics. Parallel bars were chosen since they give a somewhat more uniform field over the area between the electrodes. This type of electrode subjects a considerable area of the specimen to a high voltage gradient; therefore, the characteristics obtained are more typical of the general surface conditions of the materials than would be obtained by

CONTROL CIRCUIT FOR 100 KV TRANSFORMER

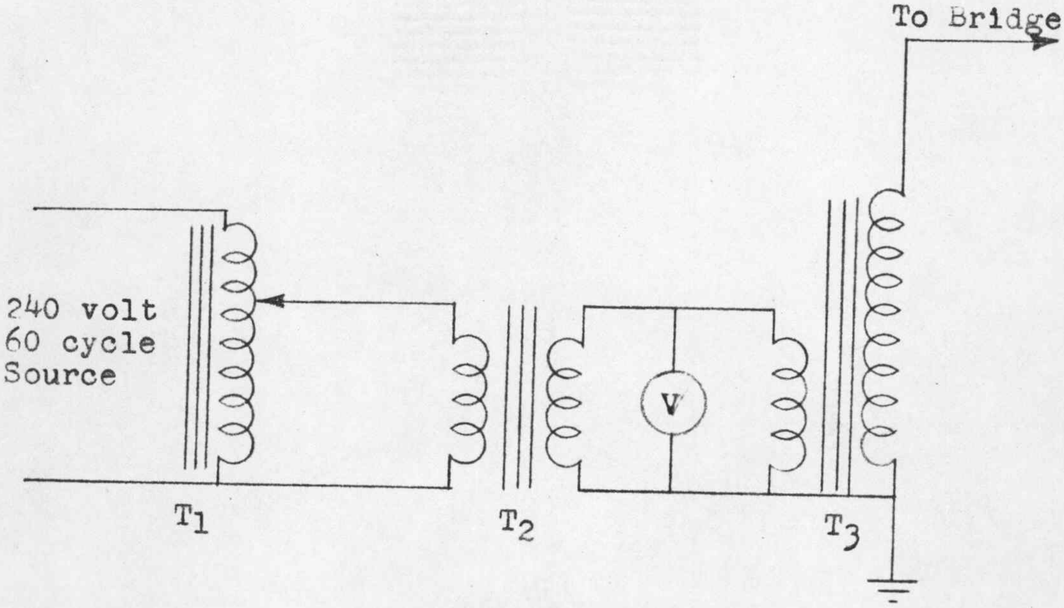

T_1 230 Volt Variable Autotransformer

T_2 Isolation Transformer, 240:100
Maloney Electric Company
Single Phase Distribution Transformer
No. 711398

T_3 100 KV Transformer OSC No. 3566

V AC Voltmeter
Weston Model 155 No. 42071 0-75-150
G.E. Type P-3 No. 3320351 0-15-30

Figure 4

HIGH VOLTAGE BRIDGE

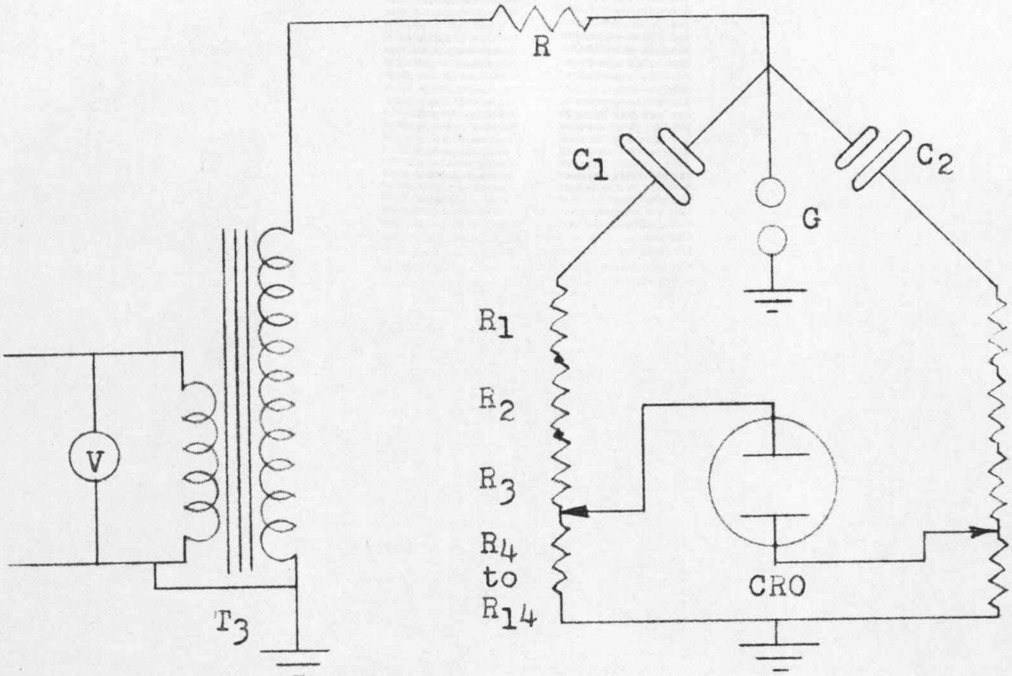

V A-C Voltmeter

T_3 100 KV Transformer OSC No. 3566

R 0.270 Megohm Current Limiting Resistor Carborundum Type

C_1 Exploratory Electrodes 3.5 to 15 mmf

C_2 Balancing Electrodes Immersed in oil to suppress corona

R_1 0.247 Megohm Metal Film Resistor

R_2 0.146 Megohm Metal Film Resistor

R_3 0.118 Megohm Metal Film Resistor

R_4 to R_{14} Ayrton-Perry Type Resistors Total 62,290 ohms

G 2.0 cm Sphere Gap

CRO Tektronix Oscilloscope, Type 511AD No. 3797

Figure 5

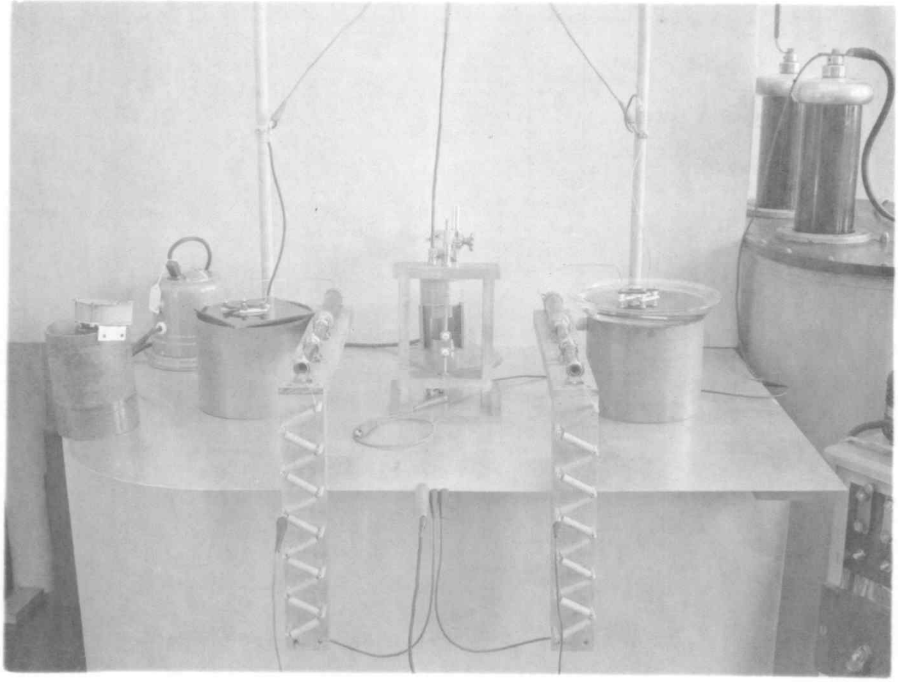

Figure 6.
Arrangement of high voltage
bridge elements.

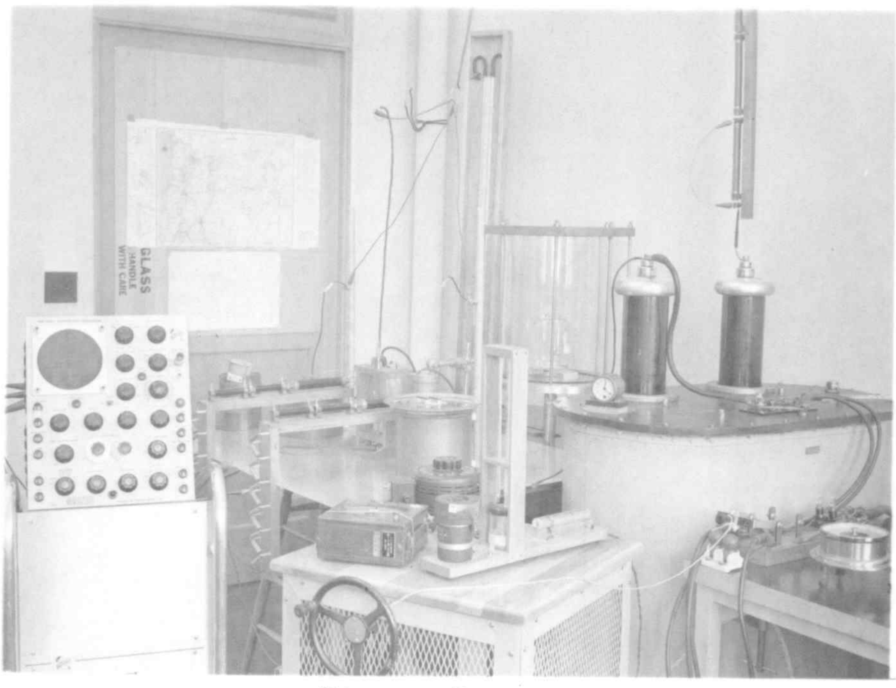

Figure 7.
General view of transformer and high voltage
bridge with cathode ray oscilloscope.

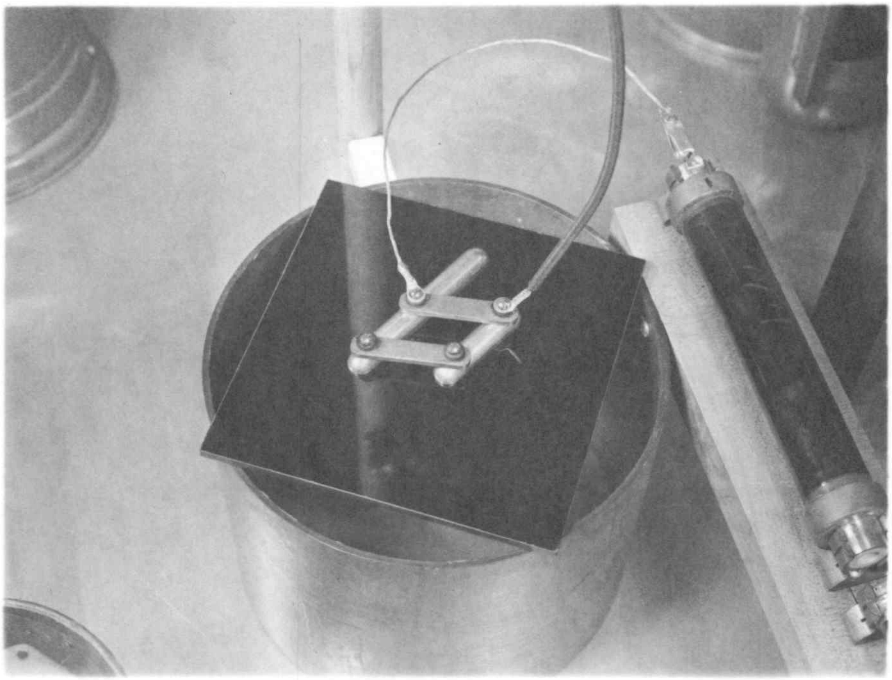

Figure 8.
Half round parallel electrodes
on specimen under test.

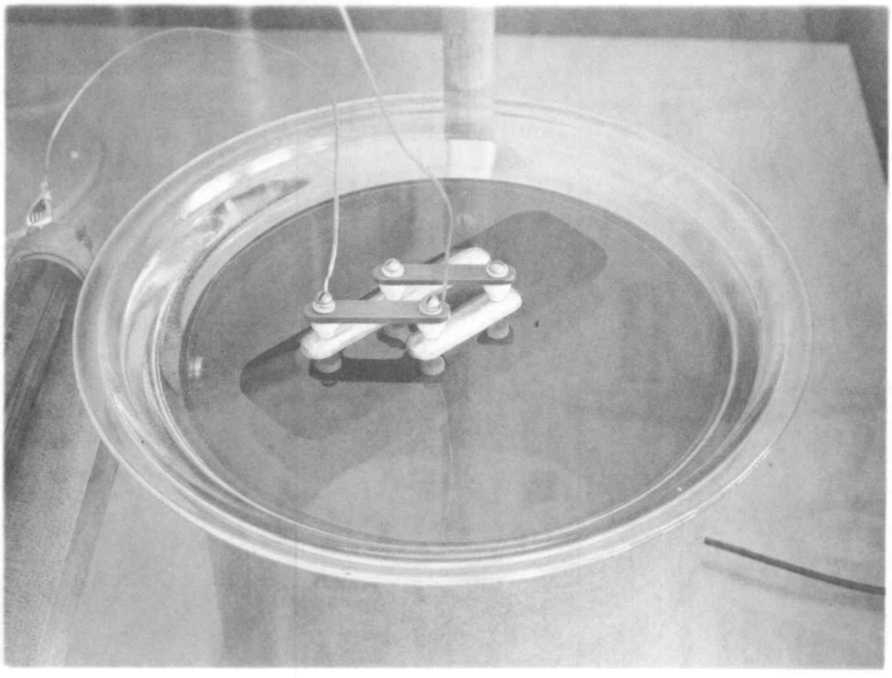

Figure 9.
Half round parallel balancing electrodes
immersed in oil to suppress ionization.

smaller electrodes concentrating the field in a more localized area. Half-round bar stock was used to concentrate the field close to the surface of the material. The ends of the electrodes were rounded to eliminate points of high electric stress. A parallel rule arrangement was employed using strips of micalex insulation as spacers. This combination was used for two reasons. First, it permitted ready adjustment of the electrodes parallel to each other at any desired spacing, and secondly, it provided a ready means for holding the electrode spacing fixed against the electrostatic forces tending to pull them together. The electrostatic forces do become large enough to pull the unsupported electrodes together. Measurements showed that the micalex arms did not disturb the tests, because the length of path over the micalex is very much greater than that over the specimen under test and because the micalex is a superior dielectric for this purpose. Measurements of the capacitance of the electrodes for different spacings on the various insulating materials gave a range of 3.5 to 15 mmf when measured on the General Radio Type 716-C capacitance bridge by the substitution method at 100 cycles. The 100-cycle frequency was chosen to avoid the 60 cycle background noise which is present in the building at a level high enough to make the measurements difficult.

The electrodes used as a balancing capacitor in the high-voltage bridge are shown in Figure 9. These are duplicates of the exploring electrodes. This set of electrodes is immersed to a shallow depth in General Electric type 10-C insulating oil to suppress the edge and surface ionization around and between the electrodes. The electrodes are placed on a specimen which is of the same material and surface treatment as the one under test. The specimen is then placed on an inverted pyrex cover dish which is in turn placed in a pyrex pie plate. The oil level is brought up just high enough to wet the surface of the specimen and the edges of the electrodes. Because the dielectric constant of the oil is approximately two, and only a small portion covers the electrodes, the capacitance of the balancing electrodes is not altered enough to disturb the balance of the bridge beyond what can be readily compensated for. Pyrex was chosen for the cover dish and the pie plate because it has a lower dielectric constant than soft glass and hence its presence is less of a disturbing influence.

In a search for a suitable detector for the bridge, several measuring devices were investigated. One of these was the vacuum tube voltmeter. The response of a vacuum tube voltmeter is determined by the circuit used.

The diode input type of instrument may indicate either the average value or the crest value depending on a minor circuit change. The amplifier input type of instrument may have three possible types of response depending on the grid bias. They are a square-law response with no wave form error, a square-law response with wave form error, and average value response. Various types of vacuum tube voltmeters were tried and found to be unsatisfactory because the only ones available were made for single ended input and had an inadequate frequency response. Also, the readings taken at a given attenuator setting could not be made to match those taken for adjacent attenuator settings. This difficulty was caused by bringing the feed-back loop to the input attenuator, coupled with the fact that in this investigation it was necessary to connect the device to a low impedance source from which the non-sinueoidal ionization pulses are obtainable.

Other types of detectors were considered and experimented with. Thermocouples and thermistors were tried as a means of measuring the effective value of the ionization current. Thermocouples could not stand the overload imposed by flashover. Thermistors proved to be of insufficient sensitivity. Observations made with the cathode ray oscilloscope showed that the effective value of the ionization current is relatively very much less than the crest value. This great difference in the relative magnitudes of the crest values and the effective values of the ionization current is due to the fact that the ionization current is made up of sporadic unsustained bursts of ionization current with very high crest values, but with very low effective values because of the discontinuity of the corona. This relation between the effective and crest values has been shown by Professors F. O. McMillan and H. G. Barnett in their work on radio interference measurements (7, pp. 857-862).

The most suitable detector for the bridge proved to be the oscilloscope shown in Figure 7, which is proveded with short direct connections to the vertical deflector plates. This direct connection was necessary because of the steep rise of the ionization pulses and the bridge circuit which made it necessary to operate the detector with both deflector plates above ground. The oscilloscope was used to measure the crest values of the ionization pulses.

The resistive arms of the bridge were calculated to have sufficient resistance to give a reliable deflection on the cathode ray tube even for the specimens showing little ionization. Metal film non-inductive resistors were used for the larger values of resistance, and Ayrton-Perry type, wire-wound, non-inductive resistors were used for the low values. The resistance values used are given in Figure 5.

The ionization and breakdown over the surface of a solid dielectric is a function of the crest value of the applied voltage. The most reliable method of measuring this crest voltage is by means of a sphere gap. The range of voltage covered by the ionization measurements was such that the two-centimeter sphere gap was of the proper size. In the use of the two-centimeter sphere gap it was found to be very important that the spheres be polished and cleaned frequently, since the voltage at which the clean gap fires is lower than that for the oxidized gap. For this series of experiments, the sphere gap was also irradiated by the light from a mercury-arc lamp. This ultraviolet radiation produced the ions enabling the gap to fire in a more reproducible manner than would be possible without irradiation. The convenience this afforded led to more consistant results and a great saving in time in determining the ionization and flashover voltages. The difference in the break-down voltage between the irradiated and the unirradiated gap was found to be negligible.

Ionization Current Measurements

The crest values of the ionization current were measured for four different spacings of the parallel gap electrodes. The spacings were 0.25, 0.50, 0.75, and 1.00 inch. For each spacing the crest values of the ionization current were recorded from the onset of ionization to the point of flashover or beyond, depending on the specimen under test. For some of the specimens it was possible to take readings of the ionization current for a limited part of the range beyond the flashover point. This was made possible by using the air stream from a small blower to extinguish the arc after onset of flashover. Tests showed that the air stream directed toward the specimen at flashover did not alter the initial flashover voltage of the specimen. Because the cathode ray oscilloscope immediately restores itself after flashover it was possible to observe the ionization current between the flashovers at potentials in excess of the initial flashover voltage.

The ionization current characteristics for the various specimens are shown in Figures 10 to 27. These were plotted to the same scale of the coordinate axes for the sake of comparison. All measurements were made with 60-cycle alternating current. With few exceptions there

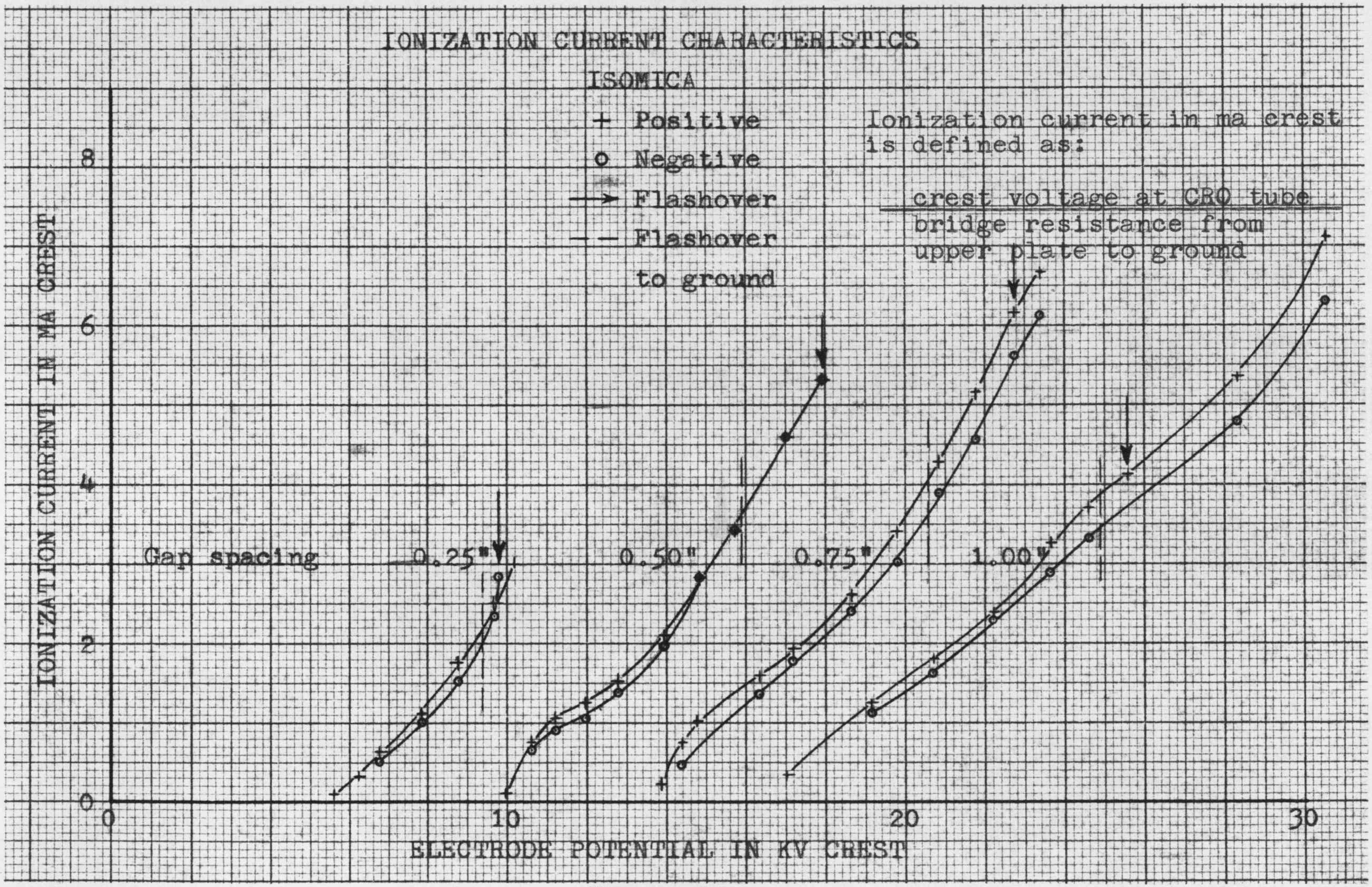
IONIZATION CURRENT CHARACTERISTICS
ISOMICA
+ Positive
o Negative
Flashover
Flashover to ground
Ionization current in ma crest is defined as:
crest voltage at CRO tube / bridge resistance from upper plate to ground
Gap spacing
0.25"
0.50"
0.75"
1.00"
IONIZATION CURRENT IN MA CREST
8
6
4
2
0
0
10
20
30
ELECTRODE POTENTIAL IN KV CREST

Figure 10

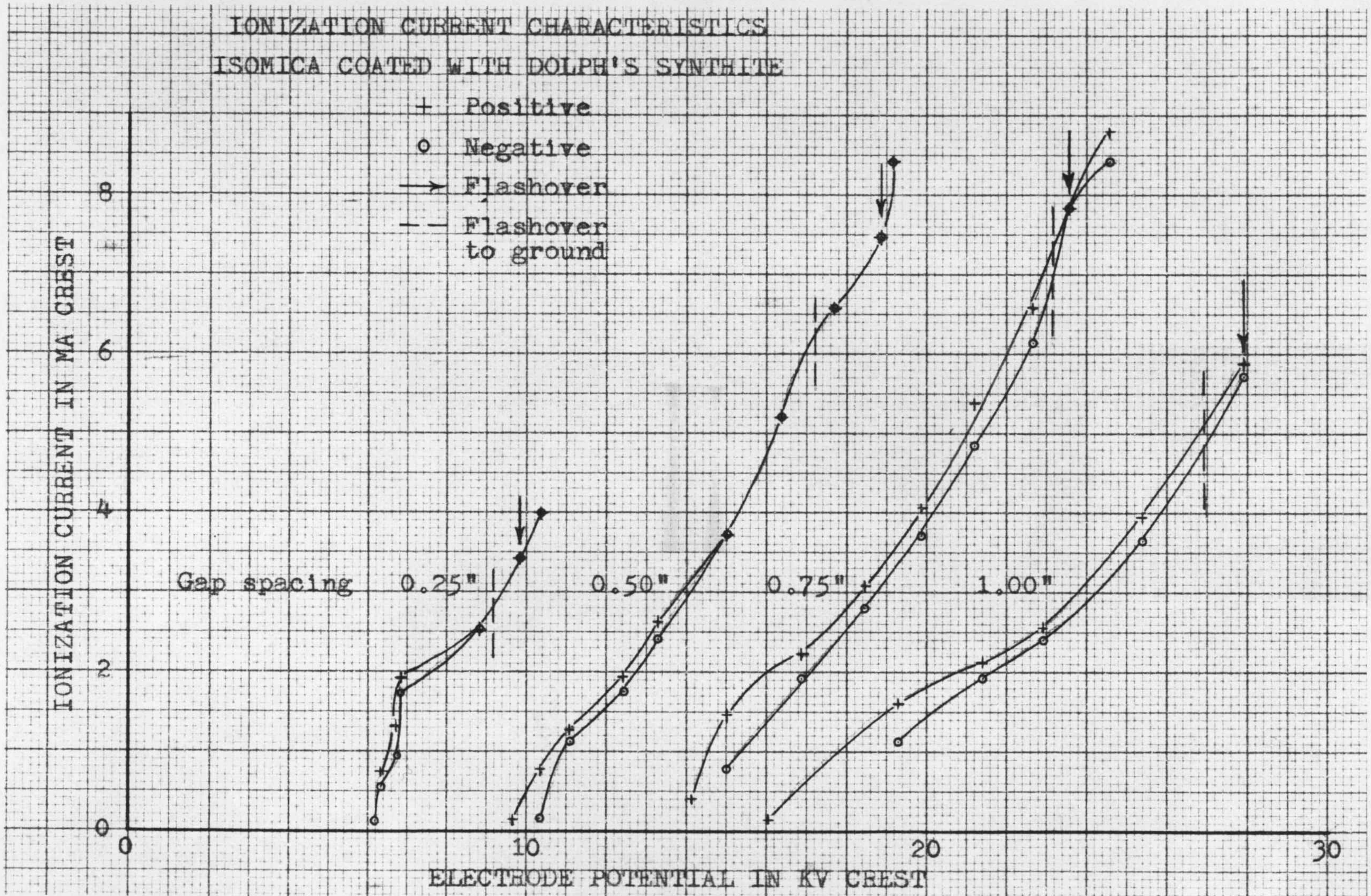
IONIZATION CURRENT CHARACTERISTICS
ISOMICA COATED WITH DOLPH'S SYNTHITE
+ Positive
o Negative
Flashover
Flashover to ground
Gap spacing 0.25" 0.50" 0.75" 1.00"
IONIZATION CURRENT IN MA CREST
0
2
4
6
8
0
10
20
30
ELECTRODE POTENTIAL IN KV CREST

Figure 11

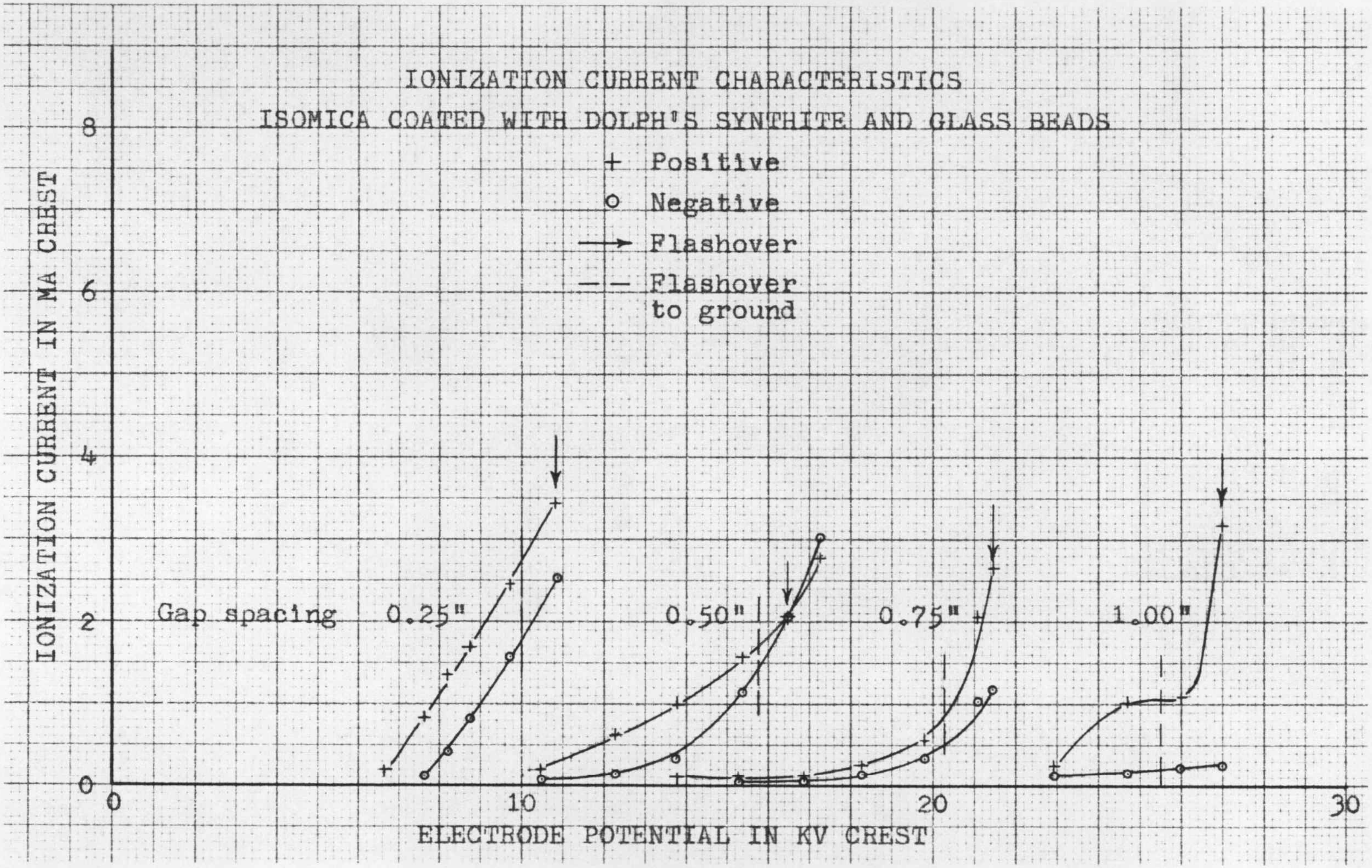
IONIZATION CURRENT CHARACTERISTICS
ISOMICA COATED WITH DOLPH'S SYNTHITE AND GLASS BEADS
+ Positive
o Negative
Flashover
Flashover to ground
Gap spacing 0.25"
0.50"
0.75"
1.00"
IONIZATION CURRENT IN MA CREST
ELECTRODE POTENTIAL IN KV CREST
0
2
4
6
8
0
10
20
30

Figure 12

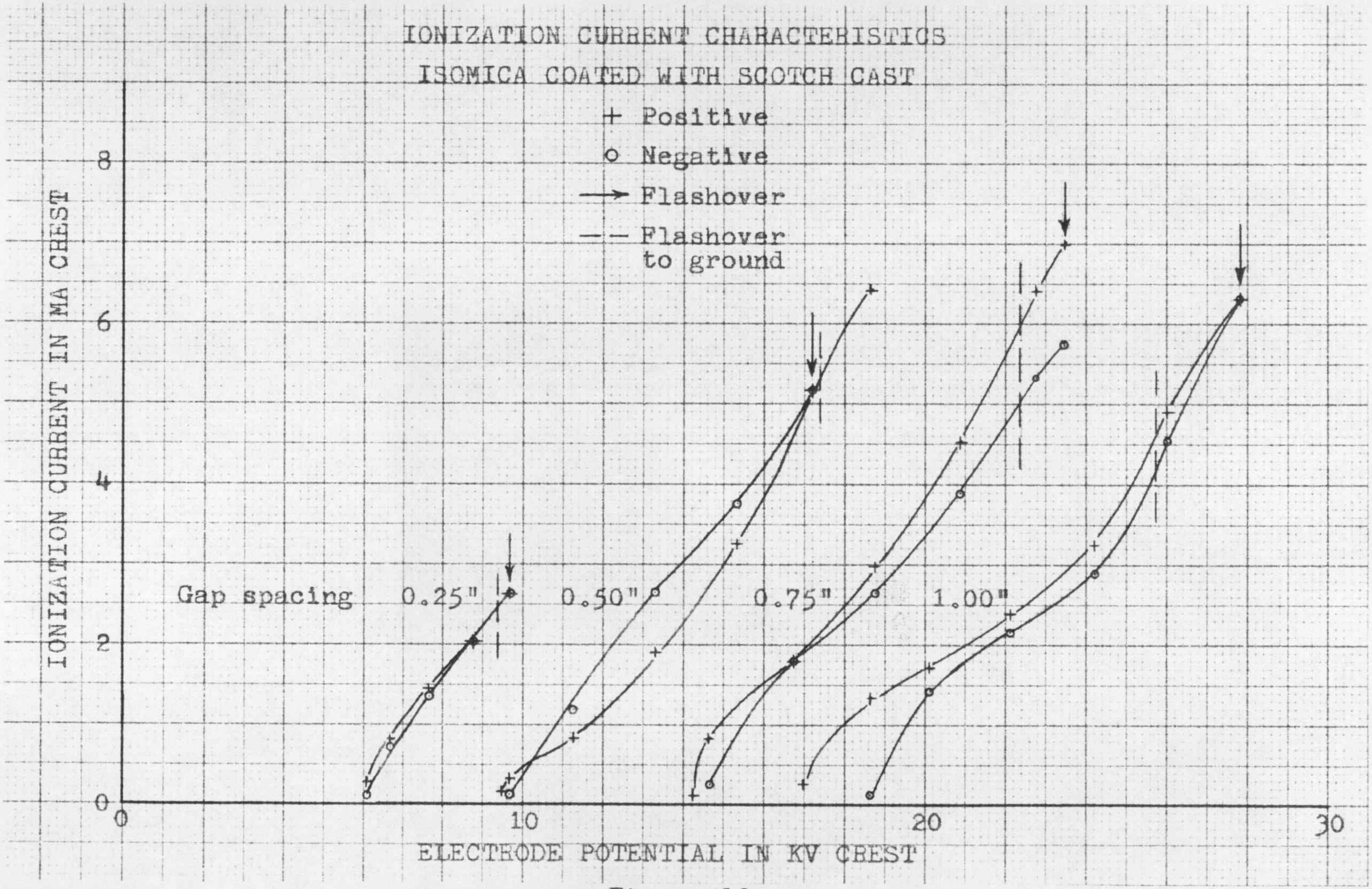
IONIZATION CURRENT CHARACTERISTICS
ISOMICA COATED WITH SCOTCH CAST
+ Positive
o Negative
Flashover
Flashover to ground
Gap spacing 0.25" 0.50" 0.75" 1.00"
IONIZATION CURRENT IN MA CREST
ELECTRODE POTENTIAL IN KV CREST
0
2
4
6
8
10
20
30

Figure 13

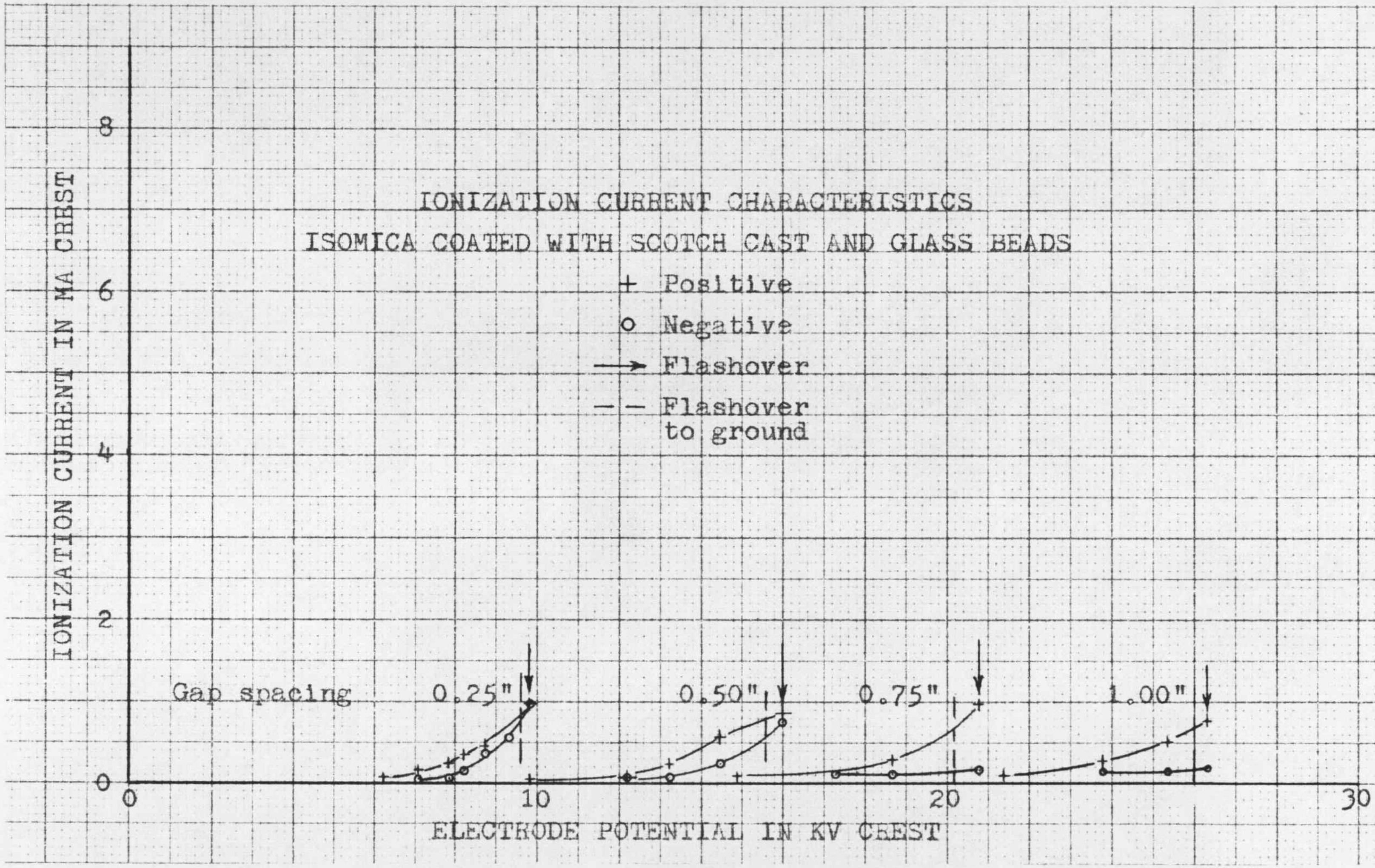
IONIZATION CURRENT CHARACTERISTICS
ISOMICA COATED WITH SCOTCH CAST AND GLASS BEADS
+ Positive
o Negative
Flashover
Flashover to ground
IONIZATION CURRENT IN MA CREST
8
6
4
2
0
Gap spacing
0.25"
0.50"
0.75"
1.00"
0
10
20
30
ELECTRODE POTENTIAL IN KV CREST

Figure 14

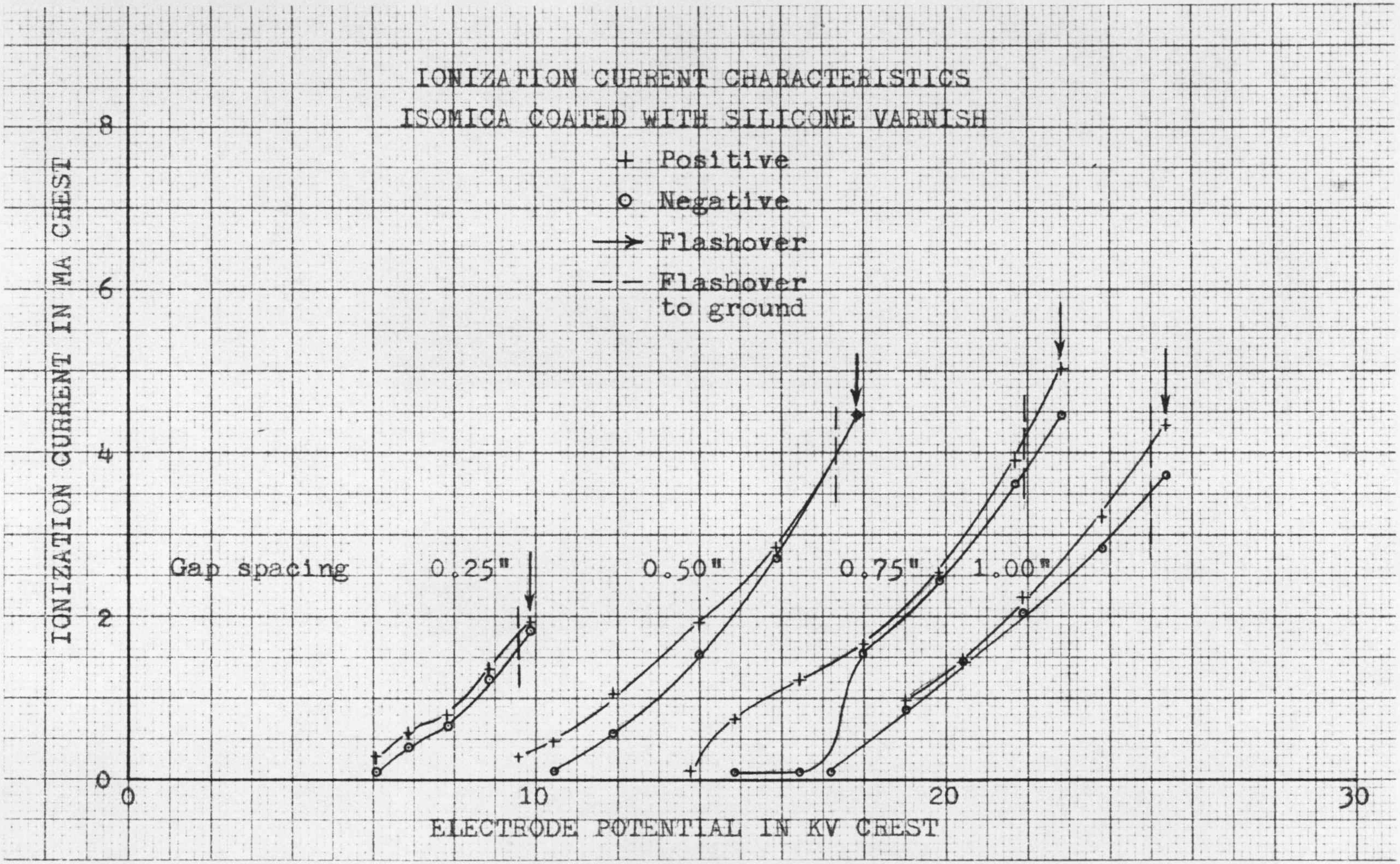

IONIZATION CURRENT CHARACTERISTICS
ISOMICA COATED WITH SILICONE VARNISH
+ Positive
o Negative
Flashover
Flashover to ground
IONIZATION CURRENT IN MA CREST
8
6
4
2
0
Gap spacing
0.25"
0.50"
0.75"
1.00"
0
10
20
30
ELECTRODE POTENTIAL IN KV CREST

Figure 15

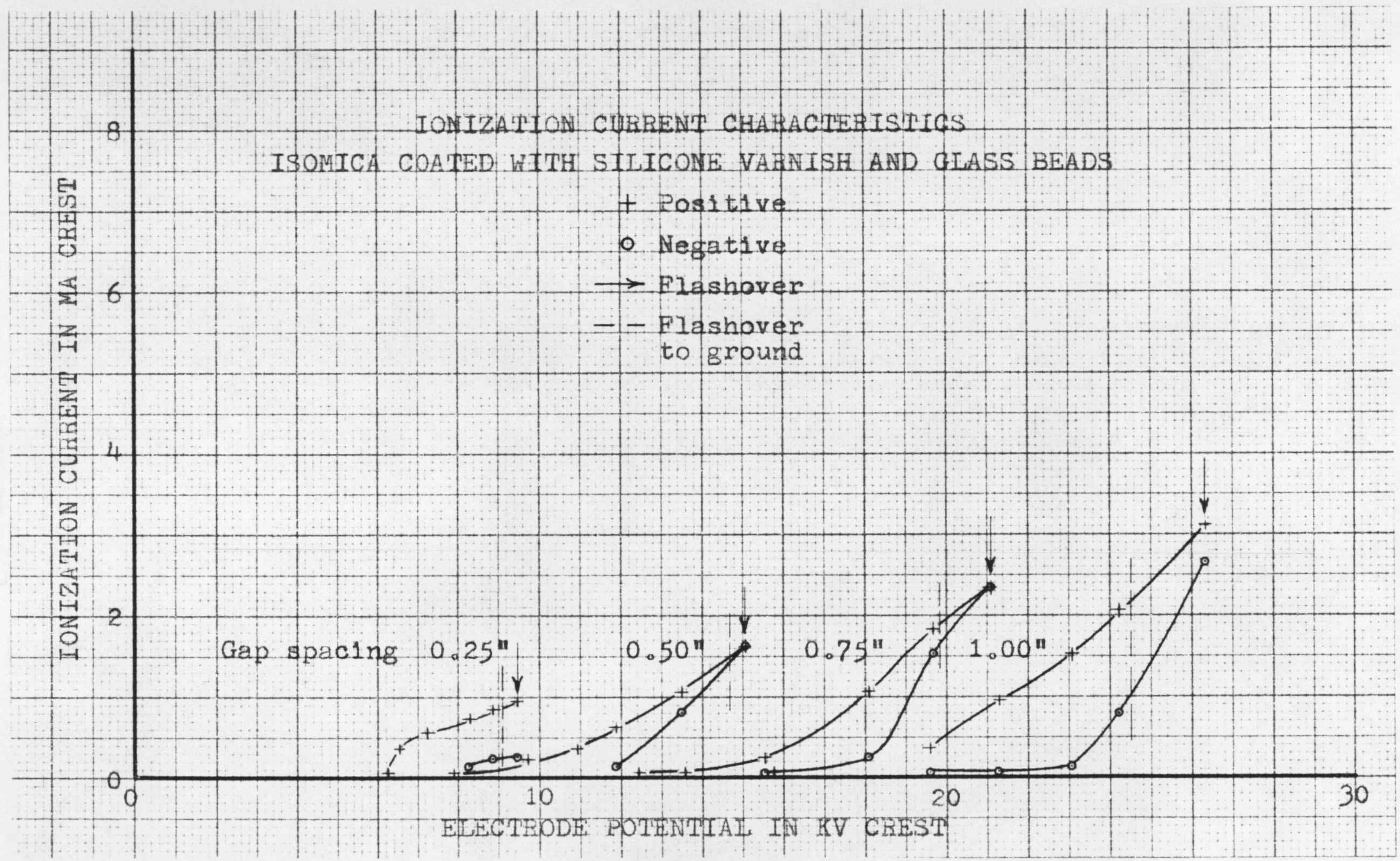
IONIZATION CURRENT CHARACTERISTICS
ISOMICA COATED WITH SILICONE VARNISH AND GLASS BEADS
+ Positive
o Negative
→ Flashover
— — Flashover to ground
Gap spacing 0.25"
0.50"
0.75"
1.00"
IONIZATION CURRENT IN MA CREST
ELECTRODE POTENTIAL IN KV CREST
0
2
4
6
8
10
20
30
Figure 16

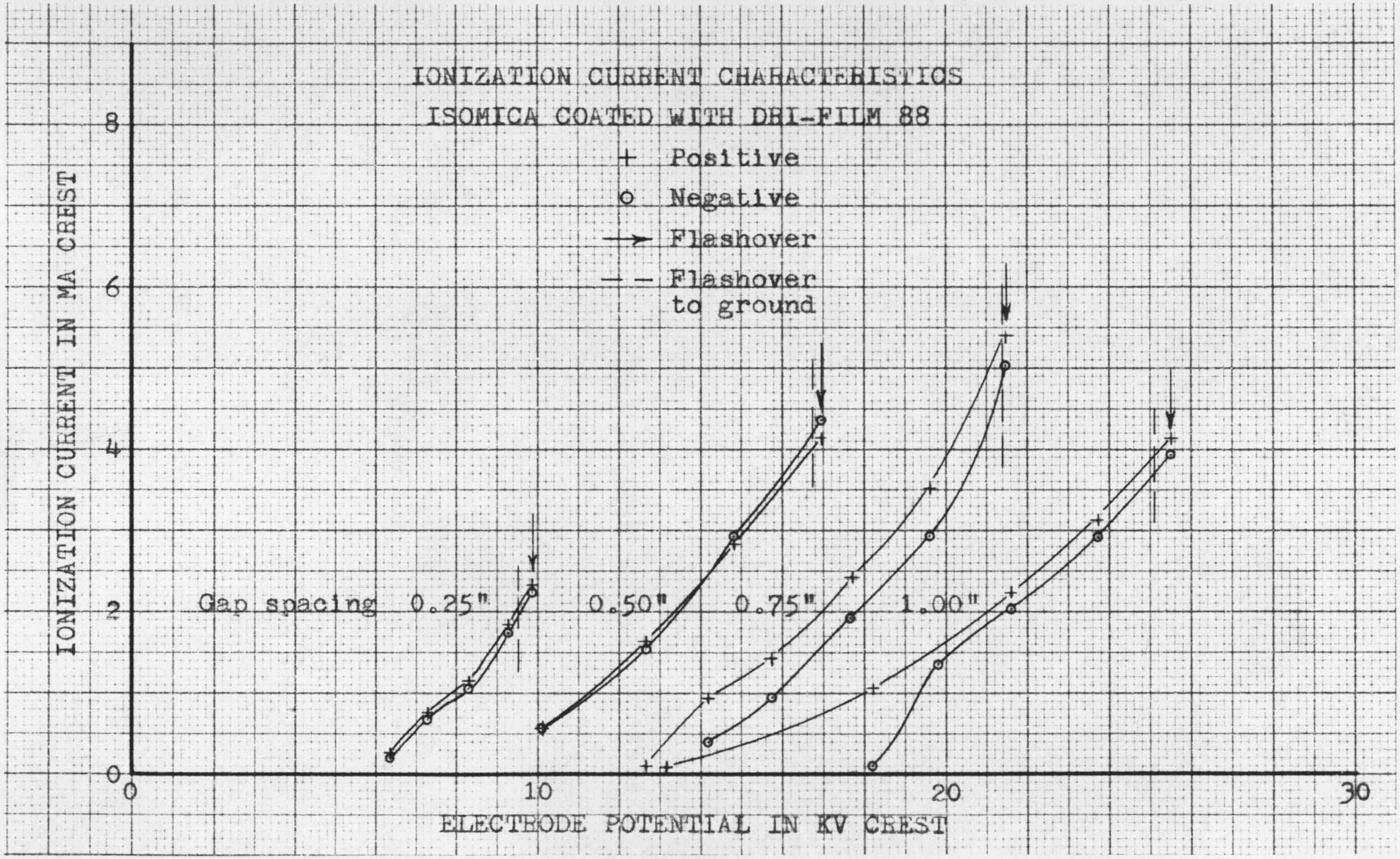
IONIZATION CURRENT CHARACTERISTICS
ISOMICA COATED WITH DRI-FILM 88
+ Positive
o Negative
Flashover
Flashover to ground
Gap spacing 0.25" 0.50" 0.75" 1.00"
IONIZATION CURRENT IN MA CREST
ELECTRODE POTENTIAL IN KV CREST
0
2
4
6
8
10
20
30

Figure 17

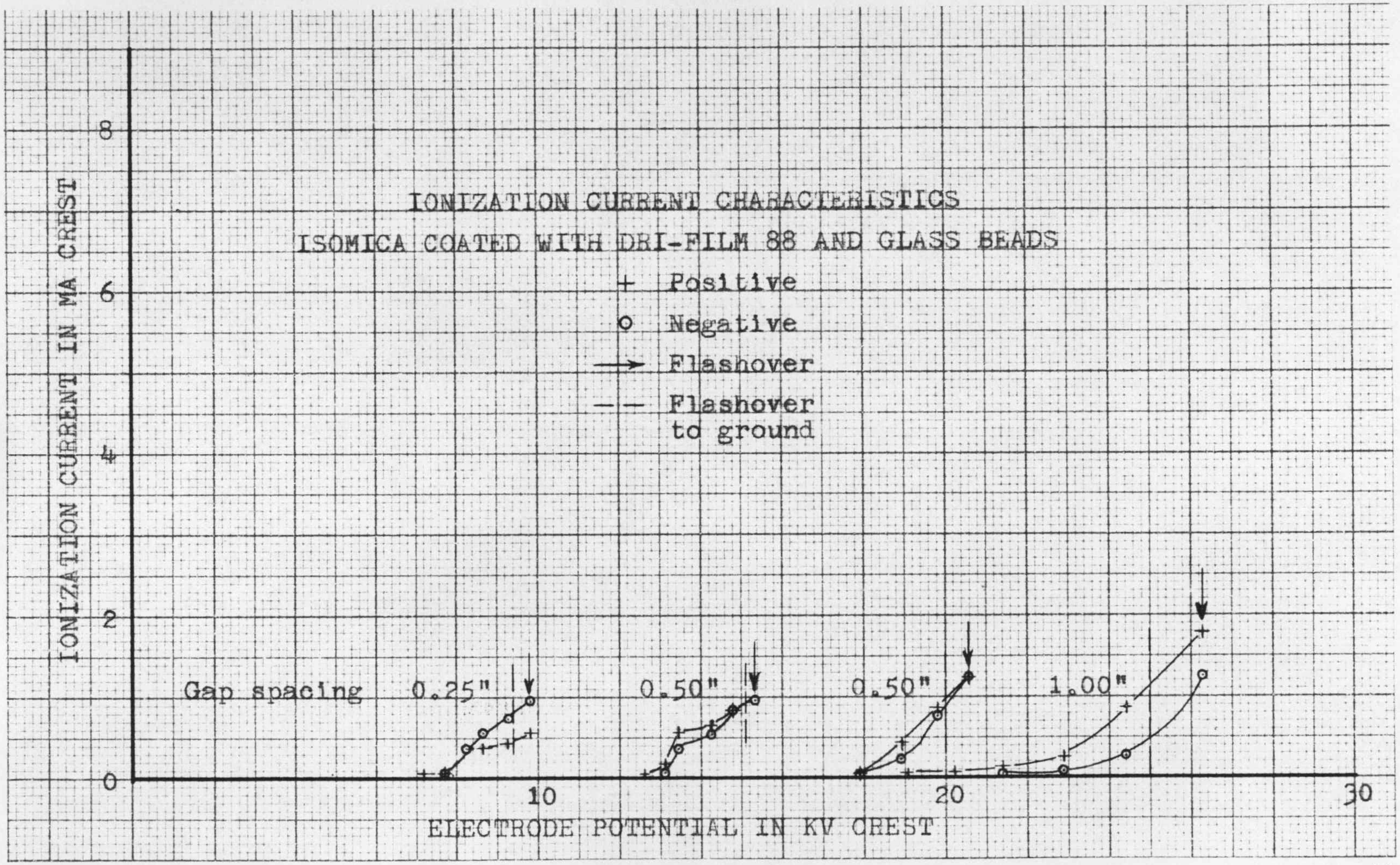
IONIZATION CURRENT CHARACTERISTICS
ISOMICA COATED WITH DRI-FILM 88 AND GLASS BEADS
+ Positive
o Negative
Flashover
Flashover to ground
IONIZATION CURRENT IN MA CREST
ELECTRODE POTENTIAL IN KV CREST
Gap spacing 0.25" 0.50" 0.50" 1.00"
0
2
4
6
8
10
20
30

Figure 18

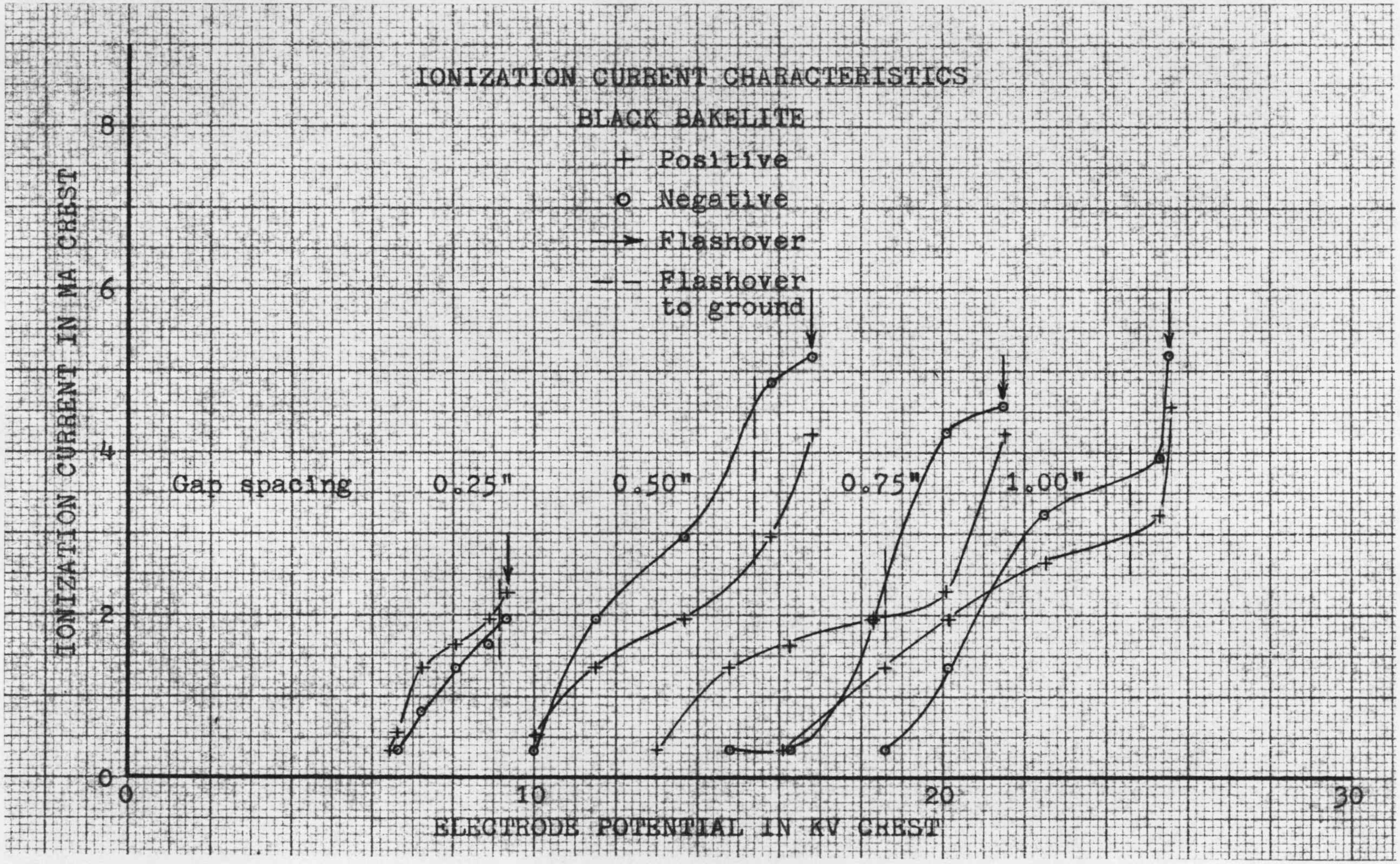
IONIZATION CURRENT CHARACTERISTICS
BLACK BAKELITE
+ Positive
o Negative
→ Flashover
-- Flashover to ground
Gap spacing
0.25"
0.50"
0.75"
1.00"
IONIZATION CURRENT IN MA CREST
ELECTRODE POTENTIAL IN KV CREST
0
2
4
6
8
10
20
30

Figure 19

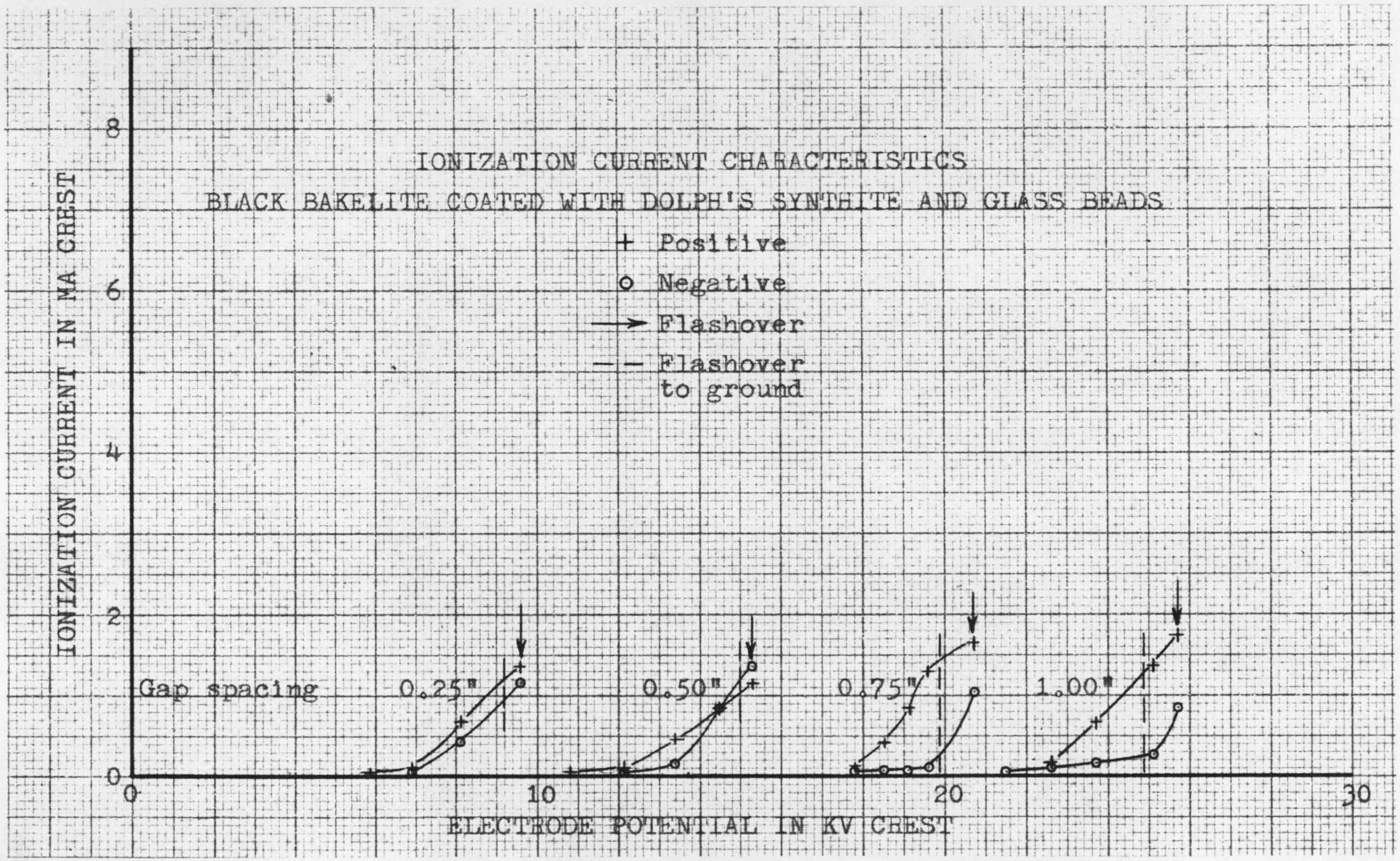
IONIZATION CURRENT CHARACTERISTICS
BLACK BAKELITE COATED WITH DOLPH'S SYNTHITE AND GLASS BEADS
Positive
Negative
Flashover
Flashover to ground
IONIZATION CURRENT IN MA CREST
ELECTRODE POTENTIAL IN KV CREST
Gap spacing
0.25"
0.50"
0.75"
1.00"
0
2
4
6
8
10
20
30

Figure 20

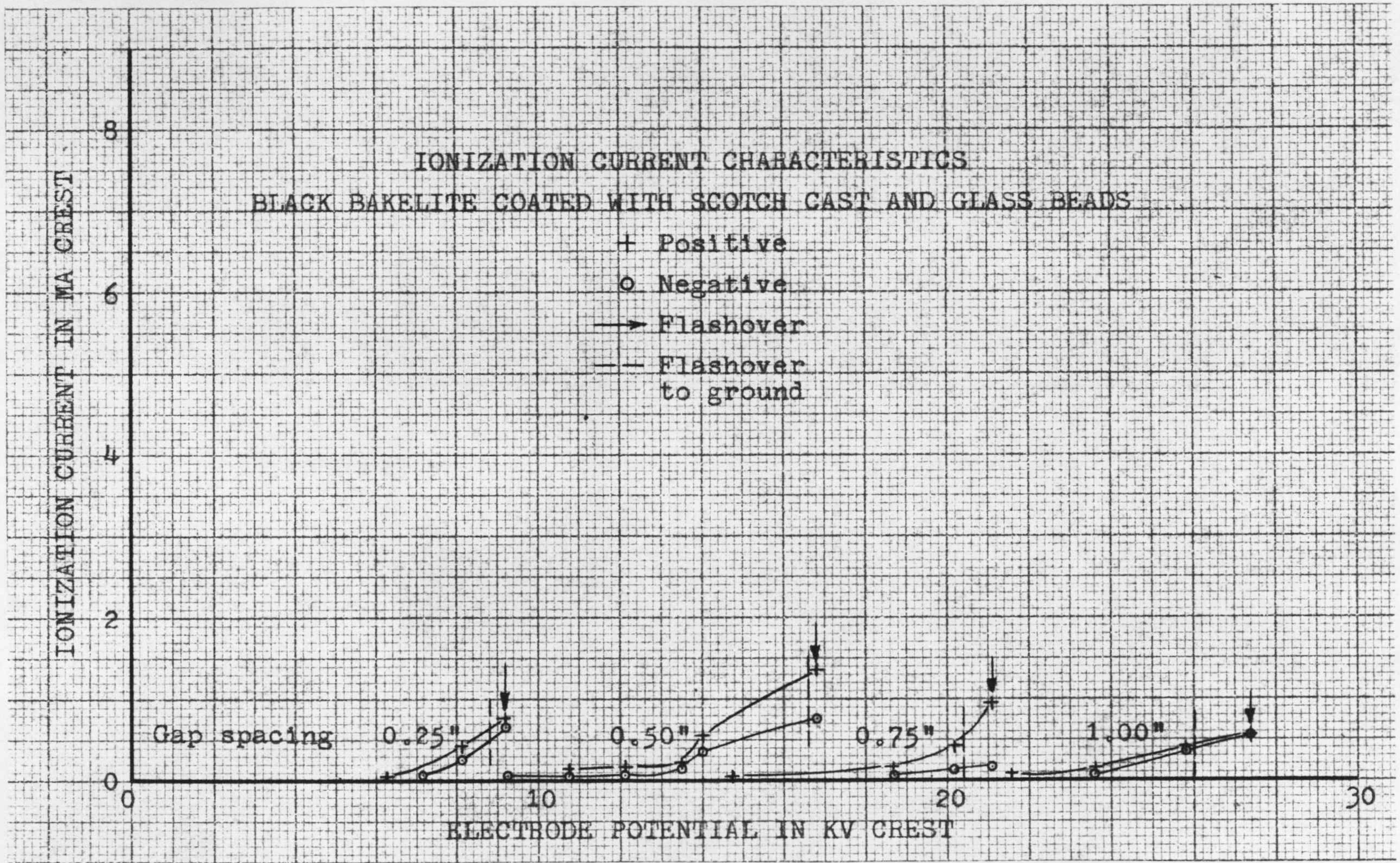
IONIZATION CURRENT CHARACTERISTICS
BLACK BAKELITE COATED WITH SCOTCH CAST AND GLASS BEADS
+ Positive
o Negative
Flashover
Flashover to ground
Gap spacing
0.25"
0.50"
0.75"
1.00"
IONIZATION CURRENT IN MA CREST
ELECTRODE POTENTIAL IN KV CREST
0
2
4
6
8
10
20
30

Figure 21

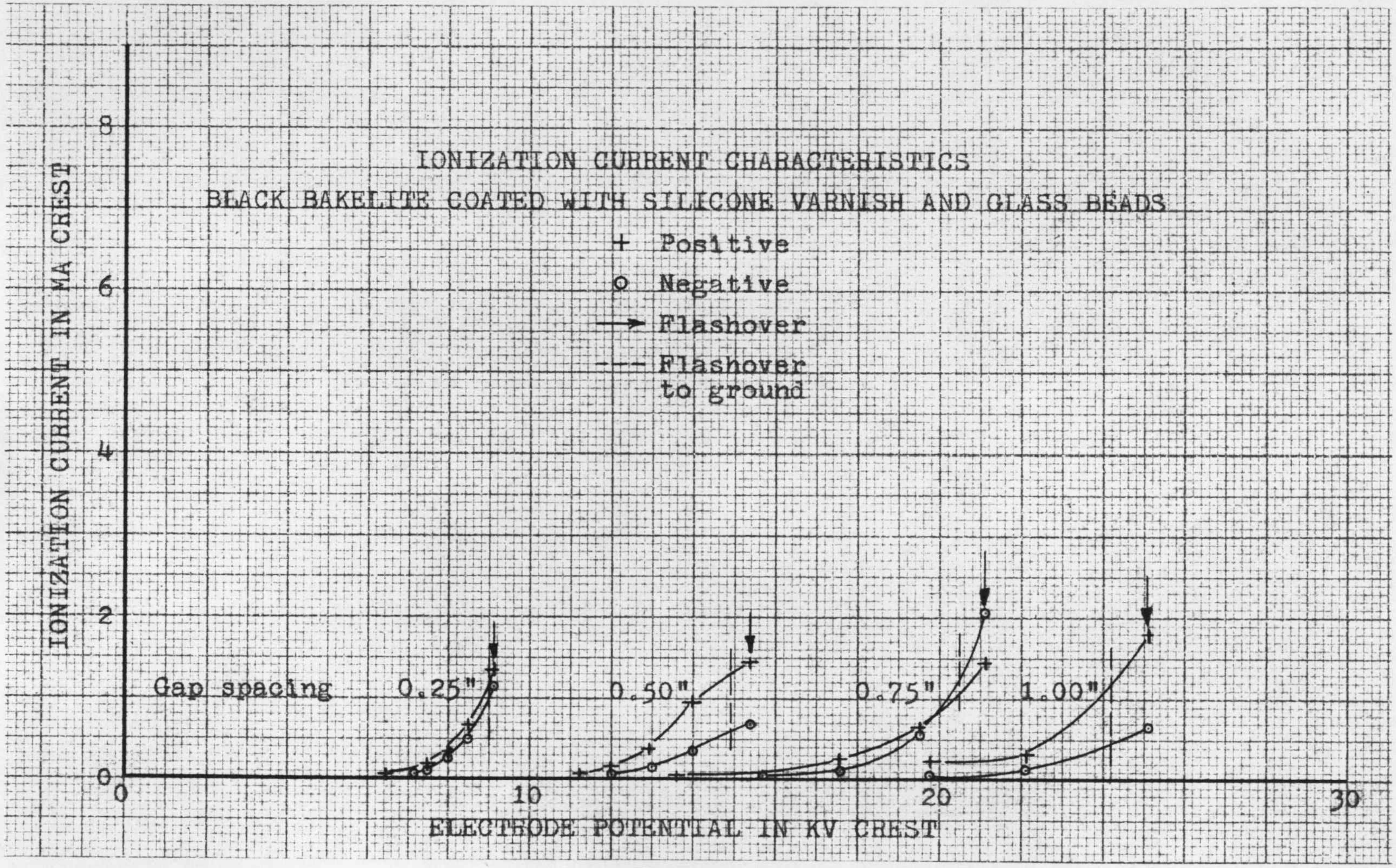
IONIZATION CURRENT CHARACTERISTICS
BLACK BAKELITE COATED WITH SILICONE VARNISH AND GLASS BEADS
+ Positive
o Negative
Flashover
Flashover to ground
Gap spacing
0.25"
0.50"
0.75"
1.00"
IONIZATION CURRENT IN MA CREST
ELECTRODE POTENTIAL IN KV CREST
0
2
4
6
8
10
20
30

Figure 22

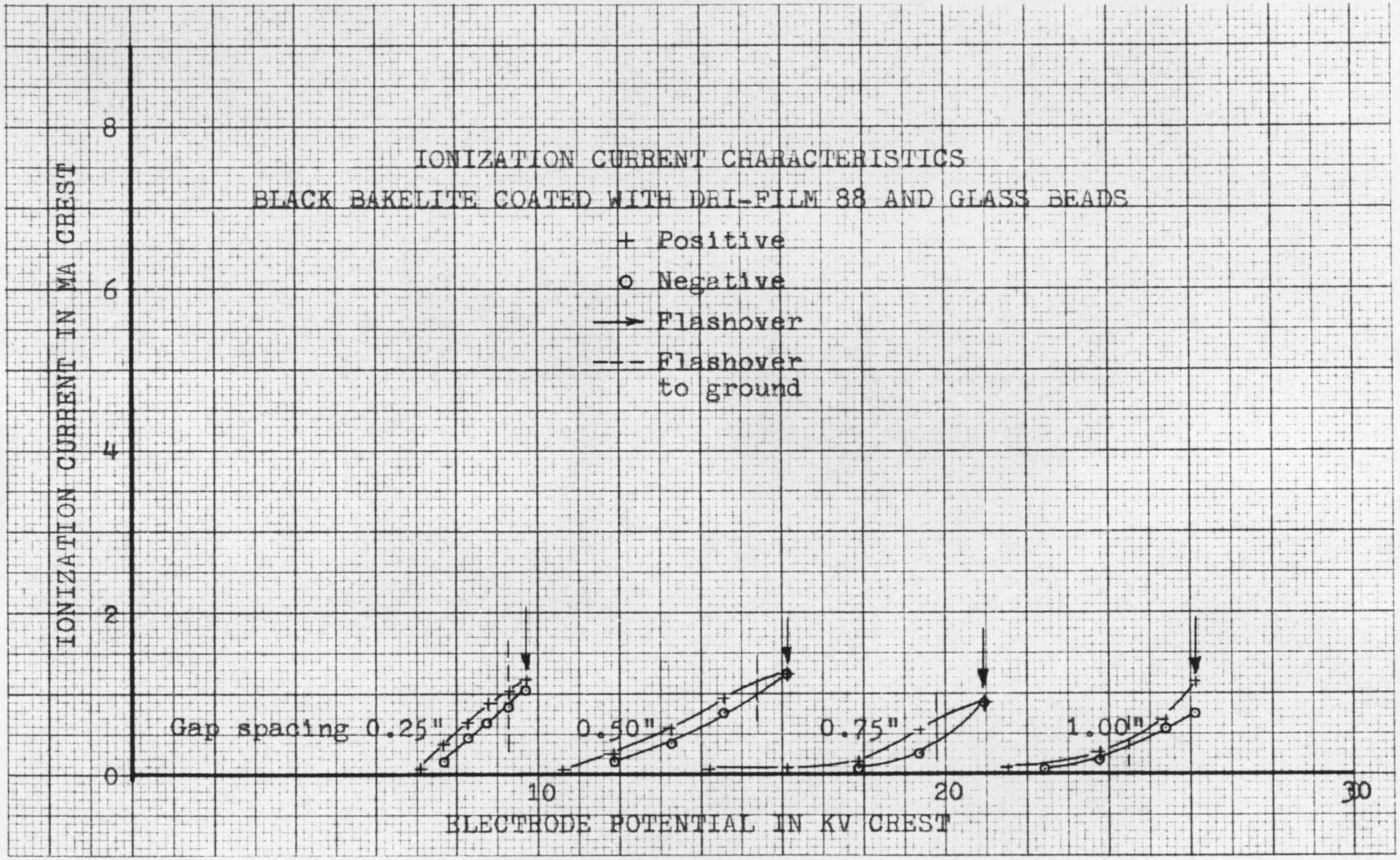
IONIZATION CURRENT CHARACTERISTICS
BLACK BAKELITE COATED WITH DRI-FILM 88 AND GLASS BEADS
+ Positive
o Negative
Flashover
Flashover to ground
IONIZATION CURRENT IN MA CREST
8
6
4
2
0
Gap spacing 0.25"
0.50"
0.75"
1.00"
10
20
30
ELECTRODE POTENTIAL IN KV CREST

Figure 23

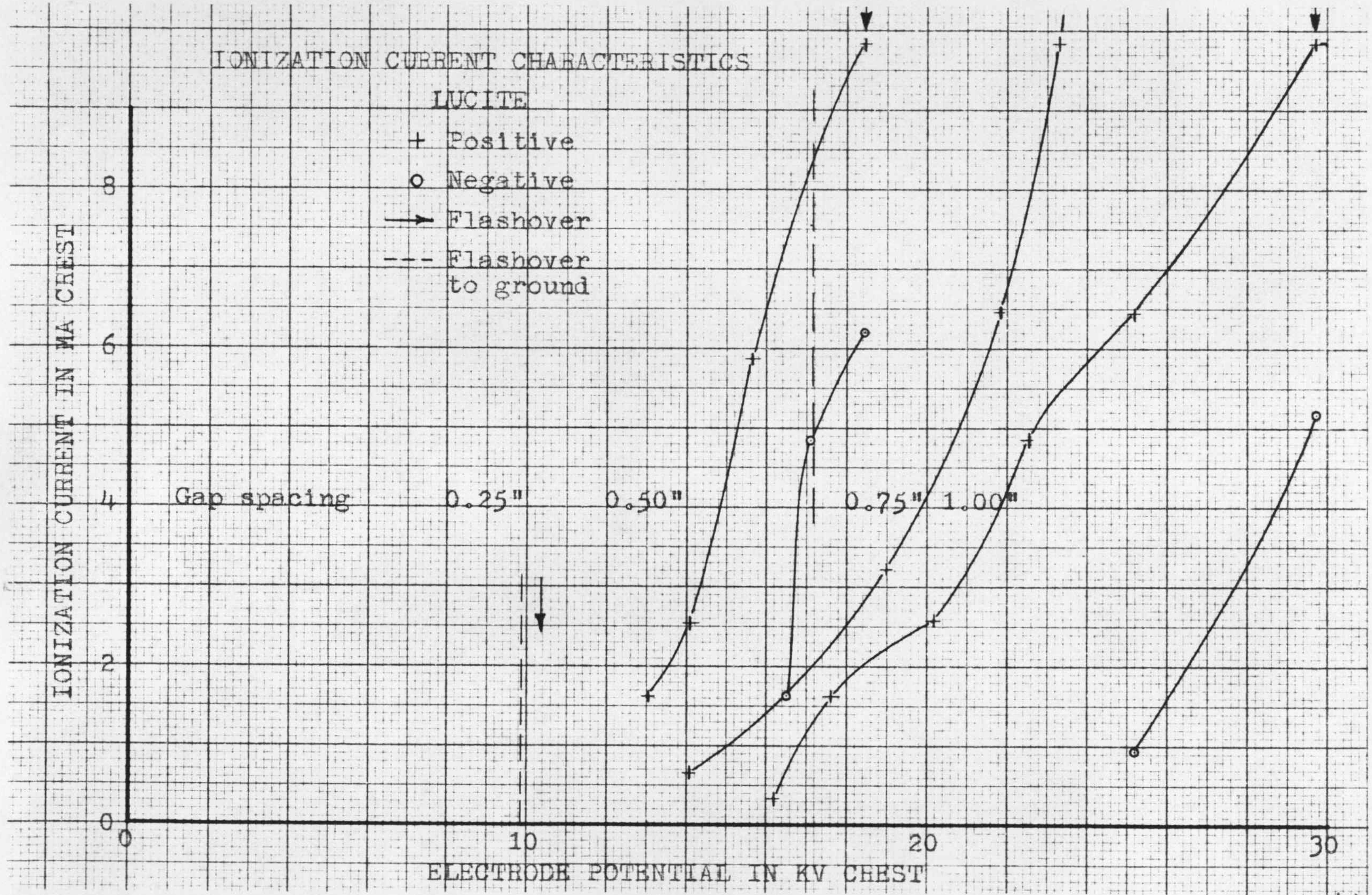
IONIZATION CURRENT CHARACTERISTICS
LUCITE
+ Positive
o Negative
Flashover
--- Flashover to ground
Gap spacing 0.25" 0.50" 0.75" 1.00"
IONIZATION CURRENT IN MA CREST
ELECTRODE POTENTIAL IN KV CREST
0
2
4
6
8
0
10
20
30

Figure 24a

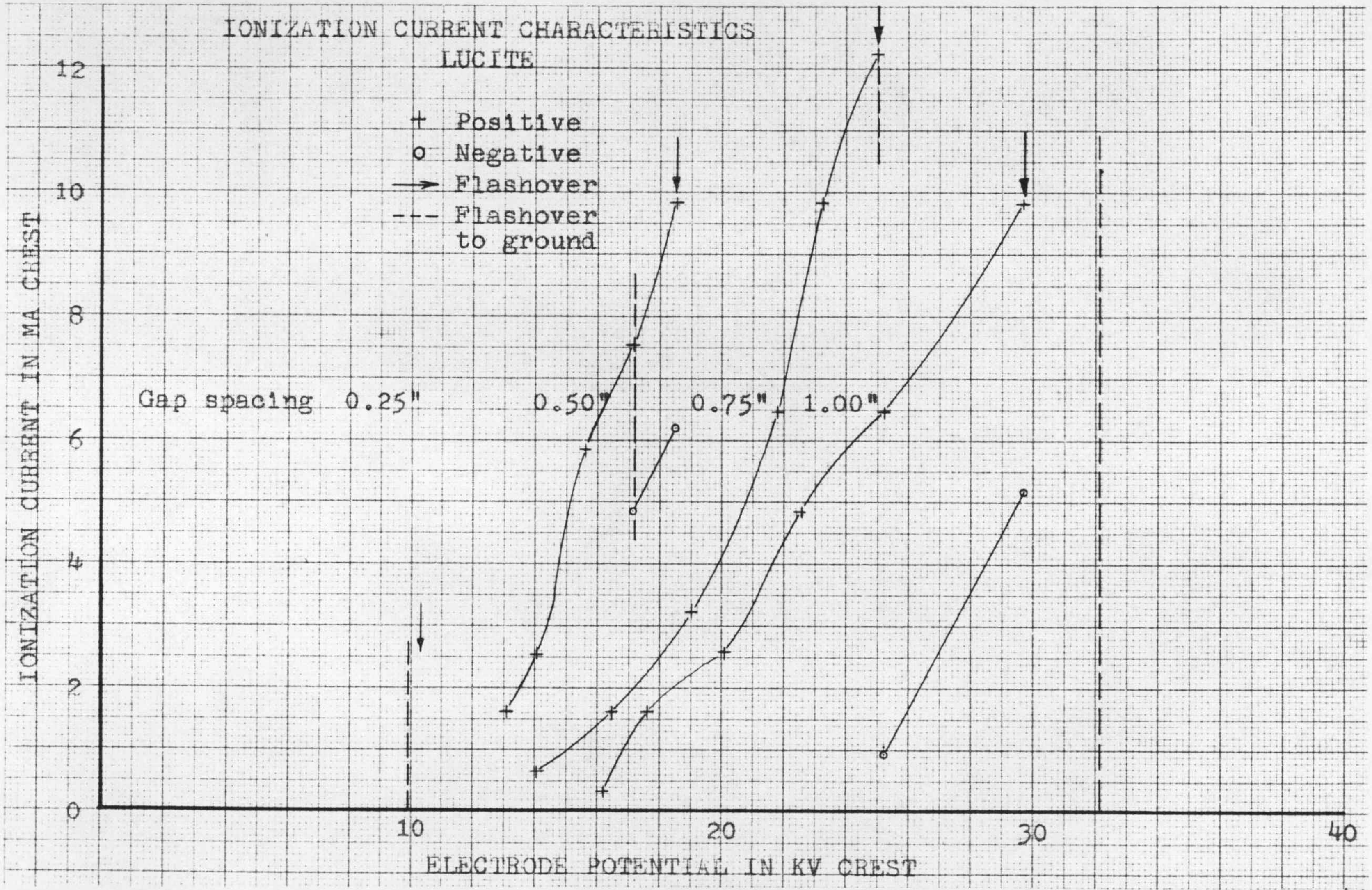
IONIZATION CURRENT CHARACTERISTICS
LUCITE
+ Positive
o Negative
Flashover
Flashover to ground
Gap spacing 0.25"
0.50"
0.75"
1.00"
IONIZATION CURRENT IN MA CREST
ELECTRODE POTENTIAL IN KV CREST
0
2
4
6
8
10
12
10
20
30
40

Figure 24b

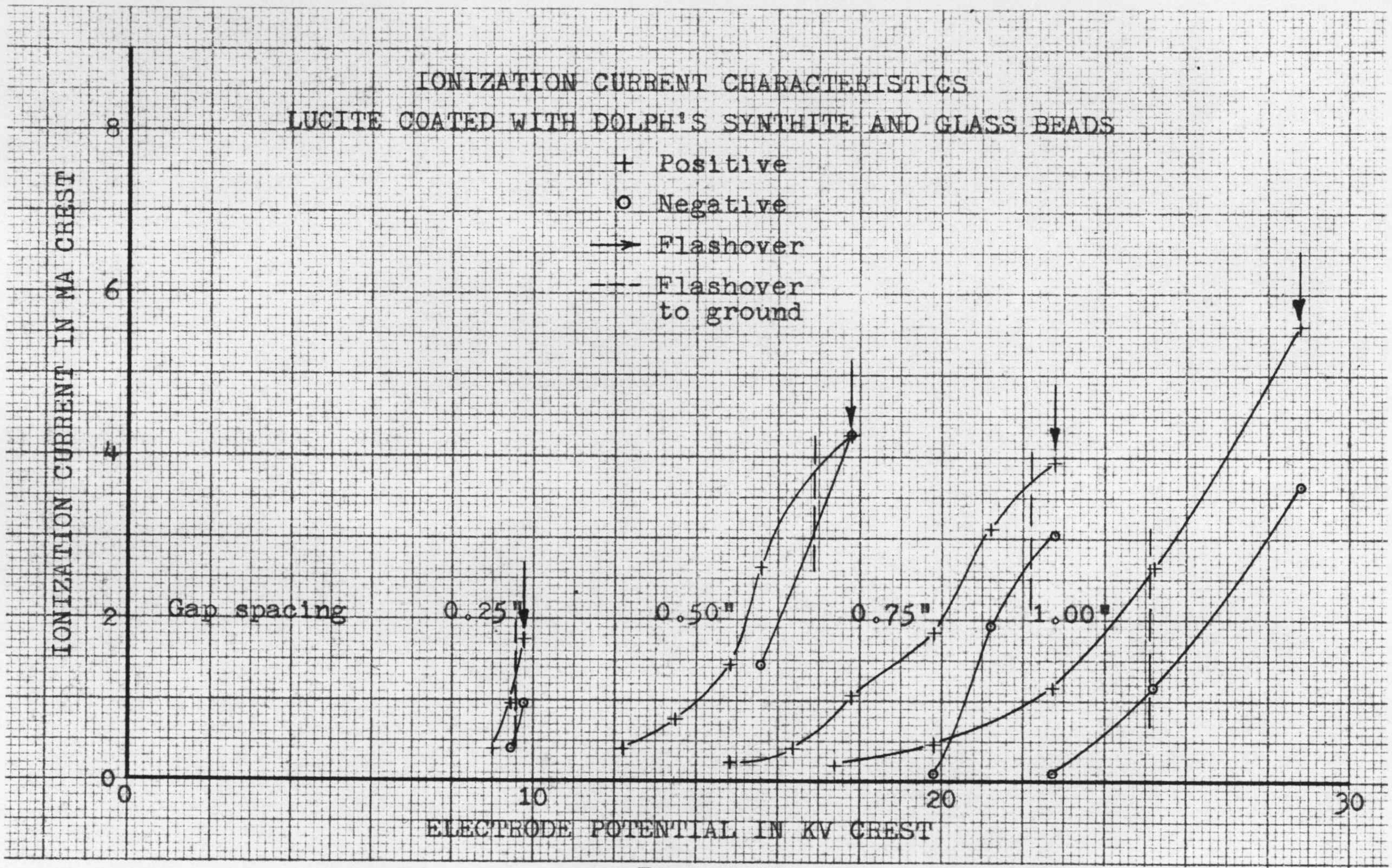
IONIZATION CURRENT CHARACTERISTICS
LUCITE COATED WITH DOLPH'S SYNTHITE AND GLASS BEADS
+ Positive
o Negative
Flashover
Flashover to ground
Gap spacing
0.25"
0.50"
0.75"
1.00"
IONIZATION CURRENT IN MA CREST
ELECTRODE POTENTIAL IN KV CREST
0
2
4
6
8
10
20
30

Figure 25

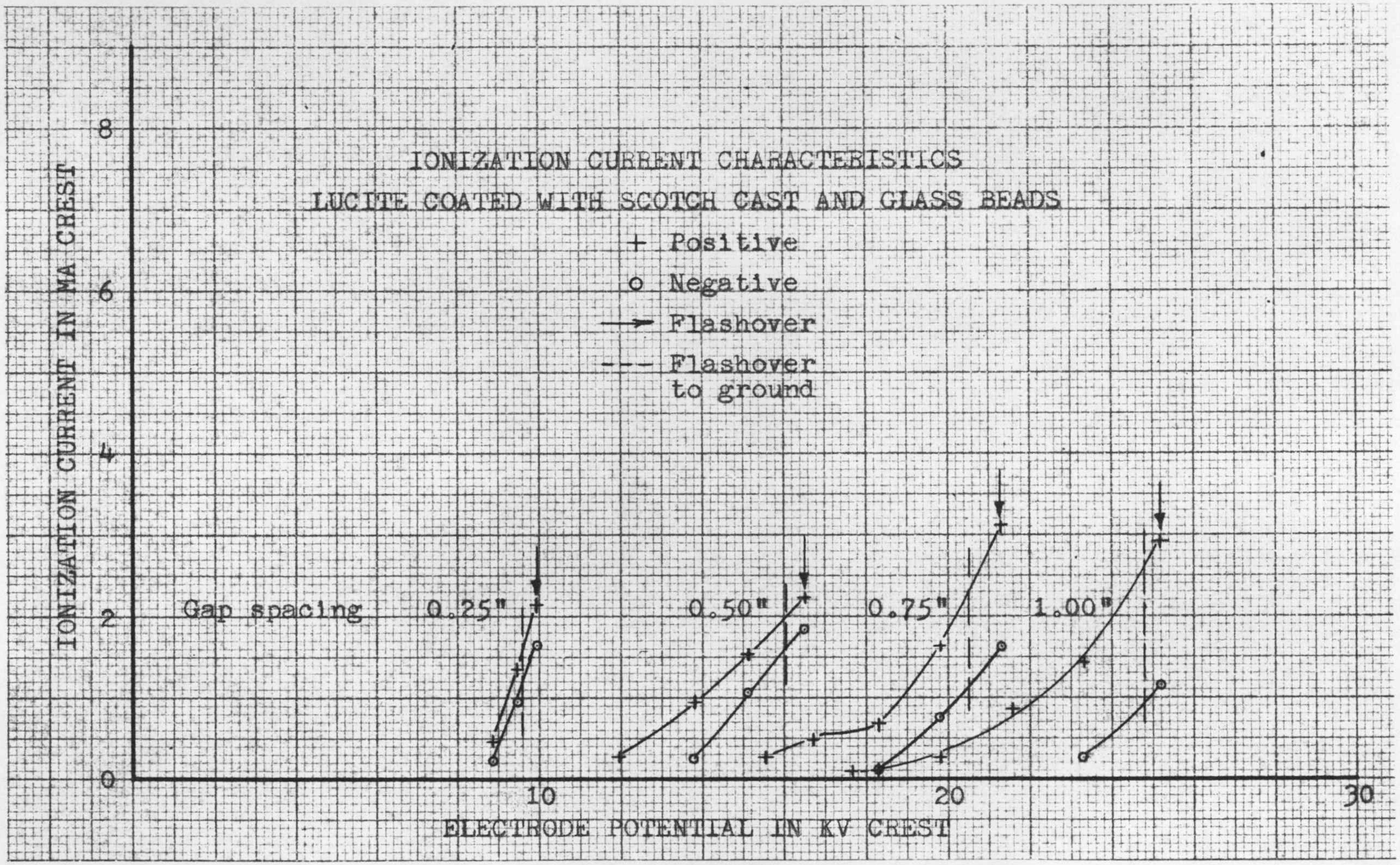
IONIZATION CURRENT CHARACTERISTICS
LUCITE COATED WITH SCOTCH CAST AND GLASS BEADS
+ Positive
o Negative
Flashover
Flashover to ground
Gap spacing
0.25"
0.50"
0.75"
1.00"
IONIZATION CURRENT IN MA CREST
ELECTRODE POTENTIAL IN KV CREST
0
2
4
6
8
10
20
30

Figure 26

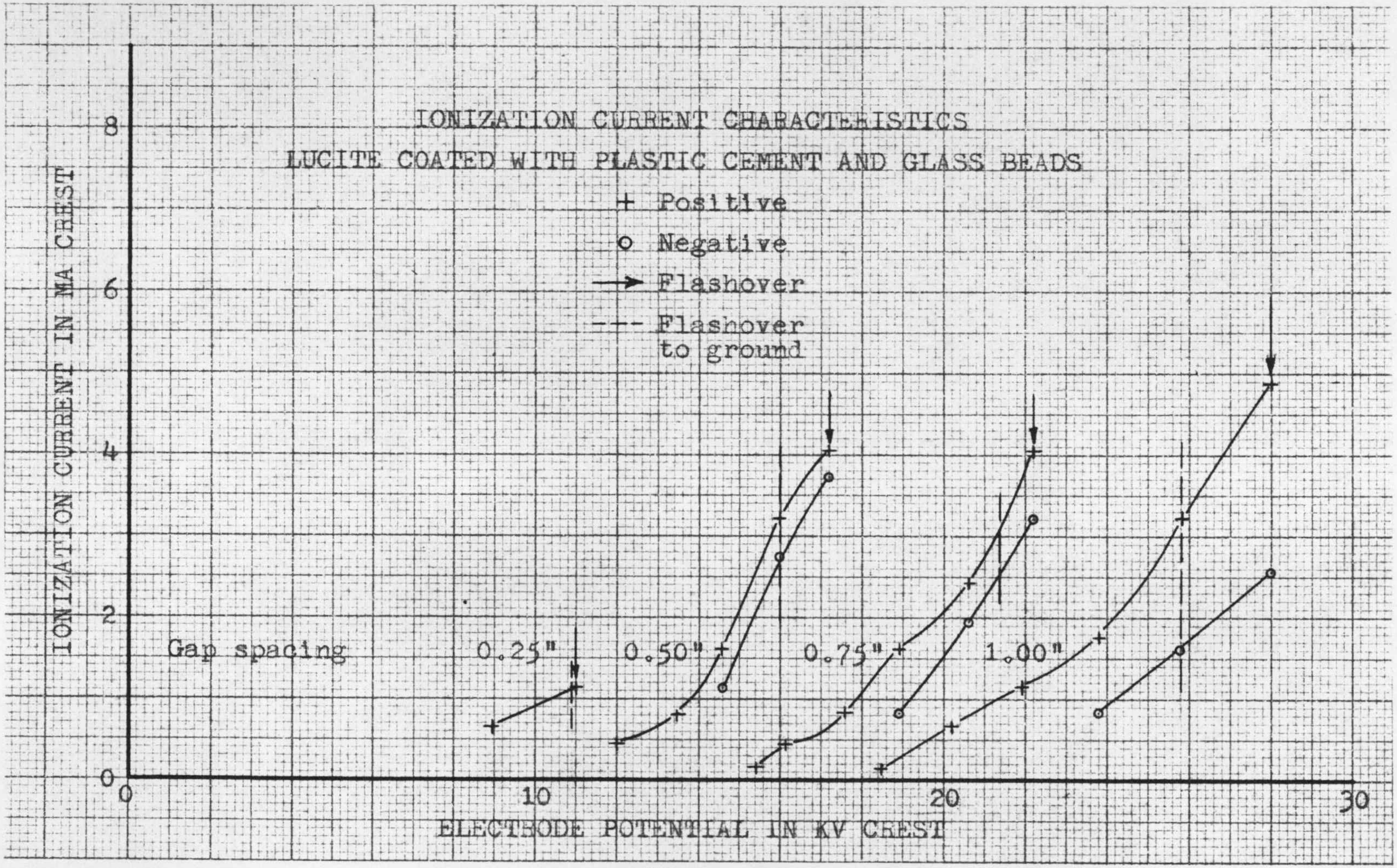
IONIZATION CURRENT CHARACTERISTICS
LUCITE COATED WITH PLASTIC CEMENT AND GLASS BEADS
+ Positive
o Negative
Flashover
Flashover to ground
Gap spacing
0.25"
0.50"
0.75"
1.00"
IONIZATION CURRENT IN MA CREST
ELECTRODE POTENTIAL IN KV CREST
0
2
4
6
8
10
20
30

Figure 27

are two curves for each spacing, one marked positive and one negative. The positive curves are for the crest values of ionization current that occur during the positive half of the 60-cycle exciting voltage, and the negative curves are for the crest values of ionization current that occur during the negative half of the 60-cycle exciting voltage, using the ungrounded exploratory electrode as a point of reference as shown in Figure 5. Vertical arrows are placed on the curves at the flashover voltage as determined for the specimen with the electrodes connected in the bridge circuit as shown in Figure 5. A dashed line shows the flashover voltage for the specimen with the lower exploratory electrode directly connected to ground and the right side of the bridge disconnected. This change produces the conventional flashover circuit described later and shown in Figure 32. When the lower exploratory electrode is directly connected to the ground, the flashover of the specimen occurs at a lower voltage than when the electrode is connected in the bridge circuit, because in the bridge circuit the electrode has a resistance of 0.573 megohms between it and ground.

Isomica With Various Surface Treatments

The ionization current characteristics for the isomica series is shown in Figures 10 to 18. The ionization currents are given at onset and flashover for all the specimens in Table II. The isomica series includes the untreated specimen and those coated with four different suspension media with and without glass beads. The suspension media are used to hold the small glass beads on the surface of the specimen. The glass beads vary in size and are less than 0.002 of an inch in diameter. Flame tests show them to be made of sodium glass. They are a product of the Minnesota Mining and Manufacturing Company and are sold as pavement marker beads. In the isomica series the specimen coated with Dolph's Synthite exhibited the strongest surface ionization. The untreated specimen and those coated with the suspension media all exhibited strong surface ionization of the same order of magnitude. Over half the curves in the group without the glass beads showed a tendency to rise, starting with the curvature concave downward, then reversing to concave upward. This tendency was found for only two of the curves in the glass bead-coated group of this series. The variation of the ionization current with spacing is not a linear relation because the field between the electrodes becomes less uniform as the separation is increased. The isomica specimen coated with Scotch Cast and glass beads showed the lowest surface ionization, and that coated with Dri-Film 88 and glass beads was very nearly as good. The ratios for both the positive and negative

TABLE II

IONIZATION DATA FOR VARIOUS SPECIMENS AT DIFFERENT ELECTRODE SPACINGS

Specimen	Ionization Voltage and Current at Flashover																							
Electrode Spacing in Inches	0.25						0.50						0.75						1.00					
	At Onset			At Flashover			At Onset			At Flashover			At Onset			At Flashover			At Onset			At Flashover		
	KV	MA		KV	MA		KV	MA		KV	MA		KV	MA		KV	MA		KV	MA		KV	MA	
		+	−		+	−		+	−		+	−		+	−		+	−		+	−		+	−
Isomica	5.68	0.09					10.0	0.08					13.9	0.25					17.1	0.37				
	6.28		0.09	9.83	2.84	2.84	10.6		0.68	18.0	5.32	5.32	14.4		0.50	22.8	6.17	5.65	19.1		1.15	30.5	7.14	6.32
Isomica & Dolph's Synthite							9.70	0.17					14.1	0.40					16.0	0.17				
	6.18	3.60	0.14	9.83	3.44	3.44	10.3		0.17	18.9	7.48	7.48	15.4		0.80	23.6	7.85	7.83	19.3		1.14	27.9	5.88	5.73
Isom. & D's. Syn. & Gl. Bds.	6.65	0.14					10.0	0.14																
	7.65		0.11	10.8	3.44	2.52	11.2		0.11	16.4	2.09	2.09	18.3	0.29	0.14	21.4	2.68	1.17	22.9	0.29	0.14	27.0	3.21	0.29
Isomica & Scotch Cast	5.77	0.12					9.49	0.12					14.3	0.12					17.0	0.25				
	6.02		0.12	9.66	2.65	2.65	9.68		0.12	17.2	5.18	5.18	14.7		0.25	23.4	7.01	5.73	18.6		0.12	27.8	6.31	6.31
Isom. & Sc. Cast & Gl. Bds.	6.17	0.04																						
	7.12		0.14	9.86	0.97	0.97	12.2	0.08	0.08	16.0	0.85	0.77	17.3	0.16	0.11	20.8	0.97	0.16	23.8	0.23	0.16	26.3	0.77	0.19
Isomica & Silicone Varnish	5.87	0.20					9.57	0.28					13.8	0.10					17.1	0.10				
	6.07		0.10	9.85	1.92	1.84	10.5		0.10	17.8	4.46	4.46	14.9		0.10	22.8	5.04	4.46	19.0		0.96	25.4	4.36	3.72
Isom. & Sil. Var. & Gl. Bds.	6.22	0.06					7.83	0.06					12.4	0.06										
	8.26		0.16	9.46	0.97	0.27	11.8		0.13	15.0	1.62	1.62	13.6		0.06	21.1	2.35	2.35	19.6	0.38	0.06	26.3	3.11	2.66
Isomica & Dri-Film 88													12.7	0.10					13.1	0.10				
	6.38	0.28	0.20	9.87	2.32	2.22	10.1	0.58	0.58	17.0	4.14	4.36	14.2		0.40	21.5	5.48	5.04	18.3		0.10	25.5	4.14	3.92
Isomica & Dri-Film 88 & Glass Beads	7.72	0.08	0.08	9.80	0.58	0.97	12.6	0.04	0.04	15.4	0.97	0.97	18.9	0.46	0.23	20.6	1.25	1.21	21.4	0.11	0.04	26.3	1.79	1.25
Black Bakelite													13.0	0.34					16.1	0.34				
	6.65	0.67	0.34	9.33	2.29	1.95	10.1	0.54	0.54	16.8	4.24	5.19	14.8		0.34	21.5	4.24	4.58	18.6		0.34	25.5	4.58	5.19
Blk. Bak. & Dolph's Synthite & Glass Beads	6.90	0.11	0.04	9.60	1.37	1.17	12.2	0.06	0.04	15.3	1.17	1.37	17.8	0.11	0.06	20.7	1.67	1.05	21.5	0.04	0.04	25.7	1.75	0.85
Blk. Bak. & Scotch Cast & Glass Beads	6.30	0.04	0.04	9.20	0.77	0.66	12.1	0.18	0.06	16.8	1.37	0.77	18.9	0.19	0.06	21.1	0.95	0.16	21.6	0.10	0.06	27.4	0.58	0.58
Blk. Bak. & Silicone Varnish & Glass Beads	7.16	0.06	0.02	9.10	1.33	1.14	11.2	0.04	0.02	15.4	1.46	0.70	15.7	0.11	0.02	21.1	1.46	2.07	19.8	0.23	0.04	25.1	1.80	0.66
Blk. Bak. & Dri-Film 88 & G.B.	7.10	0.08																						
	7.70		0.16	9.70	1.17	1.05	10.6	0.04	0.04	16.1	1.30	1.25	17.9	0.16	0.10	21.0	0.97	0.89	21.5	0.08	0.04	26.1	1.17	0.77
Lucite							13.0	1.62											16.2	0.34				
	no on set			10.3	2.42	0.00	17.1		4.85	18.5	9.84	6.20	14.1	0.67	0.00	25.0	12.2	0.00	25.2		0.94	29.7	9.84	5.19
Luc. & D's. Syn. & Gl. Bds.	9.00	0.40					12.1	0.40					14.8	0.24					17.4	0.20				
	9.45		0.40	9.79	1.74	0.96	15.6		1.44	17.8	4.26	4.26	19.8		0.10	22.8	3.94	3.04	22.7		0.10	28.8	5.60	3.64
Lucite & Sc. Cast & Gl. Bds.							12.0	0.28					15.5	0.28					17.6	0.10				
	8.85	0.48	0.20	9.93	2.12	1.64	13.8		0.28	16.5	2.22	1.84	18.3		0.10	21.3	3.12	1.64	23.3		0.28	25.2	2.92	1.16
Lucite & Plastic Cement & G.B.							12.0	0.47					15.4	0.18					18.5	0.17				
	8.87	0.67	0.00	11.0	1.14	0.00	14.6		1.14	17.2	4.05	3.71	18.9		0.80	22.2	4.05	3.21	23.8		0.80	28.0	4.89	2.57

ionization current values at flashover for the untreated isomica to that for the isomica coated with Scotch Cast and glass beads at the different electrode spacings are as follows:-

Spacing	0.25"		0.50"		0.75"		1.00"	
	+	-	+	-	+	-	+	-
Ratio	2.94	2.94	6.25	6.90	6.37	30.5	9.26	33.3

This proves that the glass bead-coated surfaces show a marked improvement over the untreated specimen in the reduction of the surface ionization.

Black Bakelite With Various Surface Treatments

Black bakelite shows strong surface ionization, but somewhat less than does isomica. In the bakelite series the test for the specimens coated with only the suspension media were not made since the data obtained from the isomica series showed that the suspension media alone did not produce any material improvement over the uncoated base material. The characteristics for the bakelite series are shown in Figures 19 to 23 and in Table II. Black bakelite showed an unusual characteristic in that the negative values of the ionization current were larger than the positive values for three of the spacings. The 0.25 inch spacing shows the usual behavior where the positive values of ionization current are larger at all times than the negative. For the 0.50 inch spacing the two currents start at about the same value after which the negative current values become larger and continue larger than the positive values. For the 0.75 and 1.00 inch spacings the curves start in the normal manner and then cross over at about the midpoint with the negative current values becoming larger for the latter portion of the curves. This behavior was checked a number of times and was found to be reproducible. The glass bead-coated bakelite group gave low values of ionization current comparable with those of the isomica group. The black bakelite specimen showing the lowest surface ionization was that coated with Scotch Cast and glass beads and the one coated with Dri-Film 88 and glass beads was very nearly as good. The ionization current ratios at flash-over for untreated black bakelite to that coated with Scotch Cast and glass beads are as follows:-

Spacing	0.25"		0.50"		0.75"		1.00"	
	+	-	+	-	+	-	+	-
Ratio	2.98	2.95	3.10	6.75	4.46	28.6	7.93	8.93

Here, as in the previous series, the specimen coated with Scotch Cast and glass beads showed the lowest surface ionization.

Lucite With Various Surface Treatments

The surface behavior of untreated lucite was very different from that of any other specimen. The untreated specimen gave the highest crest values of ionization current as shown in Figures 24a and 24b. These two figures are from the same data plotted to different scales. The scale selected as a standard for all other specimens and used in Figure 24a does not include the higher values given by lucite; therefore, a second plot was made with a change in scale to include the full range of experimental data as shown in Figure 24b. While lucite gave the highest crest ionization current, in contrast, it gave the lowest effective value of ionization current. This observation, a very striking one even though only qualitative, is based upon the consistant observation that the ionization current pulses on the untreated lucite surfaces were relatively very high and infrequent during each half cycle of the applied 60-cycle voltage. The foregoing observation applied to both the positive and negative half cycle. This behavior of lucite is due to its very high surface resistance as compared to that of the other specimens. All the coatings used on the lucite increased the surface ionization current over that for the untreated material. Untreated lucite also showed no negative ionization current pulses for some of the electrode spacings. The 0.25 inch spacing showed no positive or negative ionization prior to flashover. The only event for this spacing was flashover with no apparent prior ionization. For the 0.50 inch spacing positive ionization occured prior to flashover, but the negative pulses of ionization appeared only at flashover. The 0.75 inch spacing gave the full range of positive ionization, but no negative ionization at any time. The 1.00 inch spacing showed the usual positive ionization, but the negative ionization appeared for only a part of the range before flashover took place. Only one other specimen, lucite coated with plastic cement and glass beads, gave no negative ionization. In this case, it occured at the 0.25 inch spacing and is shown in Figure 27. The other two specimens of the series behaved in a manner which was comparable to that of other specimens and are shown in Figures 25 and 26. Again as in the two previous series, the specimen coated with Scotch Cast and glass beads gave the lowest values of ionization current. The ionization ratios at flashover for the untreated specimen to that of the glass beaded one are computed from the data in Table II and are shown as follows:-

Spacing	0.25"		0.50"		0.75"		1.00"	
	+	-	+	-	+	-	+	-
Ratio	1.14	----	4.42	3.37	3.91	----	3.91	4.48

These ratios again demonstrate the effectiveness of the glass-beaded surface in reducing surface ionization.

Results Of Ionization Current Measurements

Some characteristics are common to nearly all of the specimens. They are the following:-

1. The onset of positive ionization occurs before the onset of negative ionization.
2. The positive ionization pulses are larger in amplitude than the negative pulses.
3. The ionization current curves show a common trend. For the surfaces without glass beads, the curves rise abruptly and go through a change in curvature. For the surfaces with glass beads, the curves rise gradually and remain concave upward.
4. The specimens showed a short time-hysteresis effect due to ionic charges trapped on the surface. The time needed to adjust the equipment in order to take readings was enough in all cases to enable these surface charges to dissipate and permit the specimen to come to equilibrium for the applied voltage at which the reading was taken.

There are a few characteristics to which no exceptions were observed. They are as follows:-

1. The onset of ionization for the glass-beaded specimens is more gradual than for those without beads.
2. The onset of ionization in all cases is abrupt. The pulses appear to burst out with a definite amplitude.
3. The glass-beaded surfaces gave a much lower surface ionization than the untreated surfaces.

In most instances the glass-beaded surfaces showed ionization at a very low level for a considerable voltage range before the ionization would show an appreciable rate of rise as the 60-cycle voltage was increased. This condition was due to ionization taking place beneath the surface and around the edges of the electrodes. The glass beads on which the electrodes rest have air spaces between them in which the air becomes overstressed and gives rise to this low level ionization.

When the glass beads are present on the surface of the insulation there is a marked decrease in the visible corona discharge between the electrodes and also in the related audible noise right up to the point of flashover. The visible corona is a very narrow line around the edges of the electrodes. In other words, the glass beads act as an ionization suppressor.

IONIZATION CHARACTERISTICS OF SURFACES AT VARIOUS GAS PRESSURES

The Vacuum-Pressure System

The combined vacuum and pressure system was designed and constructed by the author. A schematic diagram of the vacuum system is given in Figure 28, and a general view of the high-voltage bridge with the vacuum-pressure cylinder in the background is shown in Figure 29. The specimen cylinder was made large enough so that the exploratory electrodes and the specimen could be placed inside and not be disturbed electrically by the proximity of the cylinder wall, base plate and top plate. This arrangement was very important in achieving a balance of the high-voltage bridge. The base plate was of cold rolled steel and was nineteen inches in diameter. The top plate was textolite of the same dimensions. Insulating material was used for the top plate to permit entry of the high voltage leads with a minimum of capacity between the leads. The glass cylinder was 12 inches in diameter and 18 inches long with ends finished by hand on a steel plate using number 80 carborundum grit. Eight vertical cold rolled steel rods were used to hold the end plates against the cylinder. These rods were placed near the outer edge of the end plates to minimize the

VACUUM-PRESSURE SYSTEM

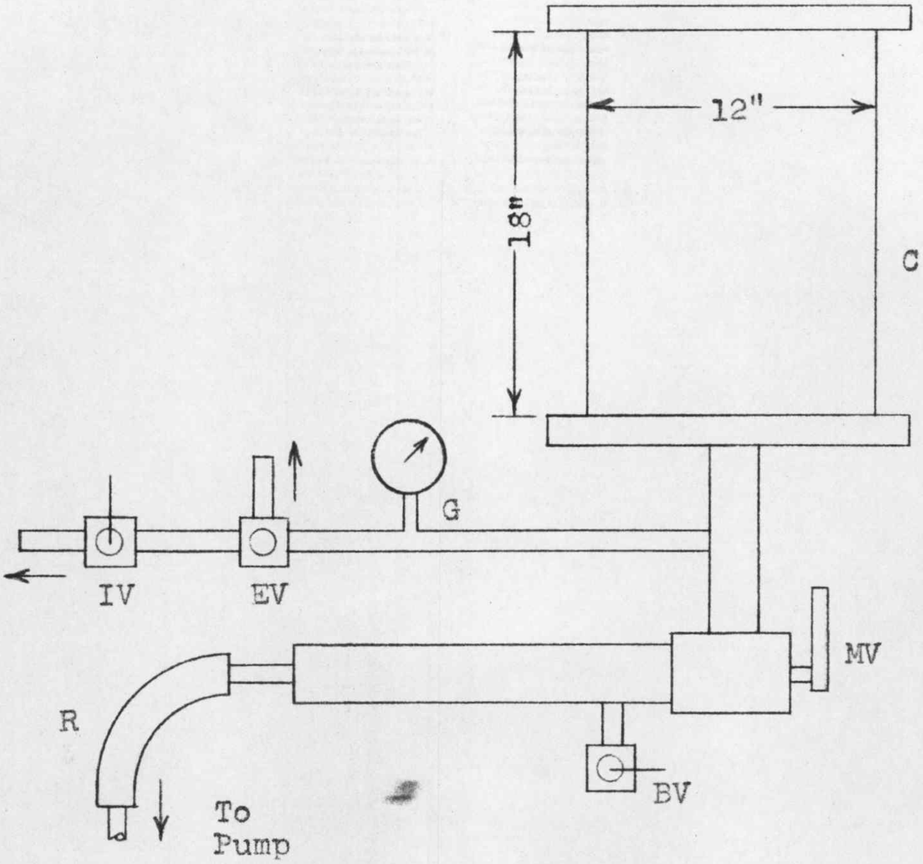

IV Intake valve to admit gas from tank

EV Exhaust valve for the system

G Vacuum and pressure gauge

C Specimen test cylinder

MV Main valve to pump

BV Bleeder valve for pump

R Rubber pressure tubing serves as electrical and vibration insulator for the system

Figure 28

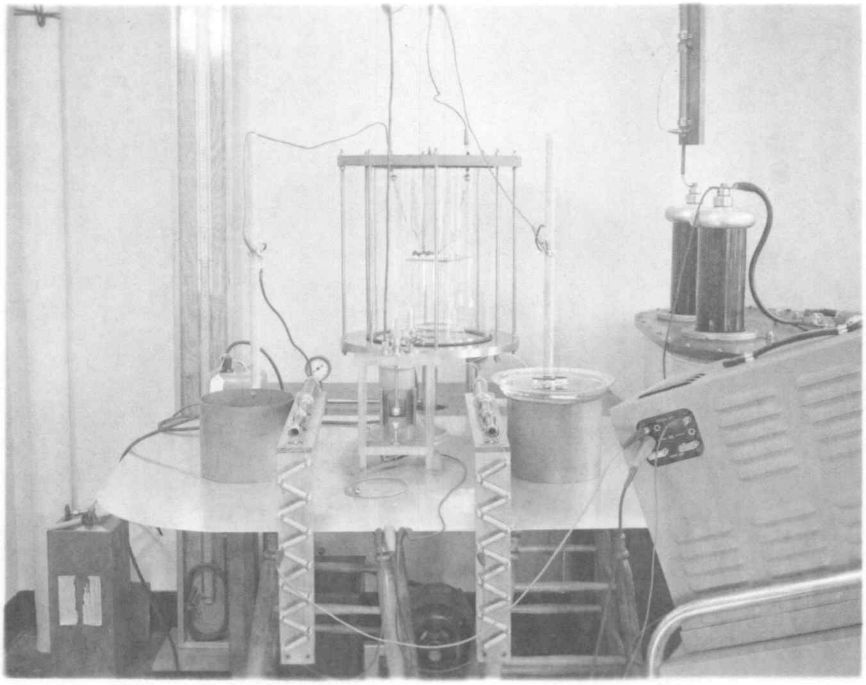

Figure 29.
Equipment for determination of ionization characteristics in gases at various pressures.

capacitance effect. The valves for the system are of the taper plug type, and were individually ground and fitted. They are lubricated with a silicone compound which has a vapor pressure of 10^{-6} mm of mercury. The function of the valves is explained in Figure 28. A mercury manometer was built to calibrate the Bourdon-type vacuum and pressure gauge. Corrections for barometric pressure and temperature were taken into account for the calibration. The manometer is shown at the left and rear of Figure 29. A length of rubber pressure tubing connects the system to the mechanical vacuum pump. The tubing serves as an electrical insulator and as a vibration insulator for the specimen cylinder. The metal parts of the cylinder must remain electrically insulated so that the high voltage bridge may be balanced. The entire system was subjected to a hydrostatic test at a gauge pressure of 35 pounds per square inch. For the safety of the operator during the tests, a sheet of 3/4-inch plywood was placed between the operator and the specimen cylinder.

Results Of Ionization Current Measurements At Various Gas Pressures

Two series of tests were made, one in air at seven different pressures and one in sulfur hexafluoride at four different pressures. Isomica coated with Dri-Film 88 and glass beads was used as the test specimen in both cases. Isomica was chosen as a base material because it is used in the construction of high-voltage equipment. Dri-Film 88 was used as the suspension medium since it contains some silicone compounds which show a minimum tendency to carbonize at flashover. The ionization curves for the two series were plotted to the same scale for the abscissa, but to different scales for the ordinates. The specimen in air gave ionization currents in the milliampere range while in sulfur hexafluoride the range was in microamperes. This is shown in Figures 30 and 31. None of the curves is for the full range of ionization current, since it was necessary to avoid flashover because the gas charge would be lost if the system had to be opened to change the specimen. Data taken from other workers were used to calculate the flashover value at each of the pressures at which tests were run (8, pp. 126-133 and 2, pp. 580-584). All tests were made at a gap spacing of 0.50 inch.

The tests in air show a greater increase in the rate of ionization for pressures below one atmosphere, and a lower increase in the rate of ionization for pressures above one atmosphere as shown in Figure 30. This decrease in rate with increase of pressure is due to the decrease of the mean free path, and because the normal process of ionization by collision has been altered. For pressures of 1.380 atmospheres and above, only negative

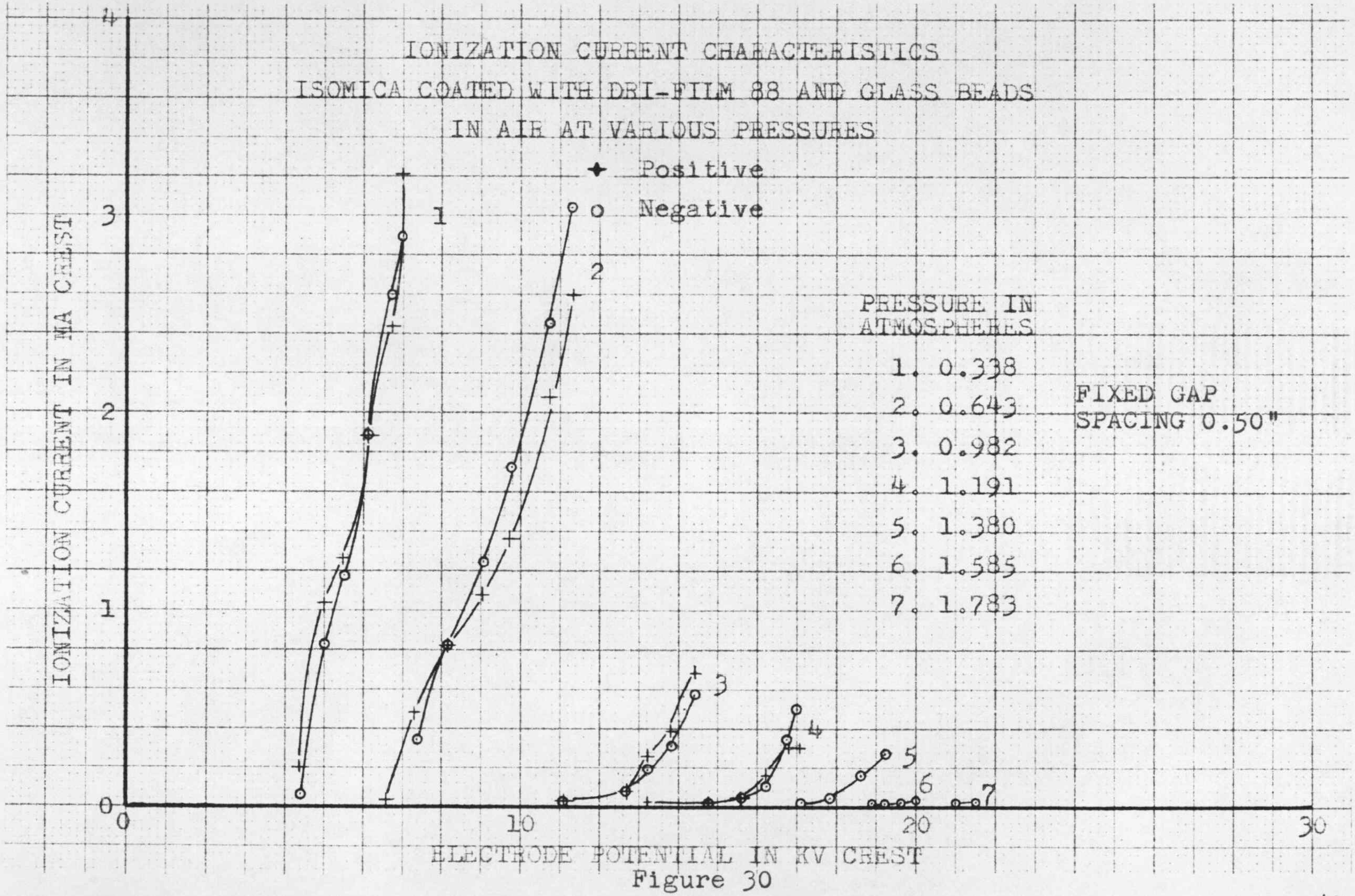
IONIZATION CURRENT CHARACTERISTICS
ISOMICA COATED WITH DRI-FILM 88 AND GLASS BEADS
IN AIR AT VARIOUS PRESSURES
+ Positive
o Negative
PRESSURE IN ATMOSPHERES
1. 0.338
2. 0.643
3. 0.982
4. 1.191
5. 1.380
6. 1.585
7. 1.783
FIXED GAP SPACING 0.50"
IONIZATION CURRENT IN MA CREST
ELECTRODE POTENTIAL IN KV CREST
0
1
2
3
4
10
20
30

Figure 30

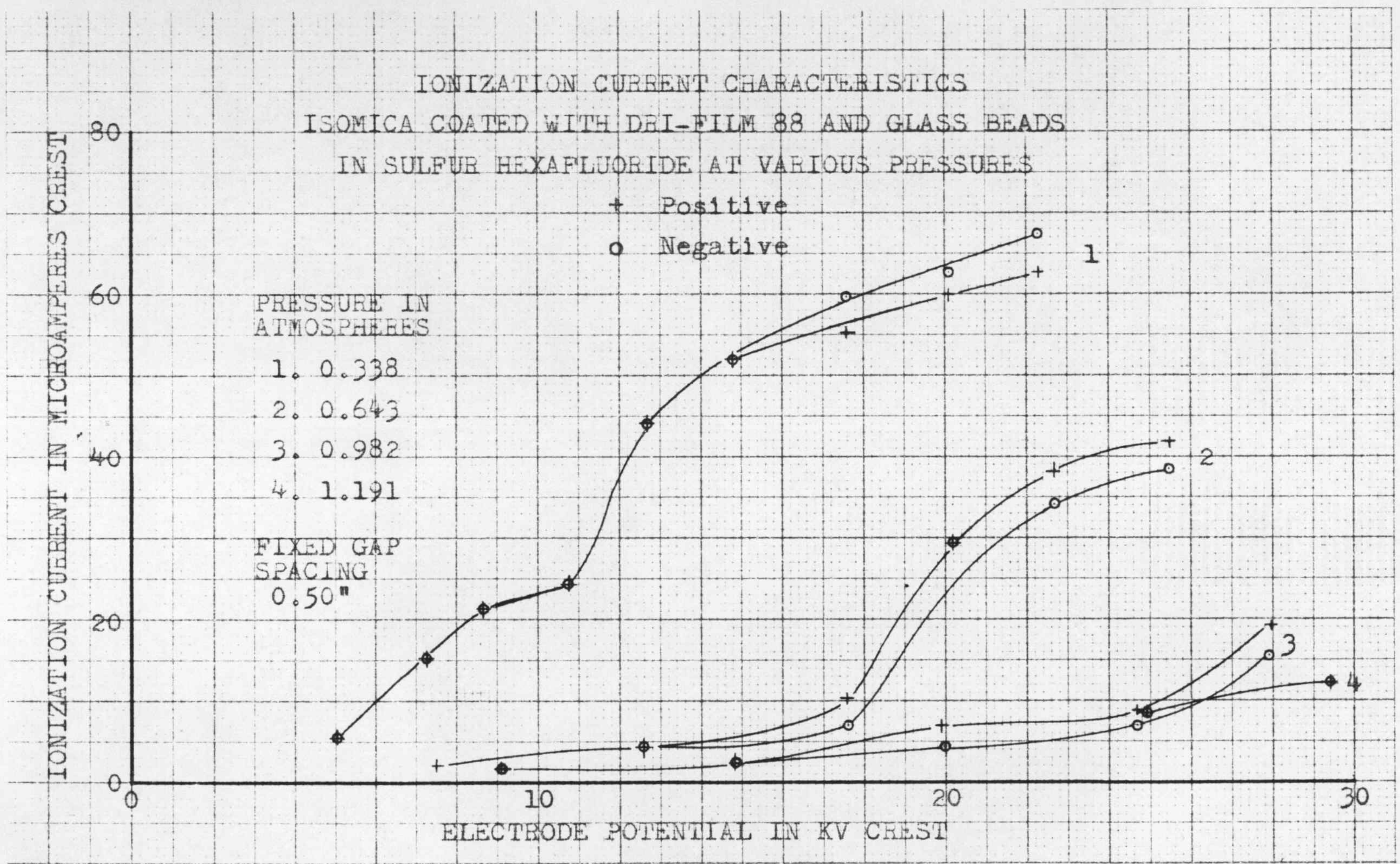
IONIZATION CURRENT CHARACTERISTICS
ISOMICA COATED WITH DRI-FILM 88 AND GLASS BEADS
IN SULFUR HEXAFLUORIDE AT VARIOUS PRESSURES
+ Positive
o Negative
PRESSURE IN ATMOSPHERES
1. 0.338
2. 0.643
3. 0.982
4. 1.191
FIXED GAP SPACING 0.50"
IONIZATION CURRENT IN MICROAMPERES CREST
ELECTRODE POTENTIAL IN KV CREST
0
10
20
30
40
60
80
1
2
3
4

Figure 31

ionization takes place because the mobility of the electrons relative to that of the positive ions has been changed.

The limited supply of sulfur hexafluoride permitted operation only at the four pressures shown in Figure 31. Both positive and negative ionization took place in these tests for the limited pressure range available. The most striking observation is the low level of ionization in sulfur hexafluoride, which is borne out by the total absence of visible ionization at any time. The structure of sulfur hexafluoride is such that it behaves as an electron trap which accounts for the extremely low level of surface ionization. At higher pressures, the gas would have a greater dielectric strength than the specimen tested.

Some of the properties of sulfur hexafluoride are as follows:

Empirical formula SF_6

Structure:

All six fluorine atoms are at the corners of a regular octahedron, with the S atom at its center. The F atoms are at distances of 1.58 Angstrom units from the S atom. These bonds, having both ionic and covalent properties, are mainly covalent.

Molecular weight: 146.06

Toxicity:

Sulfur hexafluoride has been described as a physiologically inert gas. However, in the presence of corona, arc, or spark discharge, it is slowly decomposed to the lower fluorides of sulfur which are hydrolyzable and toxic.

FLASHOVER CHARACTERISTICS OF SURFACES AT ATMOSPHERIC PRESSURE

Determination Of Flashover Characteristics

The circuit for the determination of the flashover characteristics is shown in Figure 32. Since this section of the work was the beginning of the project, the flashover tests were run as an independent series, although normally a flashover test would be made at the end of an ionization run with the aid of a circuit change that alters the high voltage bridge to that of the flashover circuit in Figure 32. No ultra violet source was available to irradiate the sphere gap for this part of the work. The flashover voltage was determined for five electrode spacings for each specimen. The spacings were 0.25, 0.375, 0.50, 0.625, and 0.75 of an inch. Untreated isomica and untreated black bakelite were tested over a range of spacings from 0.062 to 1.00 inch. These spacings were adjusted on the insulation test specimen by means of brass gauge blocks carefully made to the required width.

Flashover tests on 25 different specimens with different surface conditions were completed. Nine of these were with isomica base material, ten with a black bakelite base and six with lucite as the base material. In each case the clean base material with no treatment was tested followed by tests on the base material with a

CIRCUIT
FOR
FLASHOVER CHARACTERISTICS

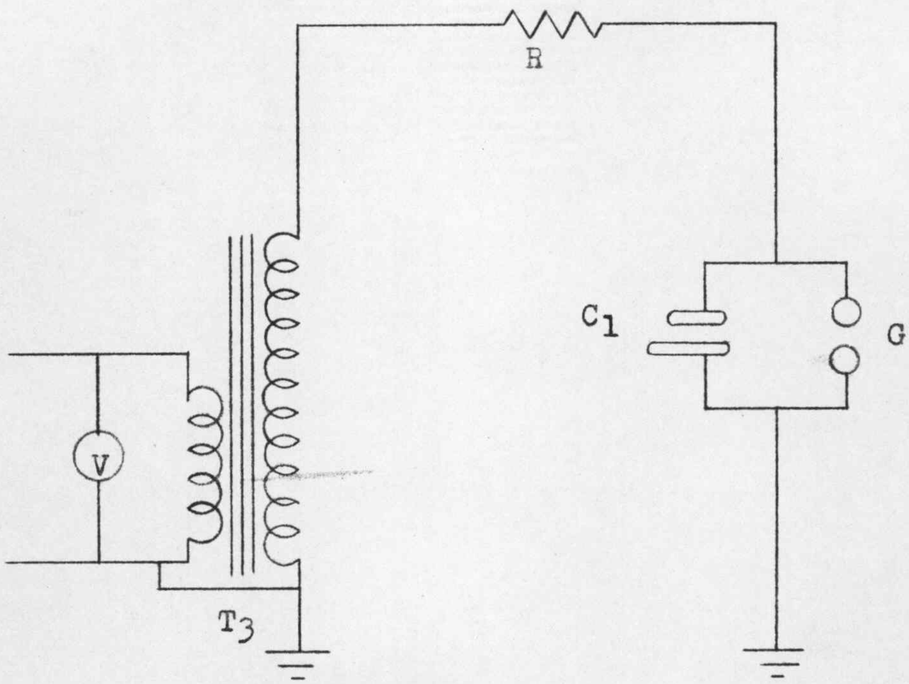

V A-C Voltmeter
Weston Model 155 No. 42071 0-75-150
G.E. Type P-3 No. 3320351 0-15-30

T_3 100 KV Transformer OSC No. 3566

R 0.270 Megohm Current Limiting Resistor
Carborundum Type

C_1 Exploratory Electrodes 3.5 to 15 mmf

G 2.0 cm Sphere Gap

Figure 32

coating of the suspension medium, and finally with the glass beads applied to the suspension medium. To insure reliable flashover results each specimen was carefully cleaned, dried in the low temperature oven and then kept in the desiccator at room temperature until tested. (This procedure is described above in the section on conditioning of specimens.)

To further increase the reliability of the flashover results at least five flashovers were made at each gap spacing for each material and the electrodes were moved to a new location for each flashover so that surface damage due to a previous flashover would not influence the later values. The average of successive flashovers at a particular spacing on a given specimen was taken as the flashover voltage when corrected for air density. Standard air density is defined as a barometric pressure of 760 mm of mercury and a temperature of 25 degrees centigrade.

Results Of Flashover Tests

The flashover characteristics are plotted for each specimen with the gap spacing as abscissa and the flashover kv rms as ordinate and are shown in Figures 33 to 56. The kv rms-distance ratio curves were obtained from the flashover characteristics by dividing the ordinate of

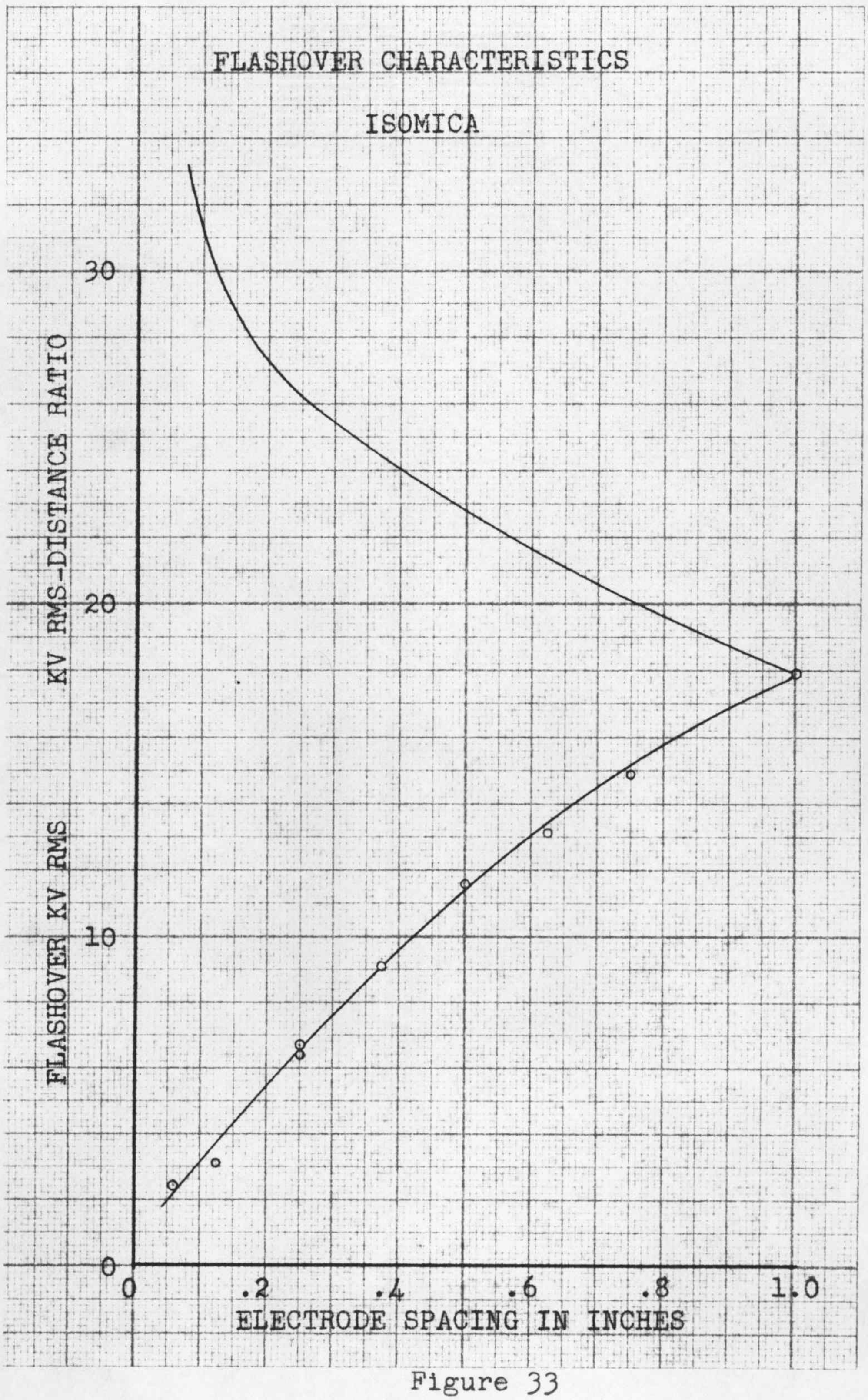
FLASHOVER CHARACTERISTICS
ISOMICA
KV RMS-DISTANCE RATIO
FLASHOVER KV RMS
30
20
10
0
0
.2
.4
.6
.8
1.0
ELECTRODE SPACING IN INCHES

Figure 33

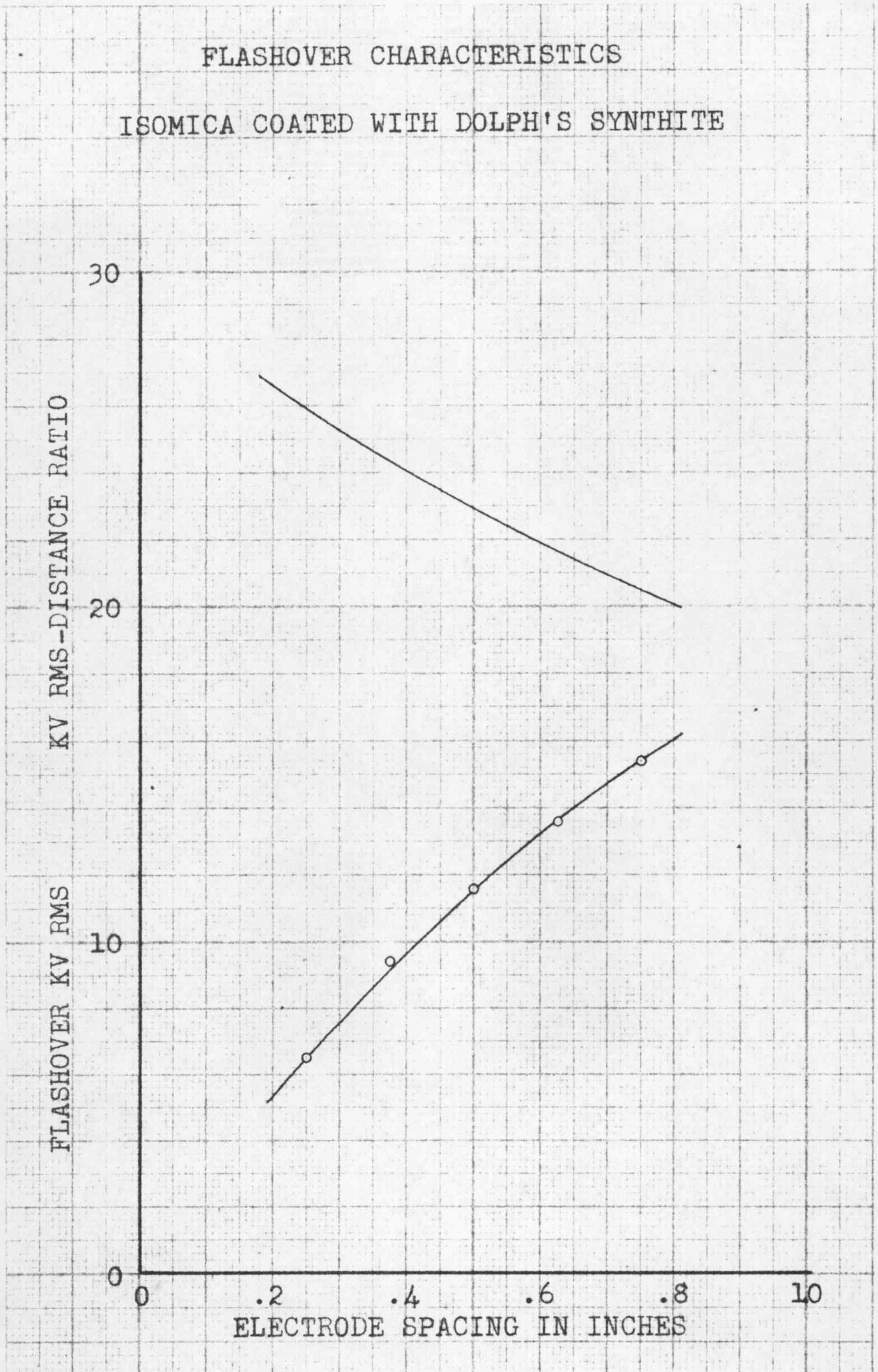
FLASHOVER CHARACTERISTICS
ISOMICA COATED WITH DOLPH'S SYNTHITE
KV RMS-DISTANCE RATIO
FLASHOVER KV RMS
30
20
10
0
0
.2
.4
.6
.8
10
ELECTRODE SPACING IN INCHES

Figure 34

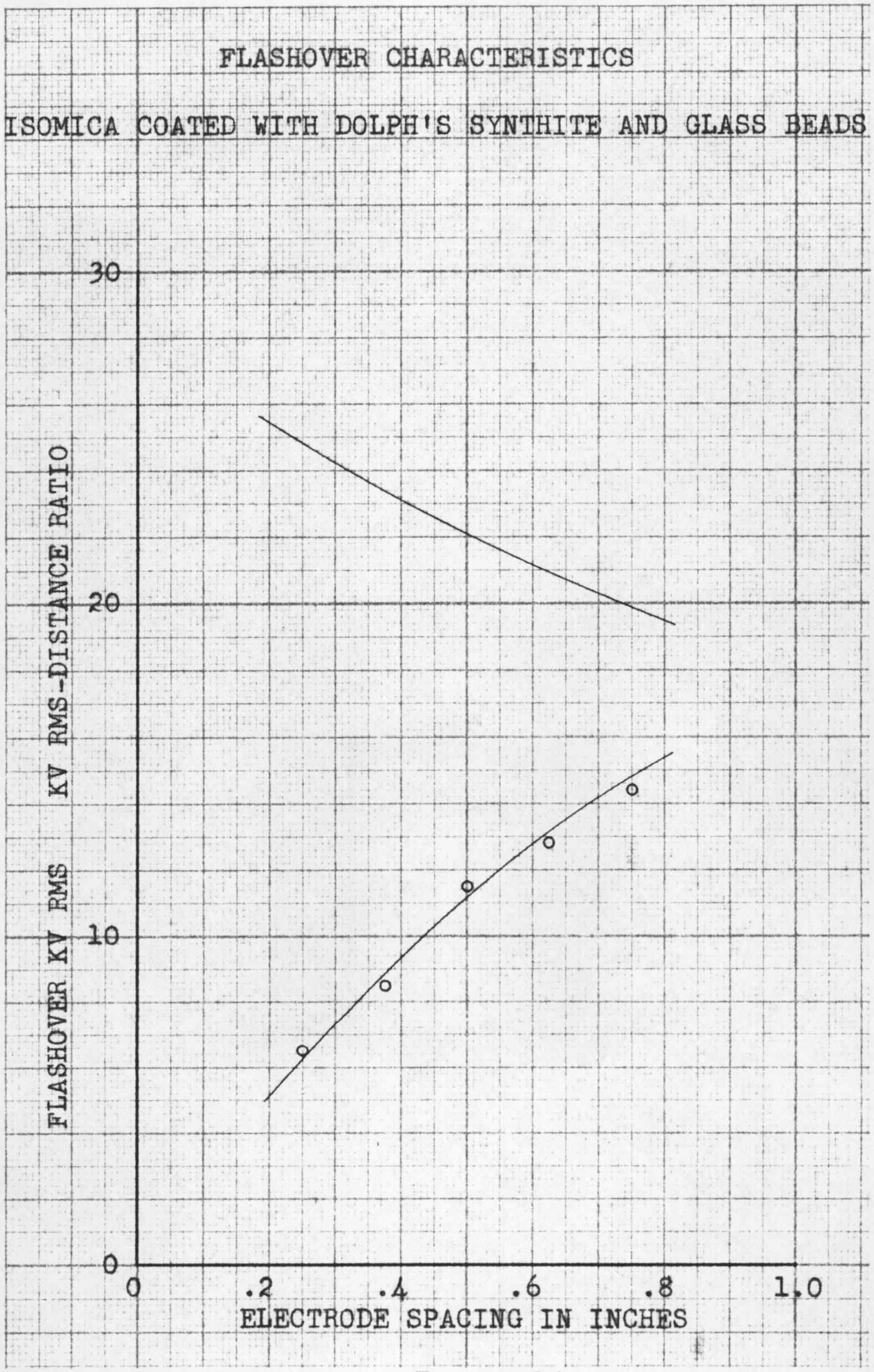
FLASHOVER CHARACTERISTICS
ISOMICA COATED WITH DOLPH'S SYNTHITE AND GLASS BEADS
FLASHOVER KV RMS   KV RMS-DISTANCE RATIO
30
20
10
0
0
.2
.4
.6
.8
1.0
ELECTRODE SPACING IN INCHES

Figure 35

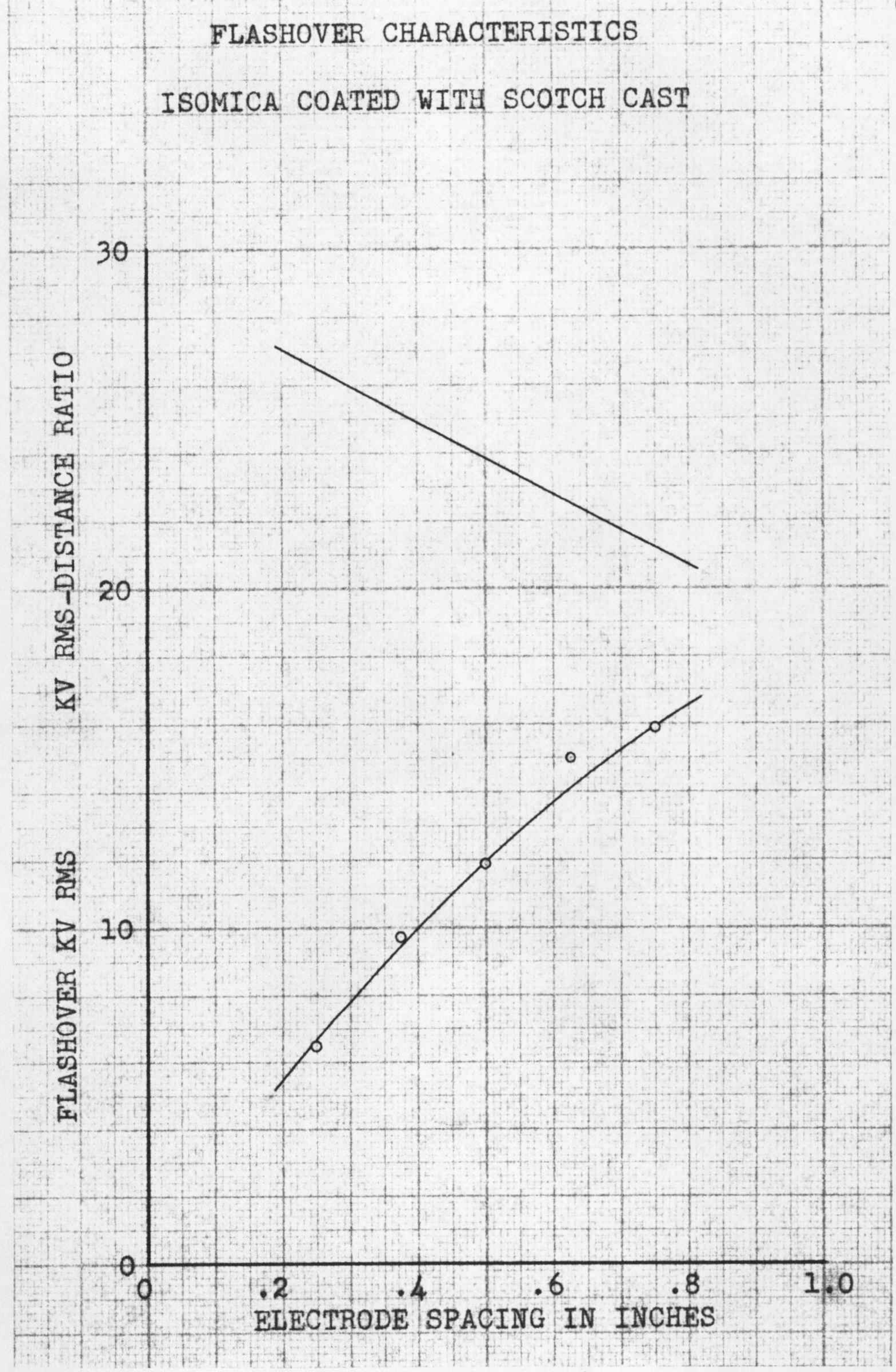
FLASHOVER CHARACTERISTICS
ISOMICA COATED WITH SCOTCH CAST
30
20
10
0
KV RMS-DISTANCE RATIO
FLASHOVER KV RMS
0
.2
.4
.6
.8
1.0
ELECTRODE SPACING IN INCHES

Figure 36

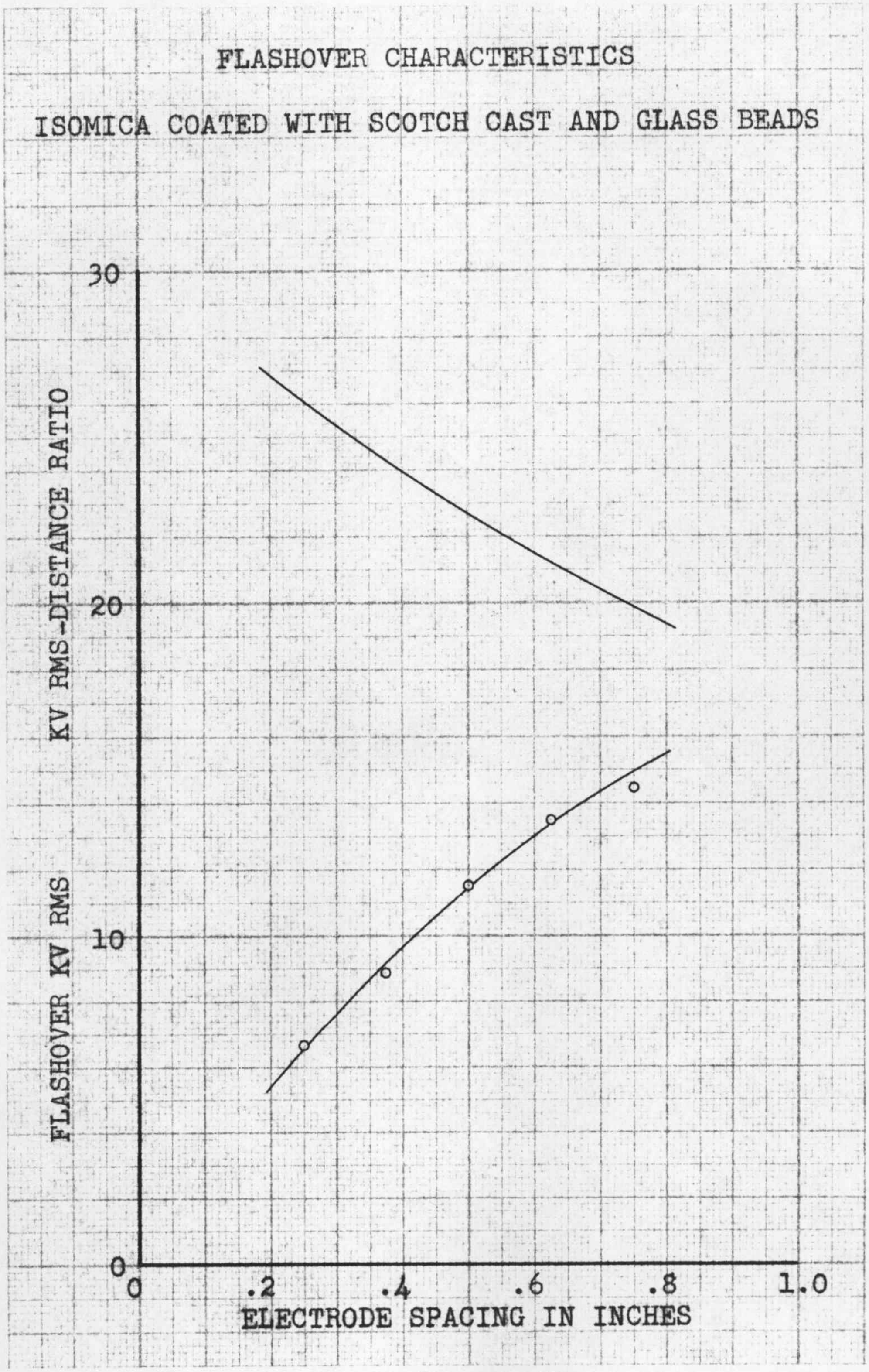
FLASHOVER CHARACTERISTICS
ISOMICA COATED WITH SCOTCH CAST AND GLASS BEADS
FLASHOVER KV RMS KV RMS-DISTANCE RATIO
30
20
10
0
0
.2
.4
.6
.8
1.0
ELECTRODE SPACING IN INCHES

Figure 37

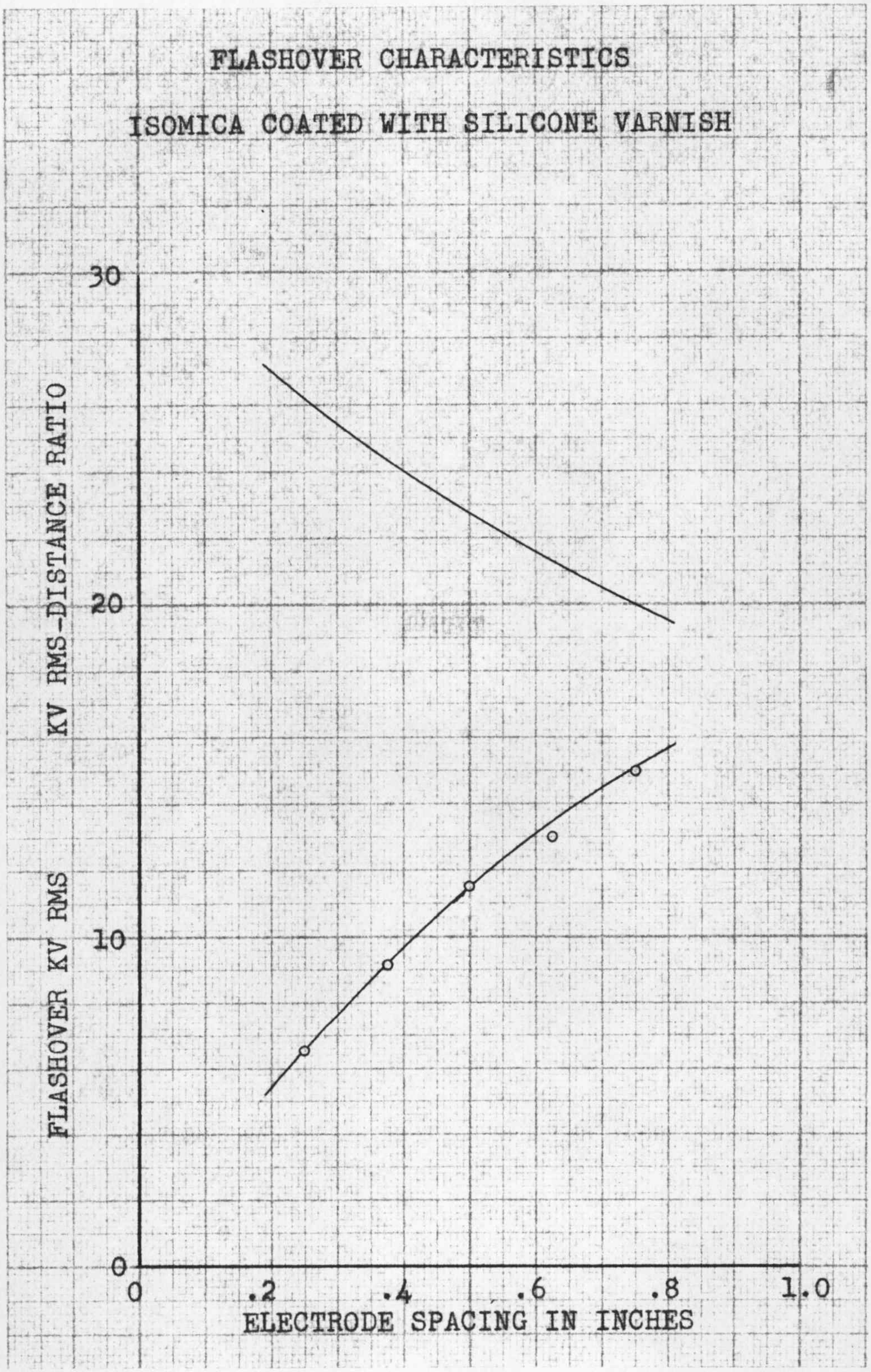
FLASHOVER CHARACTERISTICS
ISOMICA COATED WITH SILICONE VARNISH
KV RMS-DISTANCE RATIO
FLASHOVER KV RMS
30
20
10
0
0
.2
.4
.6
.8
1.0
ELECTRODE SPACING IN INCHES

Figure 38

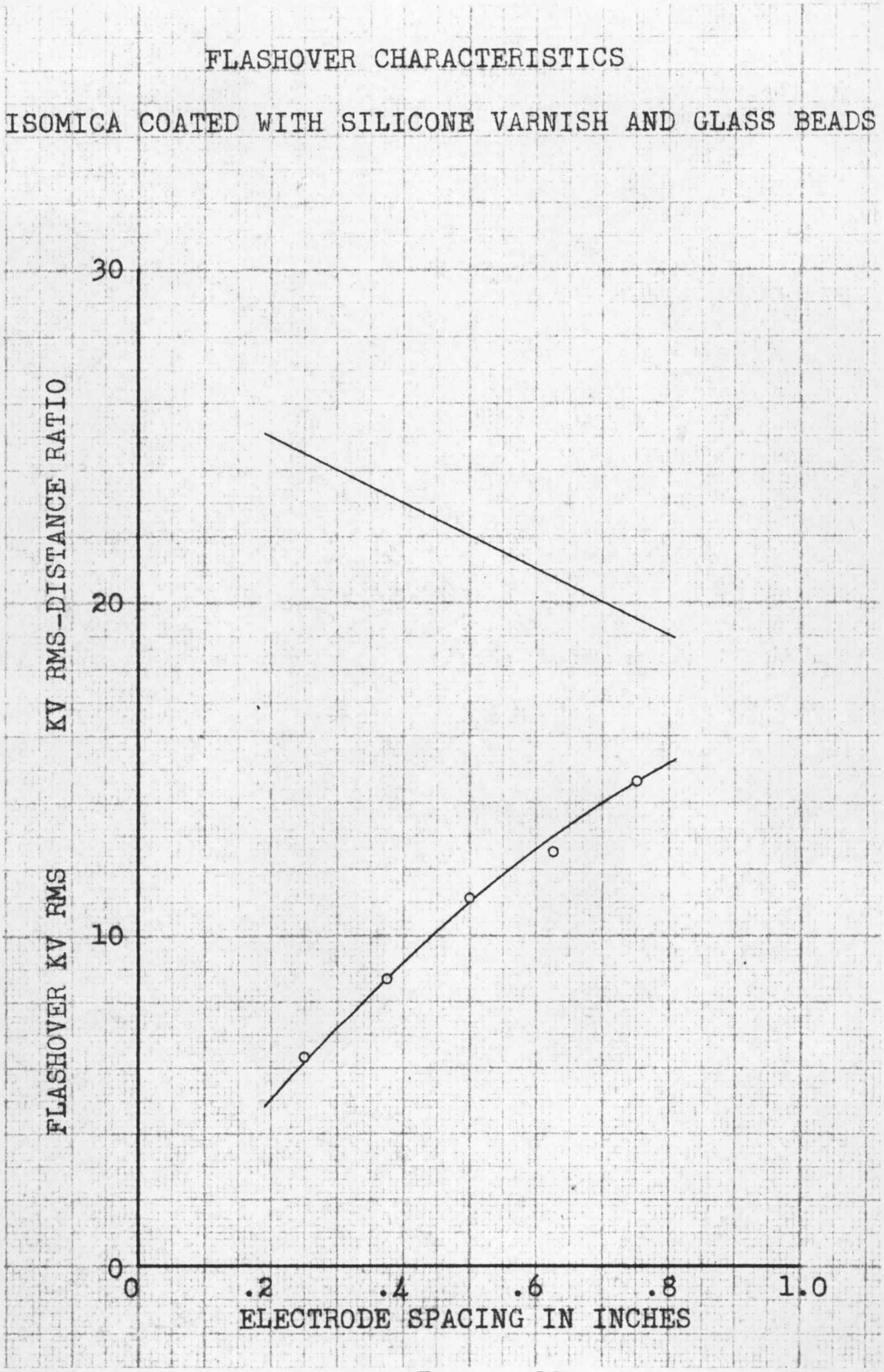
FLASHOVER CHARACTERISTICS
ISOMICA COATED WITH SILICONE VARNISH AND GLASS BEADS
KV RMS-DISTANCE RATIO
FLASHOVER KV RMS
30
20
10
0
0
.2
.4
.6
.8
1.0
ELECTRODE SPACING IN INCHES

Figure 39

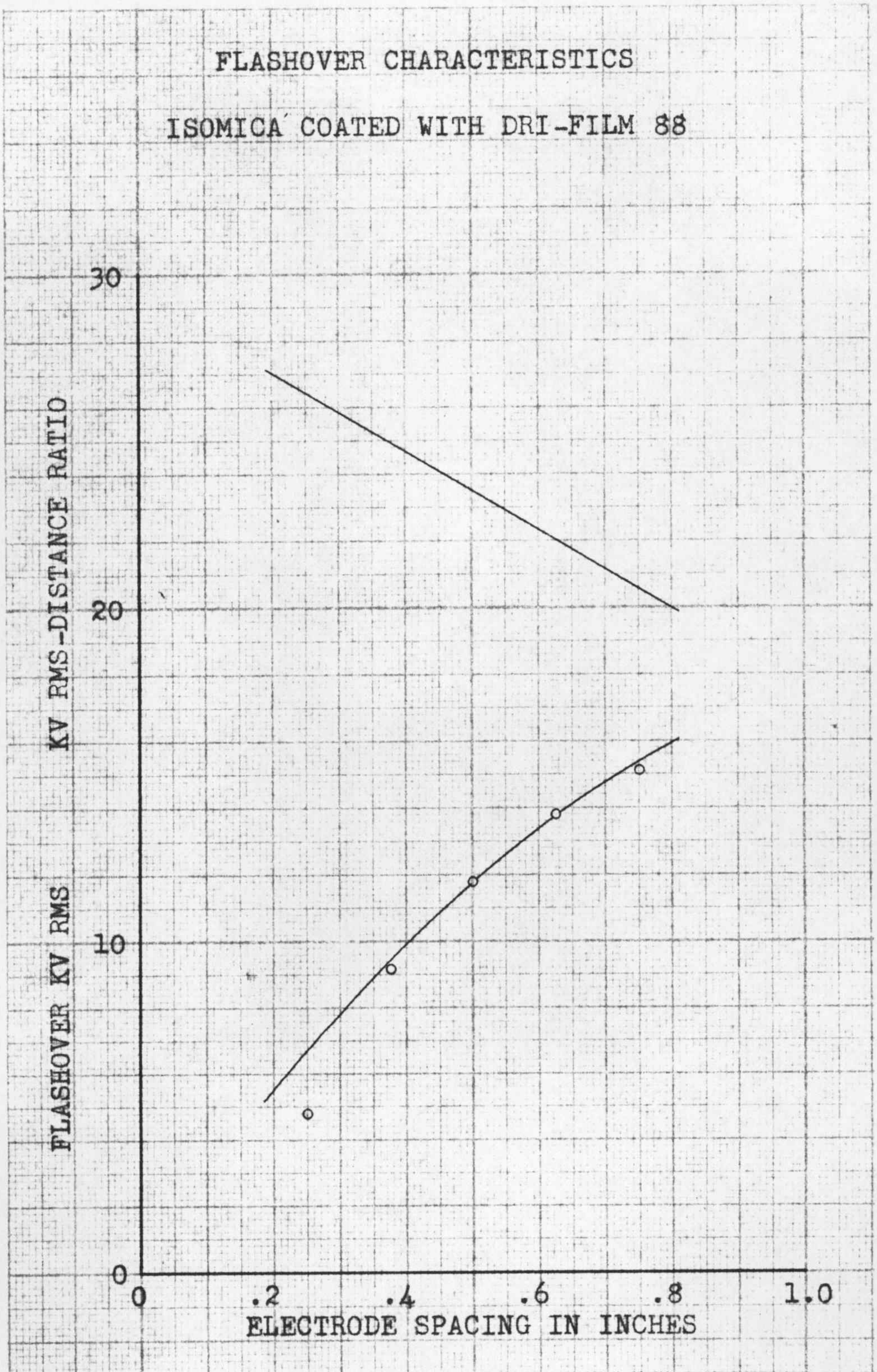
FLASHOVER CHARACTERISTICS
ISOMICA COATED WITH DRI-FILM 88
FLASHOVER KV RMS   KV RMS-DISTANCE RATIO
30
20
10
0
0
.2
.4
.6
.8
1.0
ELECTRODE SPACING IN INCHES

Figure 40

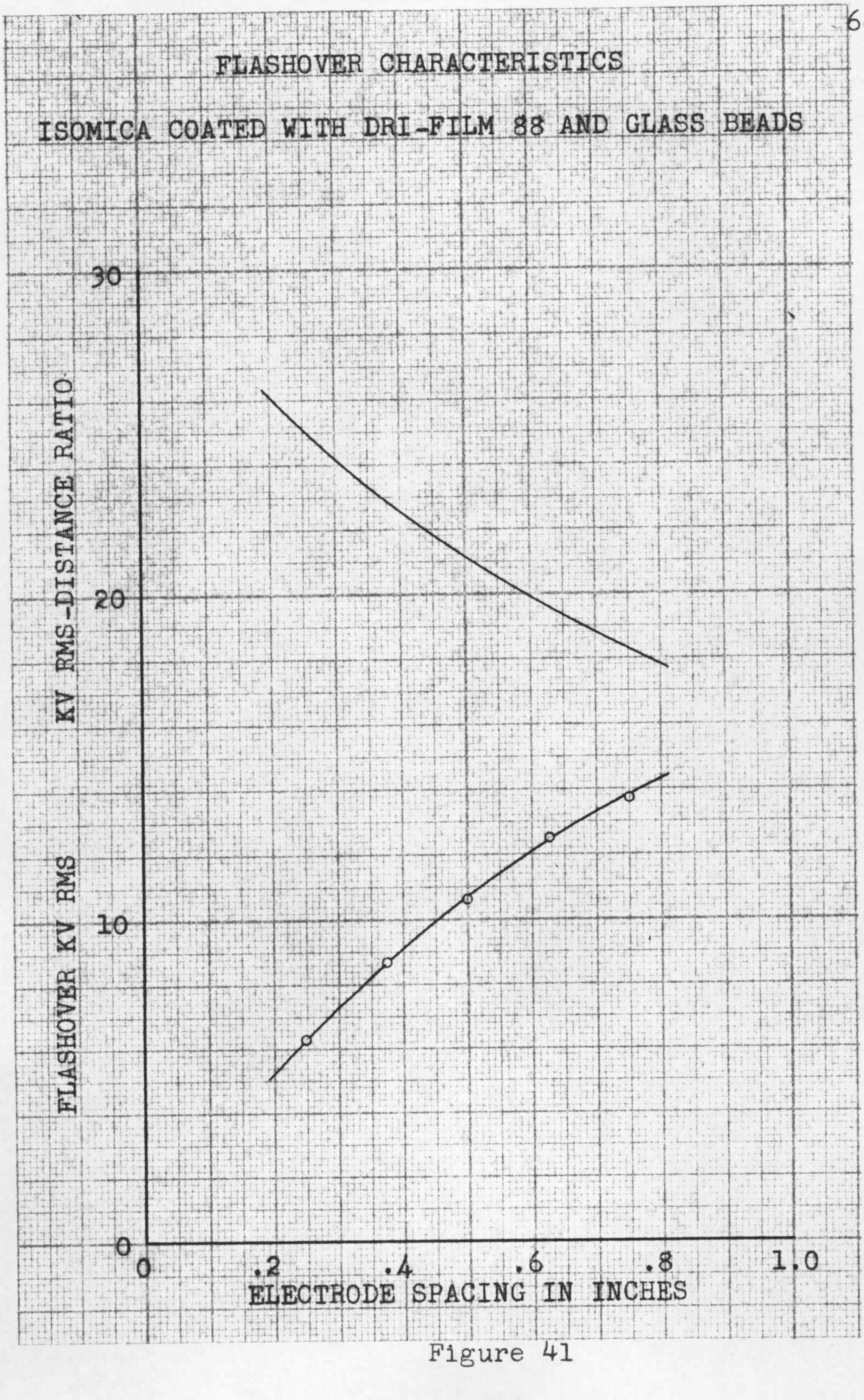
FLASHOVER CHARACTERISTICS
ISOMICA COATED WITH DRI-FILM 88 AND GLASS BEADS
KV RMS-DISTANCE RATIO
FLASHOVER KV RMS
30
20
10
0
0
.2
.4
.6
.8
1.0
ELECTRODE SPACING IN INCHES

Figure 41

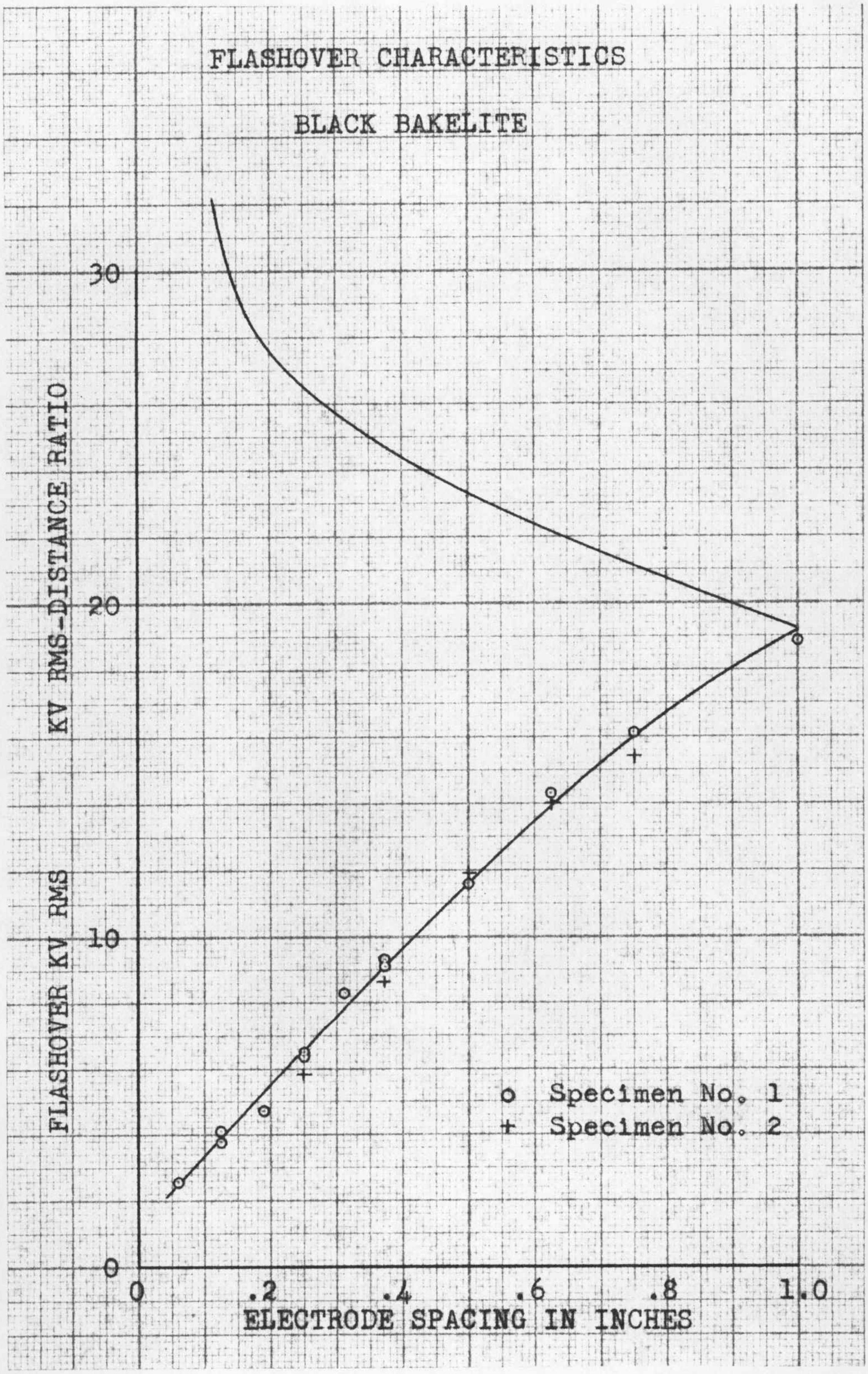
FLASHOVER CHARACTERISTICS
BLACK BAKELITE
KV RMS-DISTANCE RATIO
FLASHOVER KV RMS
30
20
10
0
0
.2
.4
.6
.8
1.0
ELECTRODE SPACING IN INCHES
o Specimen No. 1
+ Specimen No. 2

Figure 42

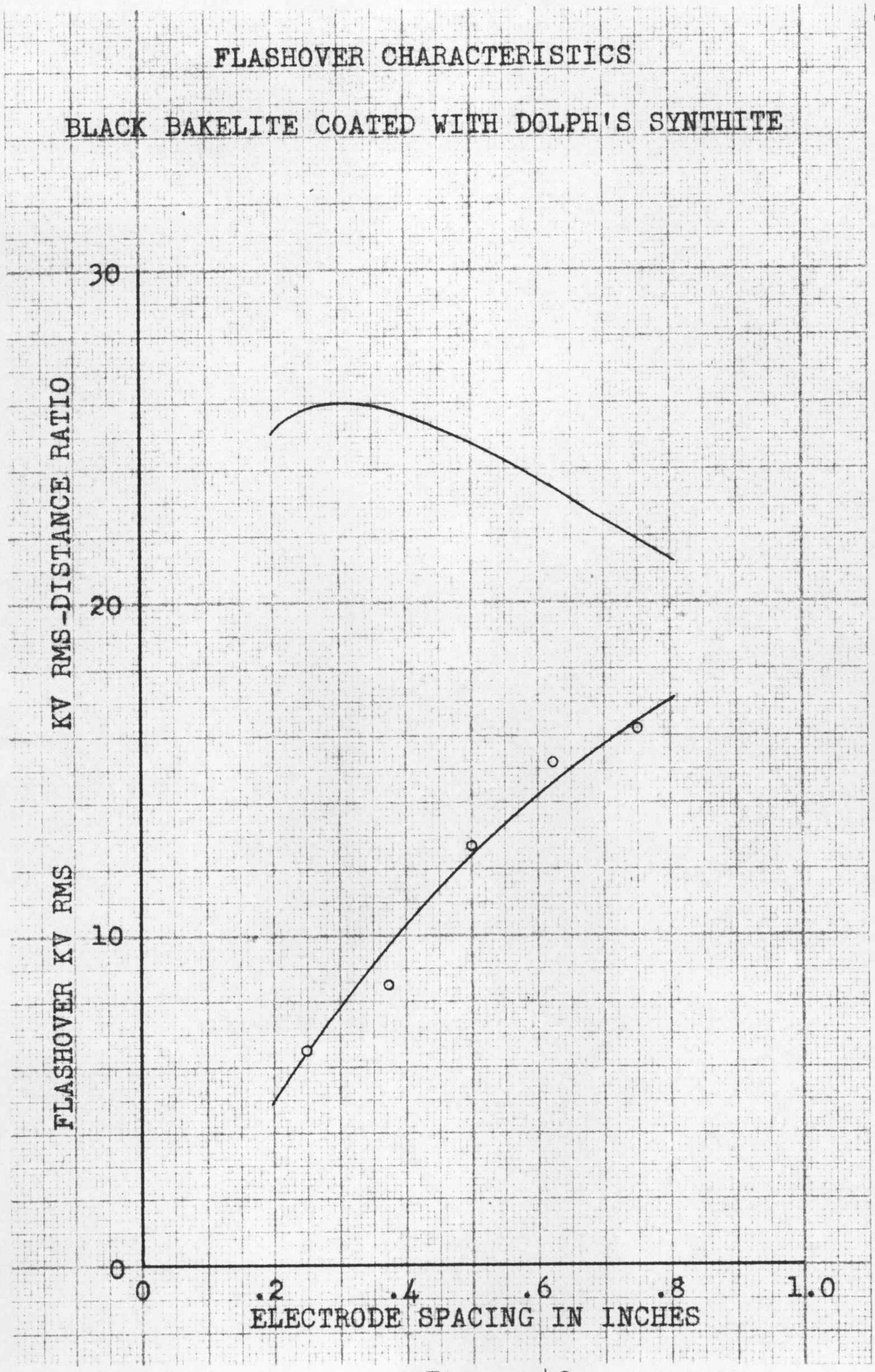
FLASHOVER CHARACTERISTICS
BLACK BAKELITE COATED WITH DOLPH'S SYNTHITE
KV RMS-DISTANCE RATIO
FLASHOVER KV RMS
30
20
10
0
0
.2
.4
.6
.8
1.0
ELECTRODE SPACING IN INCHES

Figure 43

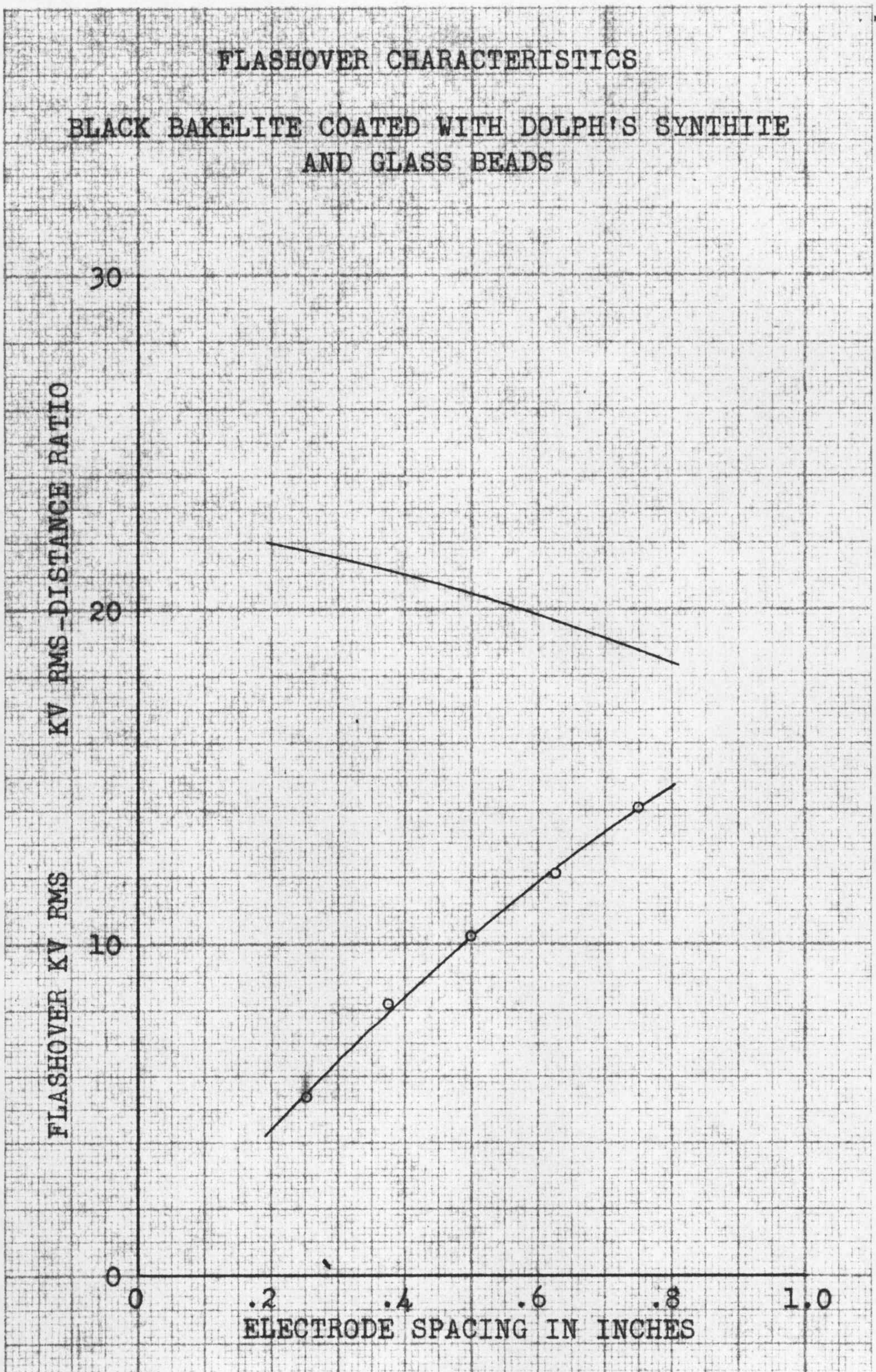
FLASHOVER CHARACTERISTICS
BLACK BAKELITE COATED WITH DOLPH'S SYNTHITE
AND GLASS BEADS
KV RMS-DISTANCE RATIO
FLASHOVER KV RMS
30
20
10
0
0
.2
.4
.6
.8
1.0
ELECTRODE SPACING IN INCHES

Figure 44

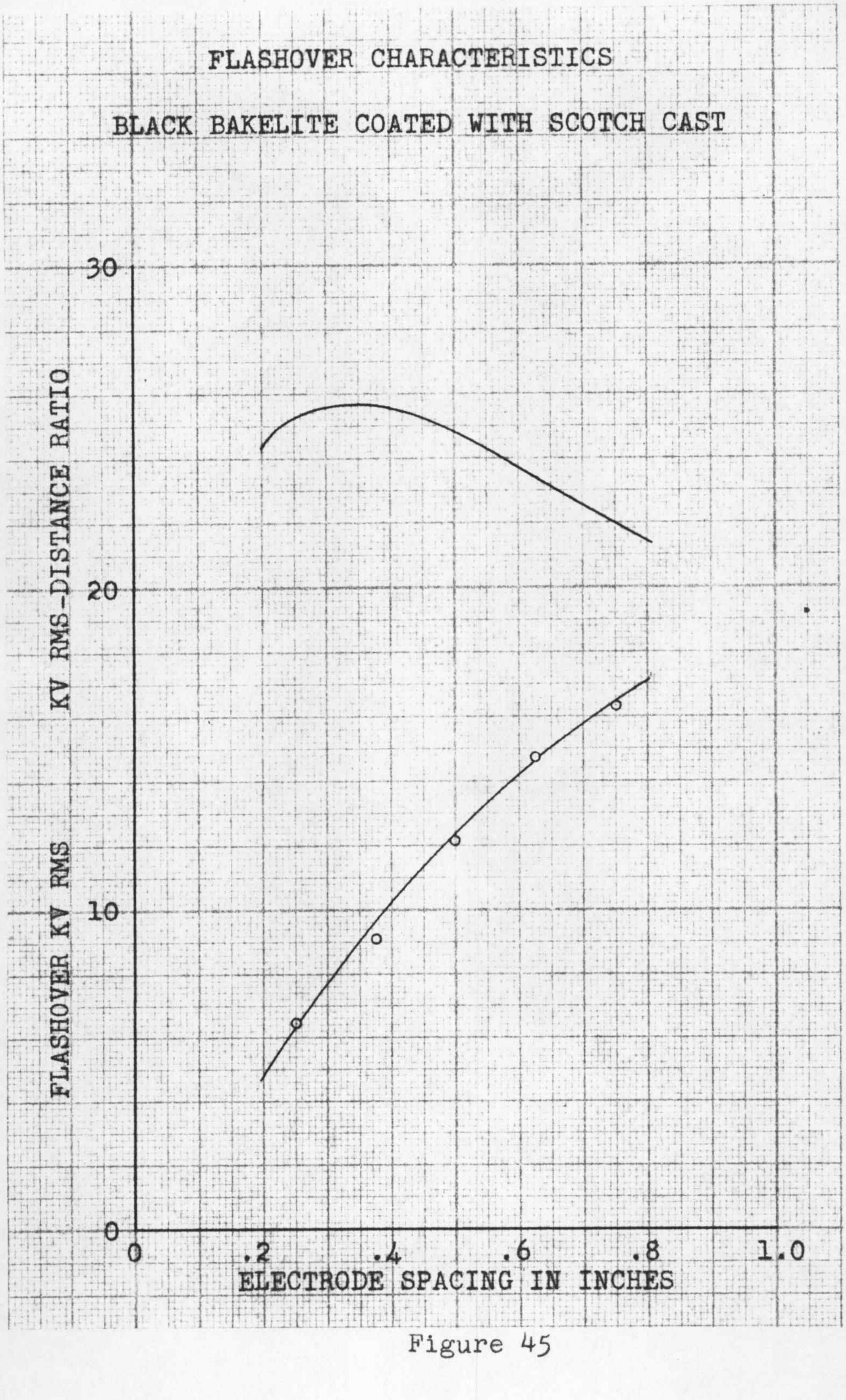
FLASHOVER CHARACTERISTICS
BLACK BAKELITE COATED WITH SCOTCH CAST
FLASHOVER KV RMS   KV RMS-DISTANCE RATIO
30
20
10
0
0
.2
.4
.6
.8
1.0
ELECTRODE SPACING IN INCHES

Figure 45

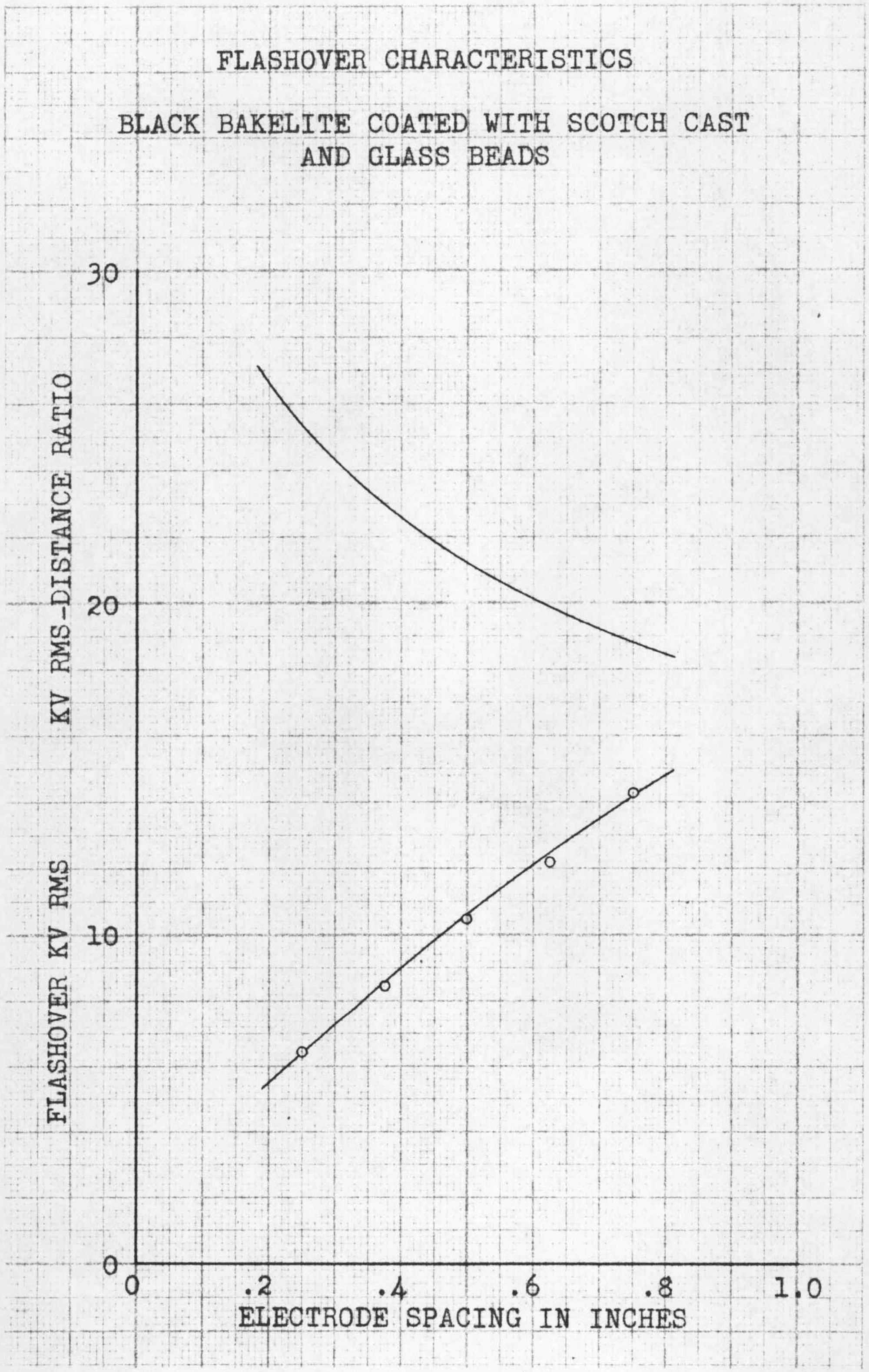
FLASHOVER CHARACTERISTICS
BLACK BAKELITE COATED WITH SCOTCH CAST AND GLASS BEADS
KV RMS-DISTANCE RATIO
FLASHOVER KV RMS
30
20
10
0
0
.2
.4
.6
.8
1.0
ELECTRODE SPACING IN INCHES

Figure 46

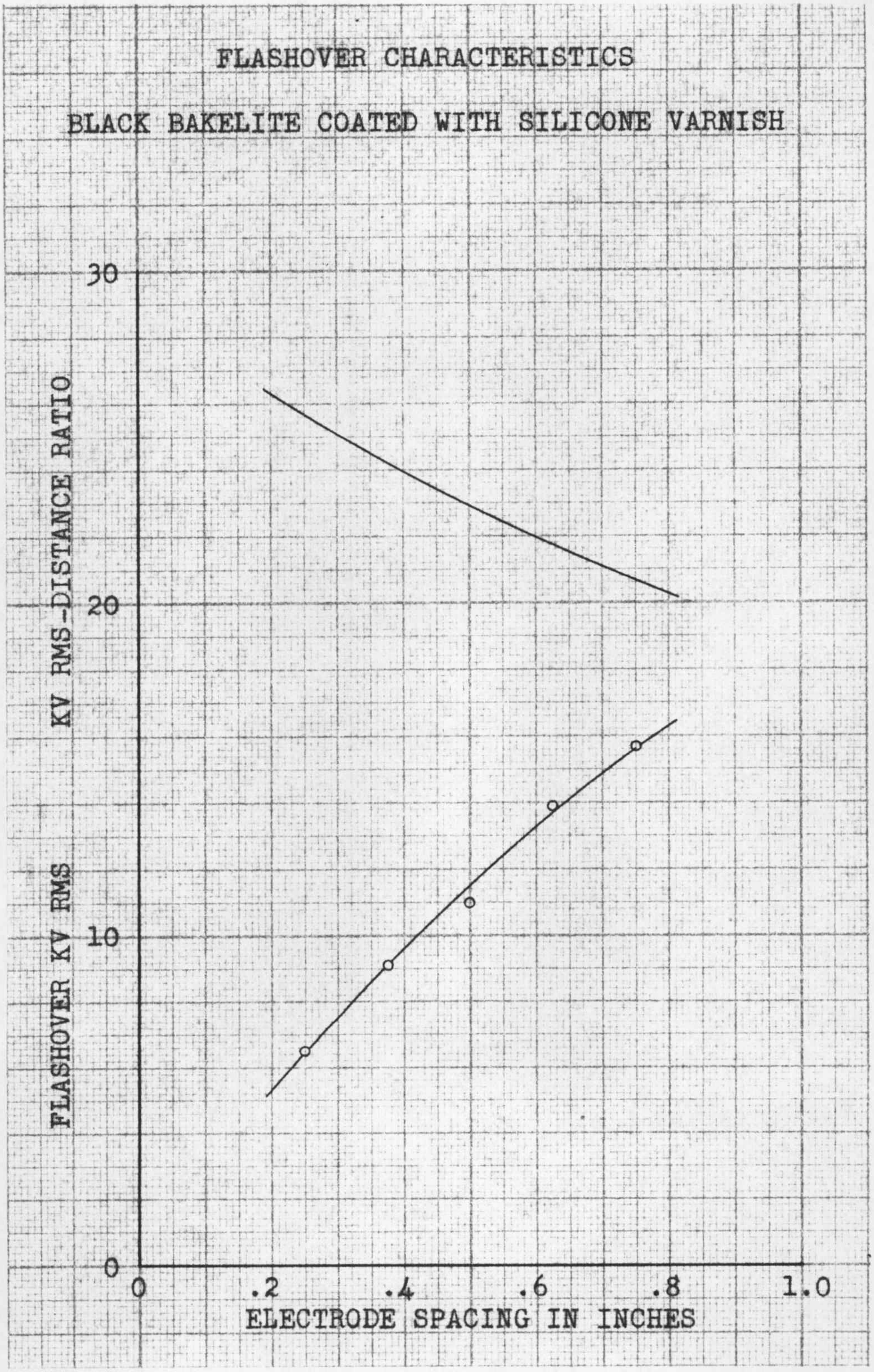
FLASHOVER CHARACTERISTICS
BLACK BAKELITE COATED WITH SILICONE VARNISH
KV RMS-DISTANCE RATIO
FLASHOVER KV RMS
30
20
10
0
0
.2
.4
.6
.8
1.0
ELECTRODE SPACING IN INCHES

Figure 47

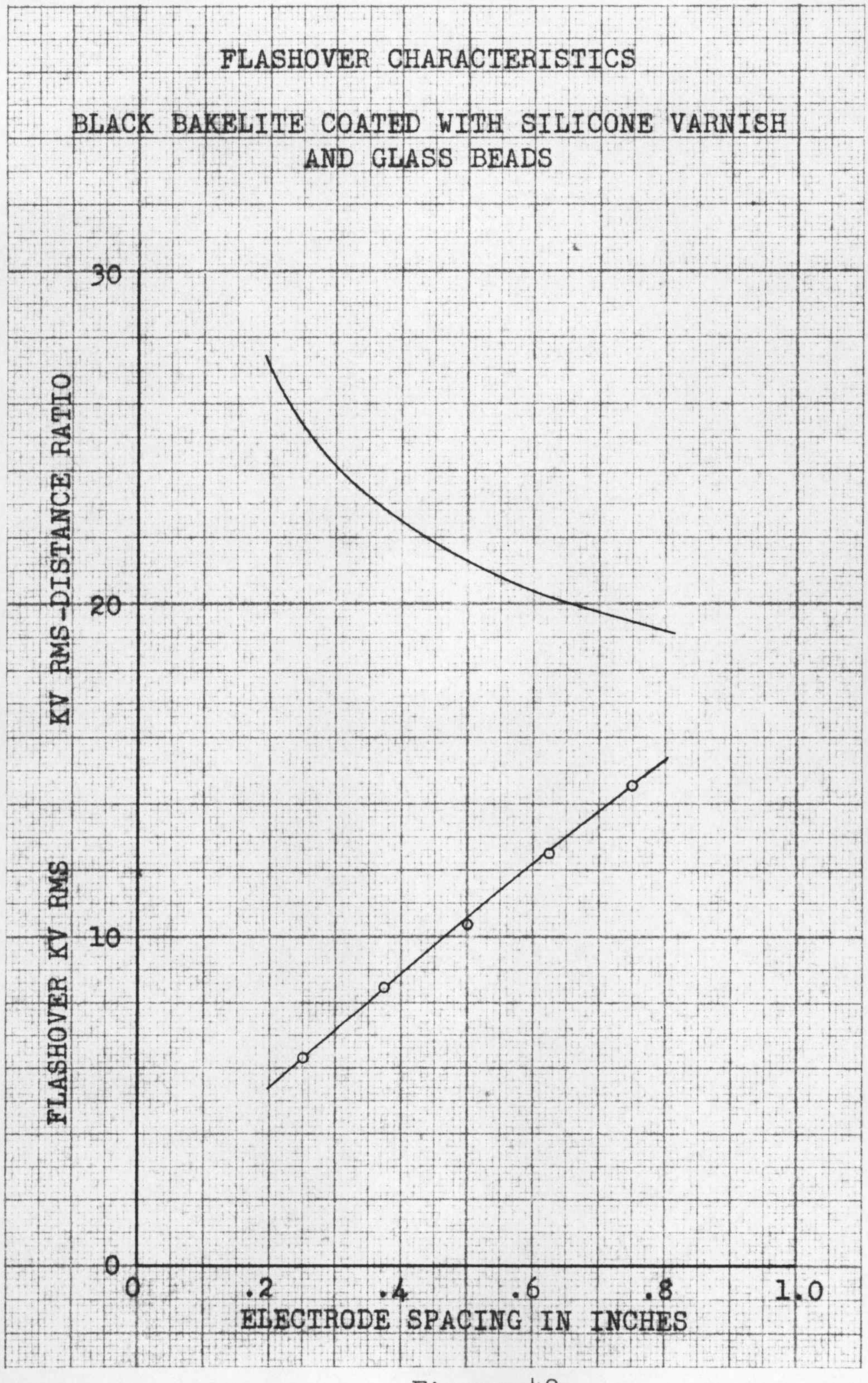
FLASHOVER CHARACTERISTICS
BLACK BAKELITE COATED WITH SILICONE VARNISH
AND GLASS BEADS
KV RMS-DISTANCE RATIO
FLASHOVER KV RMS
30
20
10
0
0
.2
.4
.6
.8
1.0
ELECTRODE SPACING IN INCHES

Figure 48

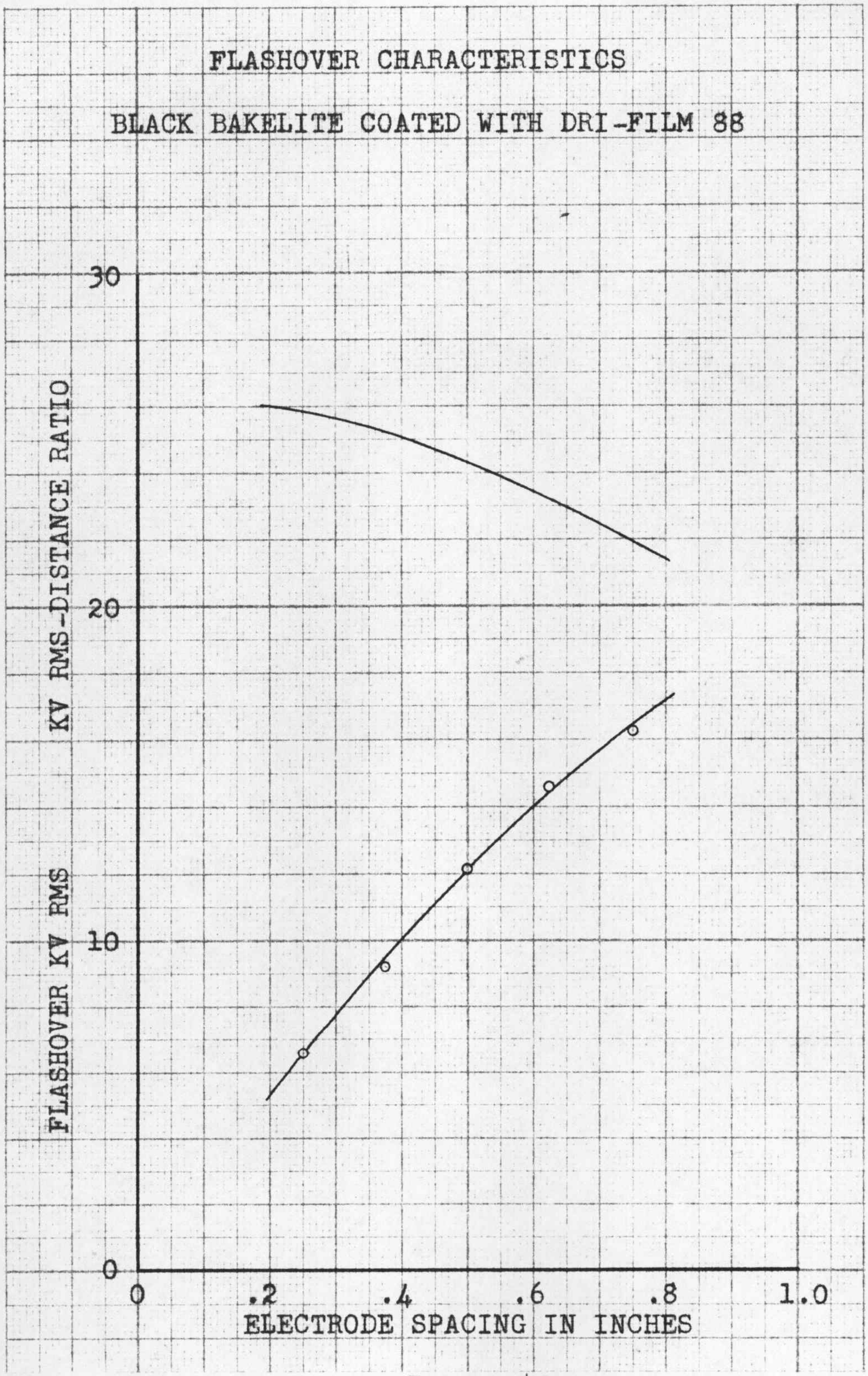
FLASHOVER CHARACTERISTICS
BLACK BAKELITE COATED WITH DRI-FILM 88
FLASHOVER KV RMS   KV RMS-DISTANCE RATIO
30
20
10
0
0
.2
.4
.6
.8
1.0
ELECTRODE SPACING IN INCHES

Figure 49

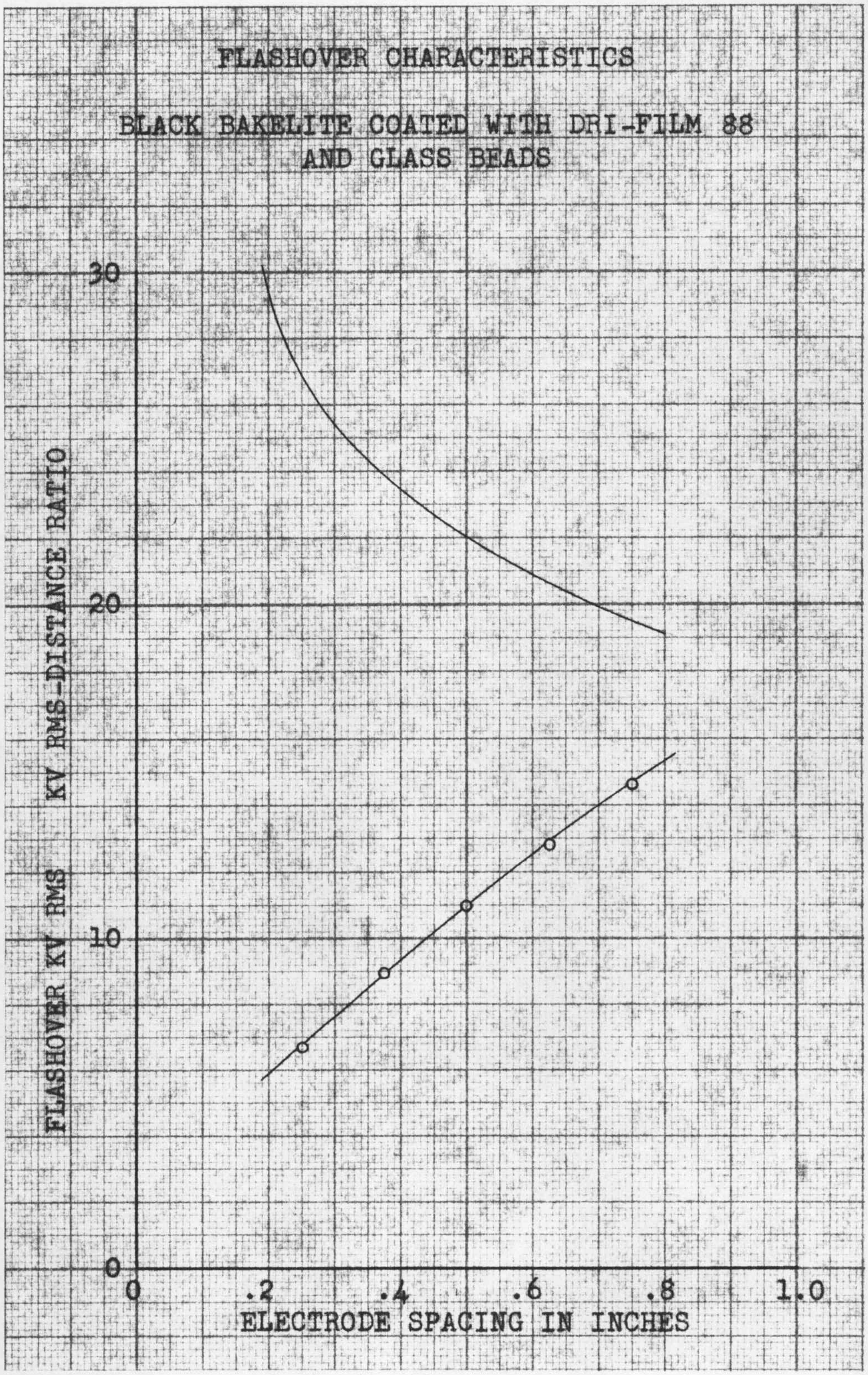
FLASHOVER CHARACTERISTICS
BLACK BAKELITE COATED WITH DRI-FILM 88
AND GLASS BEADS
FLASHOVER KV RMS   KV RMS-DISTANCE RATIO
30
20
10
0
0
.2
.4
.6
.8
1.0
ELECTRODE SPACING IN INCHES

Figure 50

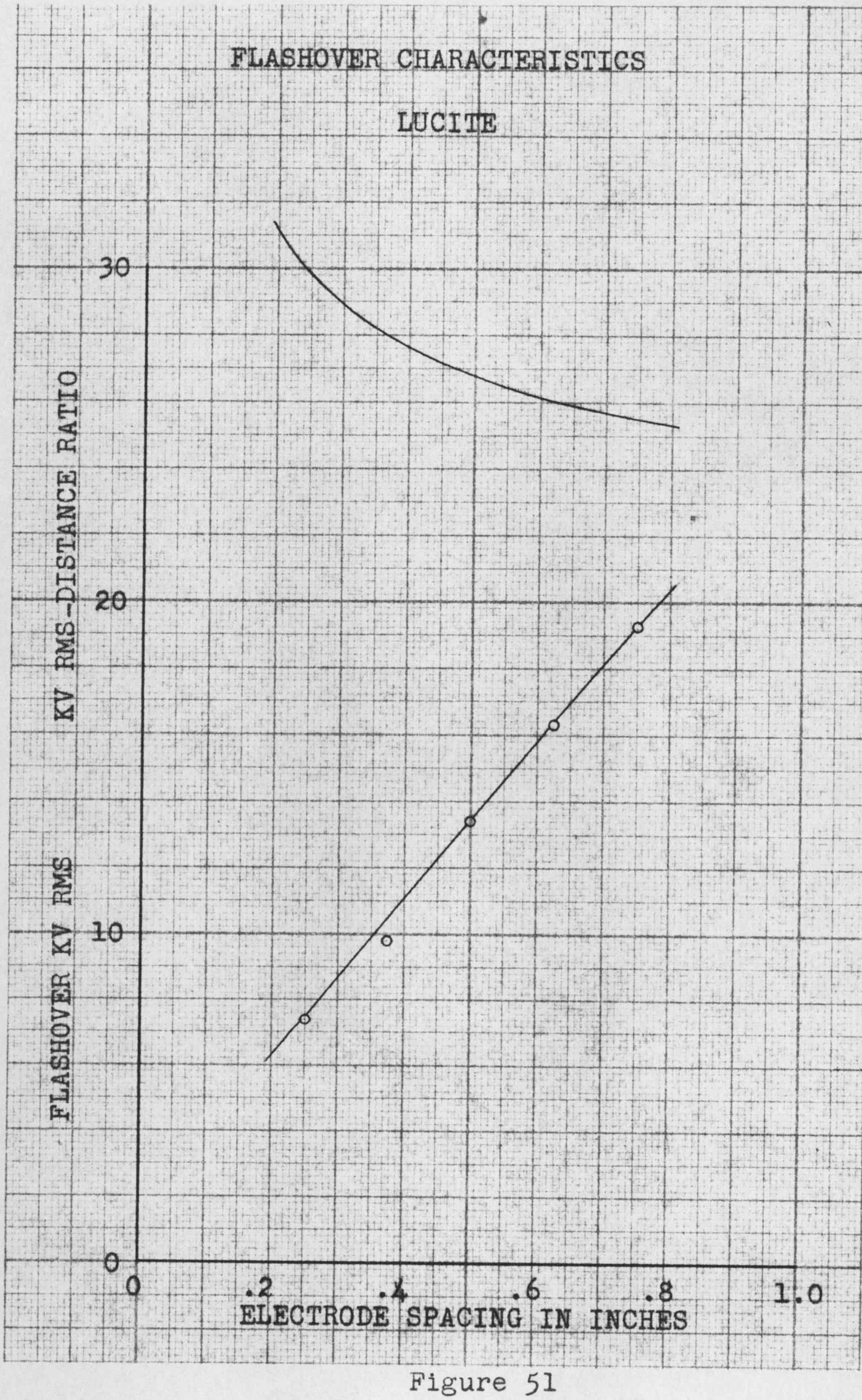
FLASHOVER CHARACTERISTICS
LUCITE
KV RMS-DISTANCE RATIO
FLASHOVER KV RMS
30
20
10
0
0
.2
.4
.6
.8
1.0
ELECTRODE SPACING IN INCHES

Figure 51

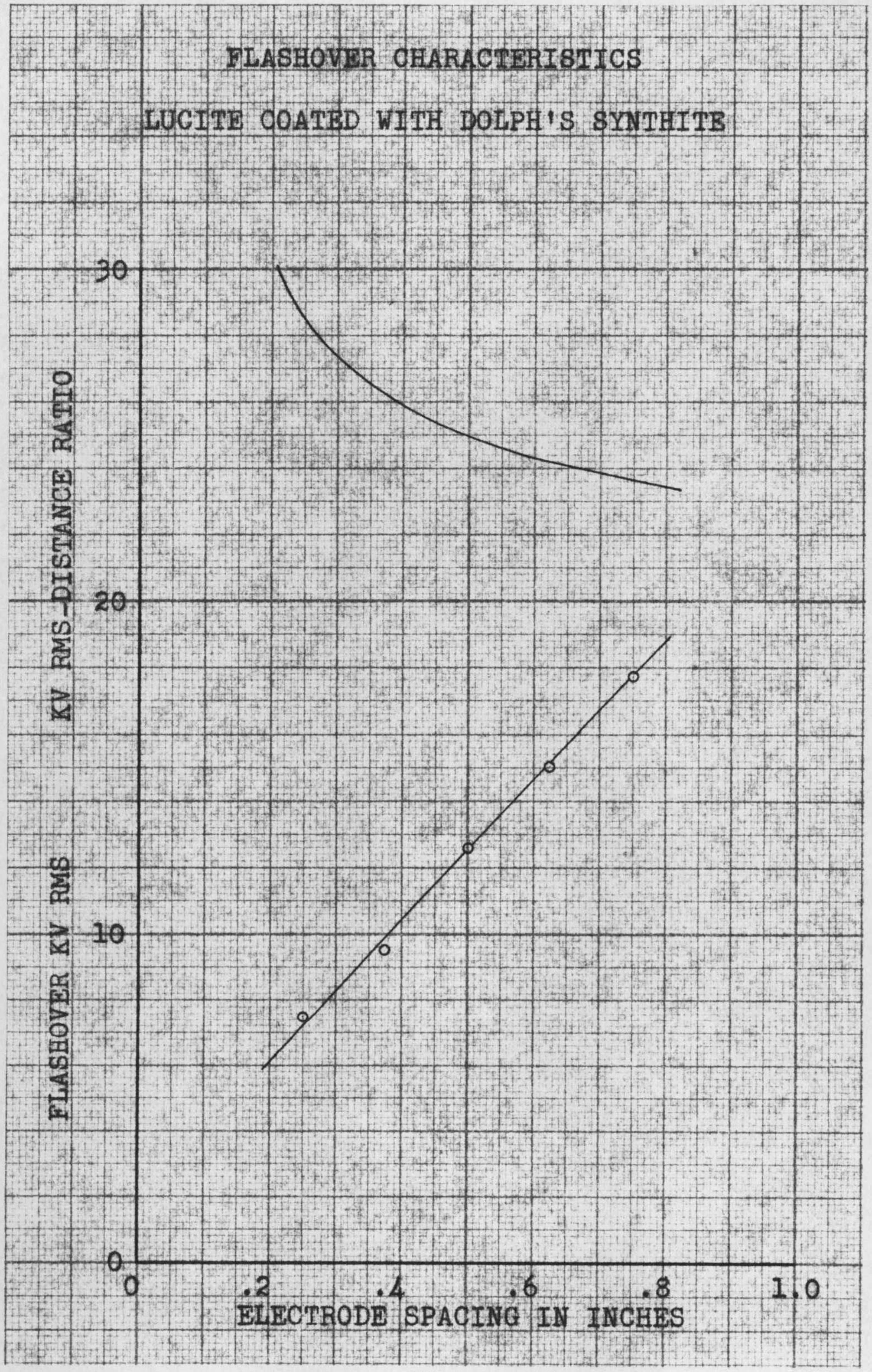
FLASHOVER CHARACTERISTICS
LUCITE COATED WITH DOLPH'S SYNTHITE
FLASHOVER KV RMS
KV RMS-DISTANCE RATIO
30
20
10
0
0
.2
.4
.6
.8
1.0
ELECTRODE SPACING IN INCHES

Figure 52

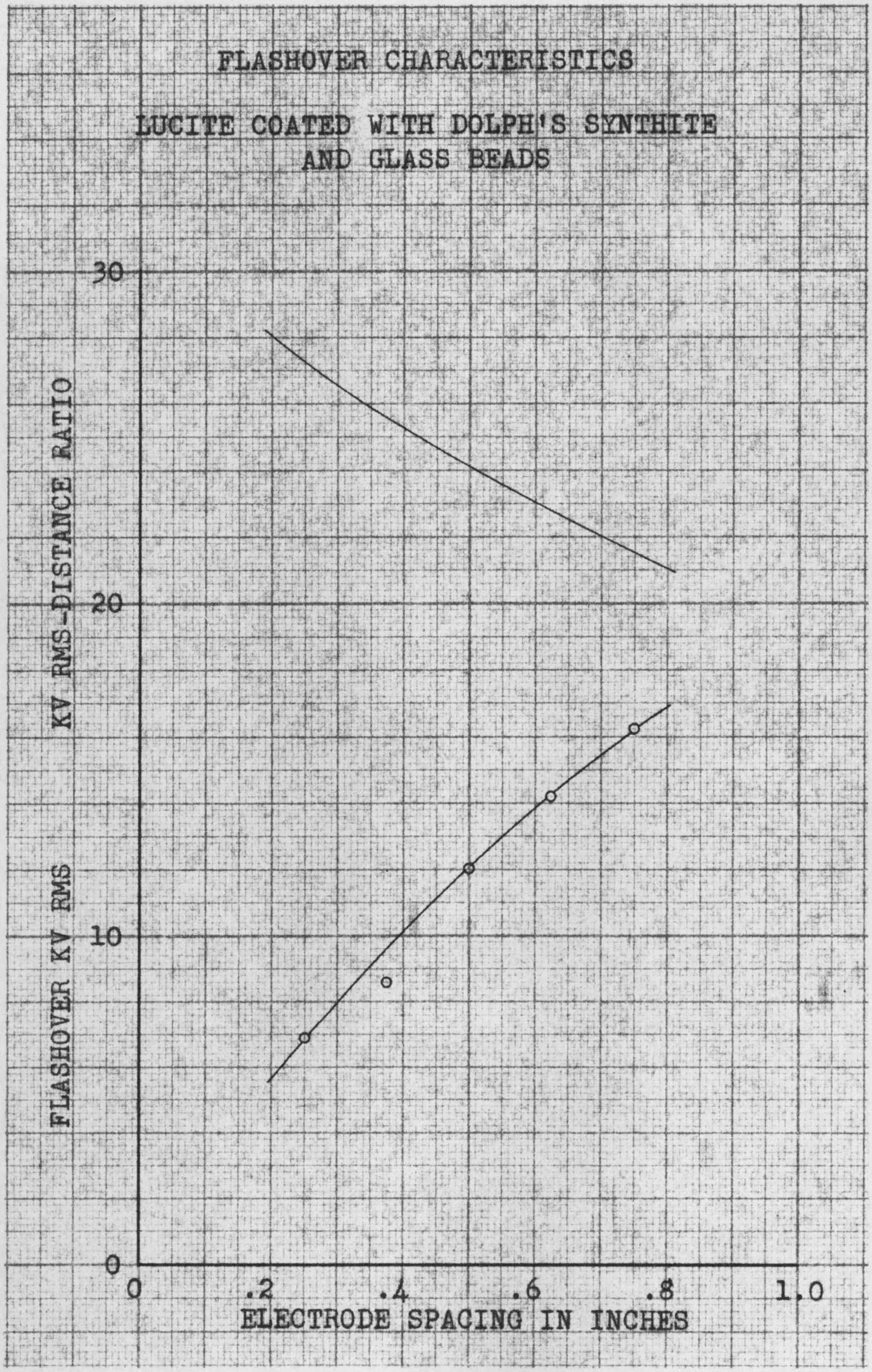
FLASHOVER CHARACTERISTICS
LUCITE COATED WITH DOLPH'S SYNTHITE
AND GLASS BEADS
FLASHOVER KV RMS   KV RMS-DISTANCE RATIO
30
20
10
0
0
.2
.4
.6
.8
1.0
ELECTRODE SPACING IN INCHES

Figure 53

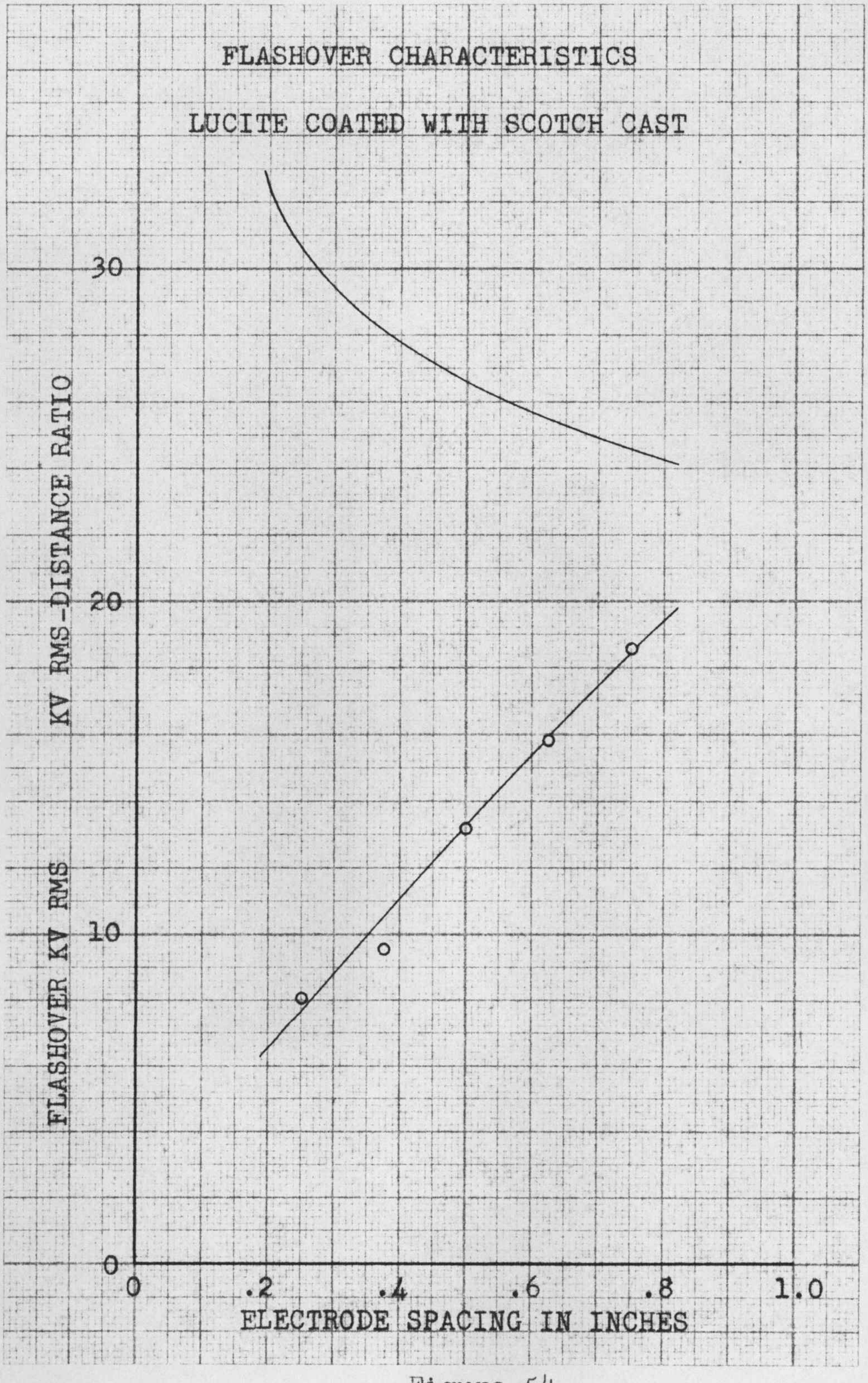

FLASHOVER CHARACTERISTICS
LUCITE COATED WITH SCOTCH CAST
FLASHOVER KV RMS
KV RMS-DISTANCE RATIO
30
20
10
0
0
.2
.4
.6
.8
1.0
ELECTRODE SPACING IN INCHES

Figure 54

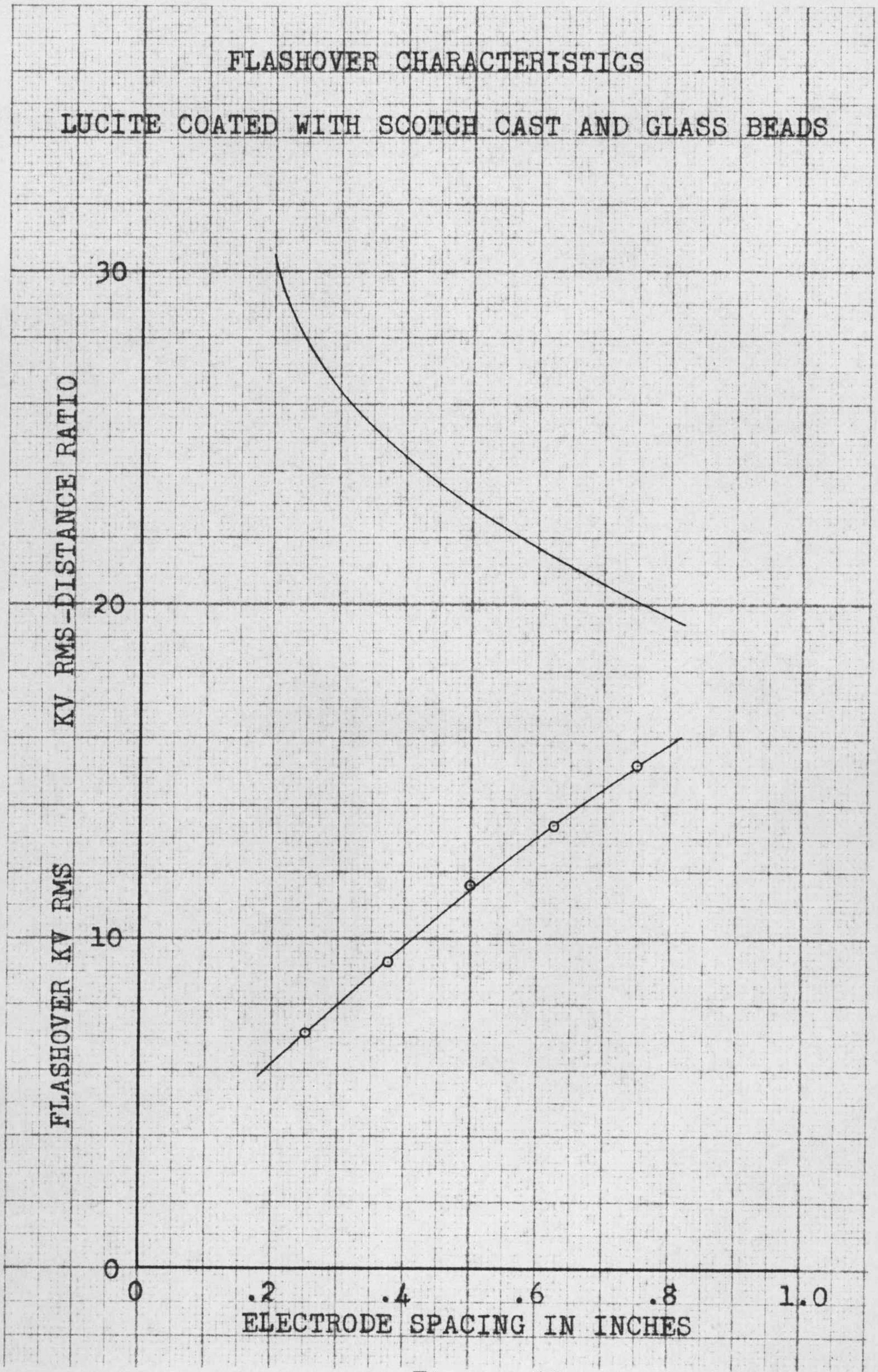
FLASHOVER CHARACTERISTICS
LUCITE COATED WITH SCOTCH CAST AND GLASS BEADS
FLASHOVER KV RMS   KV RMS-DISTANCE RATIO
30
20
10
0
0
.2
.4
.6
.8
1.0
ELECTRODE SPACING IN INCHES

Figure 55

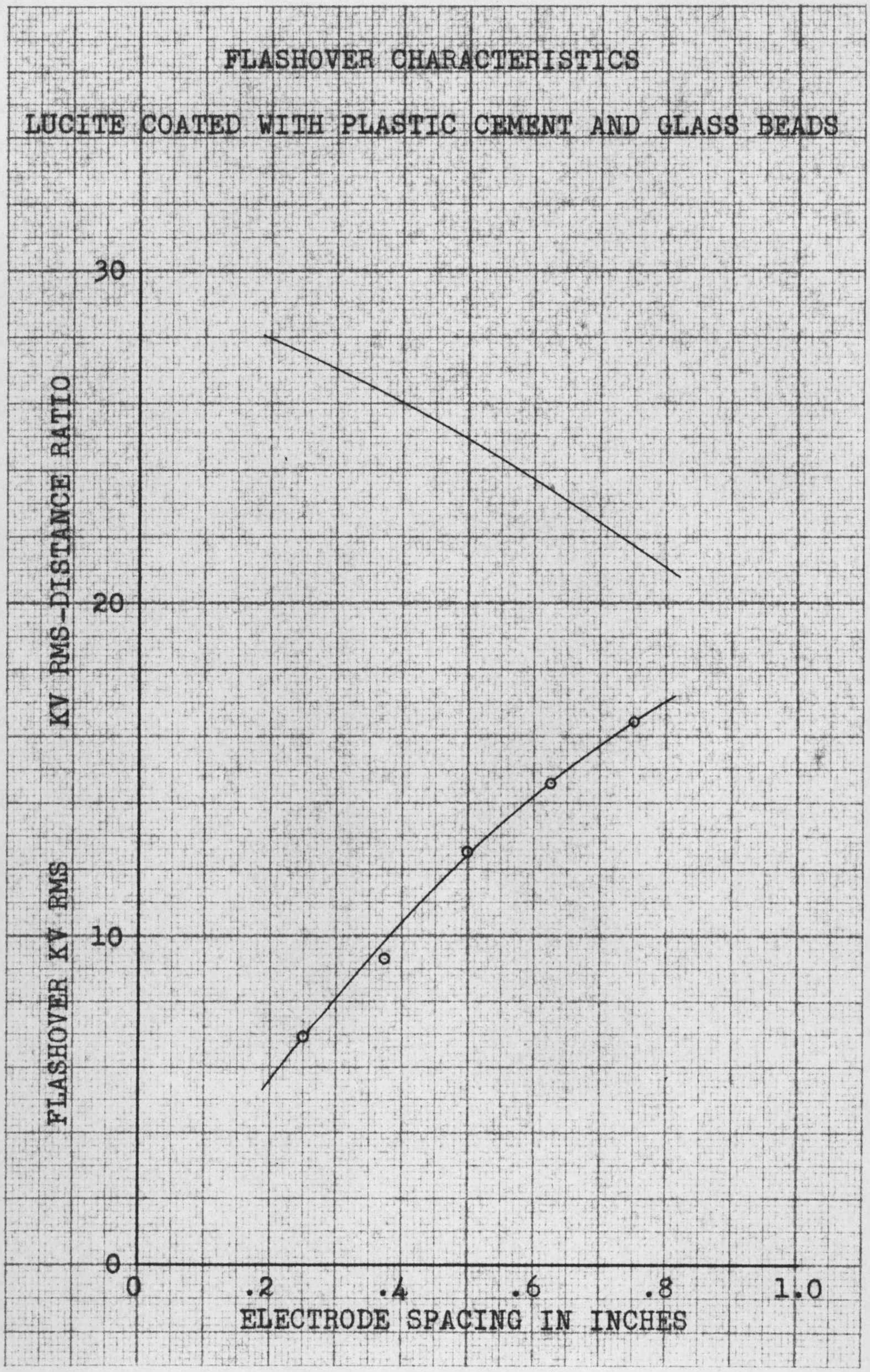
FLASHOVER CHARACTERISTICS
LUCITE COATED WITH PLASTIC CEMENT AND GLASS BEADS
KV RMS-DISTANCE RATIO
FLASHOVER KV RMS
30
20
10
0
0
.2
.4
.6
.8
1.0
ELECTRODE SPACING IN INCHES

Figure 56

a point on the flashover characteristic by its abscissa and plotting this ratio as a new ordinate for the given abscissa. This is only an approximation of the gradient, but it serves to give some notion of the electric field variation with the gap separation.

The flashover data for the various specimens taken from the curves to smooth out the experimental variations are shown in Table III at the end of this section. An examination of the table shows that without exception the addition of the glass beads to the surface of a specimen reduced the flashover voltage measureably below that for either the base material alone or the base material coated with the suspension medium. This is in agreement with theory. Any surface is weaker than the gas adjacent to it, and the rougher the surface, so long as it is not increased materially in length, the weaker it is electrically. This is due to the fact that the gas between the irregularities is subjected to much more dielectric flux and hence a higher voltage gradient because the insulating irregularities, in this case the glass beads, have a much higher dielectric constant than the air or gas between them.

TABLE III

FLASHOVER DATA FOR VARIOUS SPECIMENS AT DIFFERENT ELECTRODE SPACINGS

Specimen	Flashover KV RMS From Experimental Curves				
Inches Flashover Distance →	0.25	0.375	0.50	0.625	0.750
Isomica	6.5	9.1	11.35	13.4	15.15
Isomica + Dolph's Synthite	6.5	9.1	11.55	13.6	15.4
Isom.+ D's Syn. + Glass Beads	6.25	8.9	11.25	13.2	14.8
Isom. + Scotch Cast	6.7	9.45	11.95	14.1	15.95
Isom. +Sc. Cast + Glass Bds.	6.6	9.15	11.5	13.4	14.95
Isom. + Silicone Varnish	6.5	9.2	11.5	13.5	15.1
Isom. + Sil. Var. + Gl. Bds.	6.15	8.7	11.0	13.0	14.6
Isom. + Dri-Film 88	6.7	9.4	11.9	13.9	15.4
Isom. + D.F. 88 + Glass Bds.	6.3	8.7	10.7	12.4	13.9
Black Bakelite	6.5	9.2	11.6	13.9	16.0
Blk. Bakelite + Dolph's Syn.	6.45	9.7	12.4	14.5	16.4
Blk. Bak. +D's Syn. +Gl. Bds.	5.4	7.9	10.2	12.25	14.1
Blk. Bak. + Scotch Cast	6.3	9.6	12.35	14.8	16.45
Blk. Bak. + Sc. Cast + Gl. B.	6.4	8.55	10.65	12.5	14.2
Blk. Bak. + Silicon Varnish	6.45	9.1	11.5	13.7	15.8
Blk. Bak. + Sil.Var. + Gl.B.	6.3	8.45	10.55	12.6	14.55
Blk. Bak. + Dri-Film 88	6.6	9.5	12.1	14.45	16.45
Blk. Bak. + D.F. 88 + Gl.B.	6.75	8.9	11.0	12.9	14.65
Lucite	7.45	10.5	13.45	16.35	19.3
Lucite + Dolph's Synthite	7.2	9.9	12.55	15.15	17.75
Luc. + D's Syn. + Glass Bds.	6.85	9.6	12.1	14.3	16.2
Luc. + Scotch Cast	7.65	10.5	13.25	15.9	18.45
Luc. + Sc. Cast + Glass Bds.	7.1	9.35	11.45	13.4	15.15
Luc. + Plastic Cement + G.B.	6.9	9.8	12.4	14.6	16.4

ASTM ARC TRACKING TESTS

The arc tracking tests were performed to determine the arc resistance time of the various specimens and to relate the other experiments to a standard test.

General

These tests are described in detail as High-Voltage, Low-Current Arc Resistance Of Solid Electrical Insulating Materials by the American Society For Testing Materials (4, pp. 1136-1147). The purpose of these tests is to give a relative comparison of solid dielectrics in their ability to withstand surface flashover under conditions of high voltage and low current. The arc resistance time of a specimen is defined as the total time of operation of the test sequence until failure occurs. In the present experiment the point of failure for the specimens was determined by the formation of a carbonized track for all but two. These two were lucite and the point of failure was recorded when they burst into flame. For all the specimens tested the point of failure was very distinct.

Description Of Equipment

The circuit diagram of the arc-tracking equipment is shown in Figure 57. A general view of the complete equipment with auxiliary instruments is shown in Figure 58. The low side voltmeters were calibrated against a secondary standard. The milliammeters used to measure the arc current were calibrated with both direct and alternating current. A precision milliammeter was used for the direct current calibrations and a thermocouple and microammeter were used for the alternating current calibrations.

The 0-50 ma instrument has an iron vane movement (A_1 Figure 57). The shield made for this instrument can be seen in the interior view of Figure 59. An iron shield proved unsatisfactory as it disturbed the flux configuration of the coil surrounding the iron vanes. A brass shield proved satisfactory after it was slit with a jeweler's saw to minimize eddy current effects. The shield is connected to the high voltage terminal of this milliammeter. Since the electrostatic forces present in the equipment were large enough to move the iron vane when the milliammeter was disconnected, the shield was necessary.

When the equipment was operated at full voltage the electrostatic forces became great enough to pull apart the wires of the vacuum thermocouple of the 0-10 ma rf milliammeter (A_2 Figure 57). It was necessary to build

ARC-RESISTANCE TEST CIRCUIT
ASTM Designation: D 495-48T

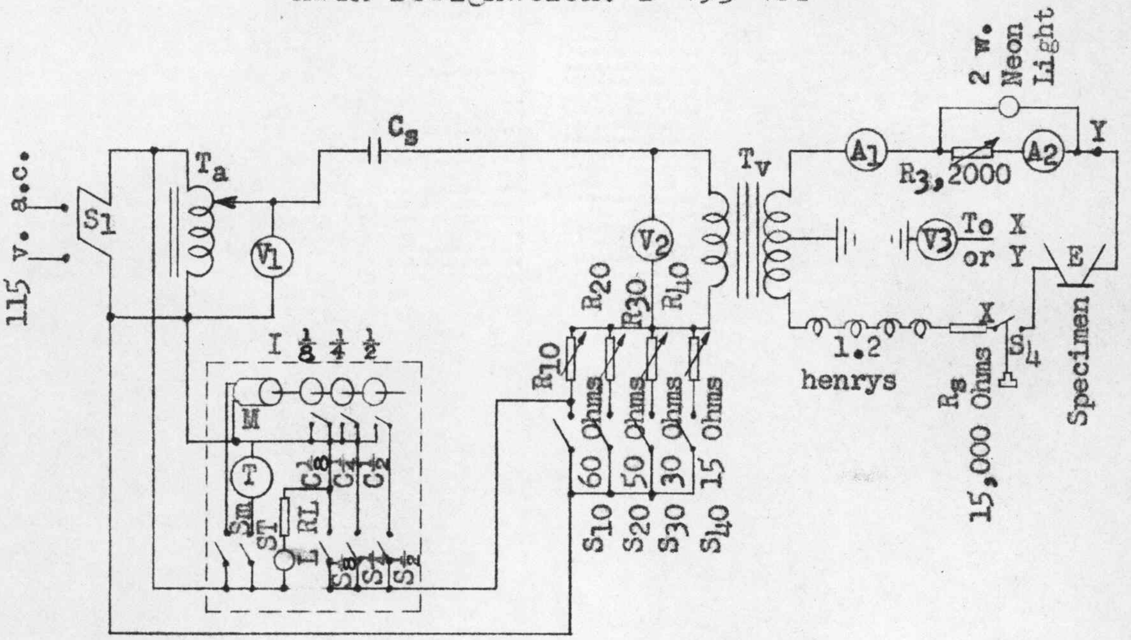

A_1	Milliammeter, 0-50 ma a-c
A_2	Milliammeter, 0-10 ma r-f
C	Contactors
E	Electrode Assembly
I	Interruptor Assembly
L	Indicator Lamp
M	Motor
R	Resistors
S	Switches
T	Timer
T_a	Autotransformer
T_v	High Voltage Transformer
V_1	Voltmeter, 0-150 v a-c
V_2	Voltmeter, 0-150 v a-c
V_3	Voltmeter, 0-10 kv electrostatic

Figure 57

Figure 58.
High voltage, low current arc resistance testing equipment.

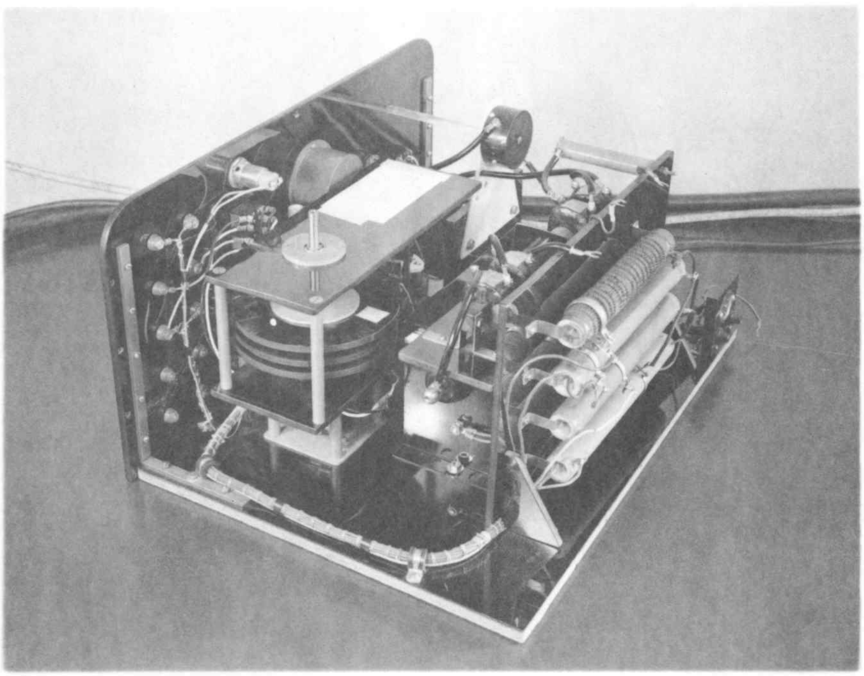

Figure 59.
High voltage, low current arc resistance testing equipment with cover removed.

a small shield of copper foil surrounding the thermocouple. The shield was connected to the high voltage terminal of the instrument.

Because electrostatic forces would otherwise pull the filaments of the pilot lamps apart, shielded cases were installed and grounded to eliminate this source of failure.

The four resistors (R_{10}, R_{20}, R_{30}, R_{40}, Figure 57) in the primary circuit are used to regulate the arc current of the secondary circuit from 10 milliamperes to 40 ma in steps of 10 ma. The resistor R_{10} is always in the circuit.

The suppressing resistor (R_s, Figure 57) found in the unit was replaced with one of the proper value. The number of inductances in the secondary circuit was reduced and the inductance of the group adjusted to the proper value on the General Radio 650-A impedance bridge by changing the mutual coupling between them. The purpose of the resistance and inductance is to suppress parasitic high frequencies in the arc circuit.

A synchronous motor (M, Figure 57) is used to drive the three bakelite timing cams shown in Figure 59. The cams operate microswitches ($S_{1/8}$, $S_{1/4}$, $S_{1/2}$, Figure 57) that open and close the primary circuit in a prescribed sequence. The time for both the open and closed intervals of the primary circuit was determined by measuring thousands of intervals with a cycle counter shown immediately to the right of the unit in Figure 58. This measurement showed that the cams originally in the unit were not properly cut. Therefore, after the necessary calculations, the cams were re-cut on the milling machine of the physics department, the only available milling machine the design of which would permit the remilling of the cams. The intervals were then checked by repeating the measurements with the cycle counter. As a further check a dual channel Brush recorder was used to measure the time intervals. One channel of the recorder carried the signal and the other the time base. A new shaft was machined for the cams because the original was not accurate enough to permit the cams to operate within the tolerance prescribed. The timing tolerance for any interval is 0.00833 seconds.

The high voltage switch (S_4, Figure 57) was entirely redesigned in order to offer less contact resistance upon closure and to offer a higher leakage path when open.

The secondary circuit was completely re-wired and greatly simplified. Over half or more than five feet of high voltage cable were removed without altering the circuit.

The electrode assembly shown in Figure 60 was taken apart and rebuilt. An additional template was made to

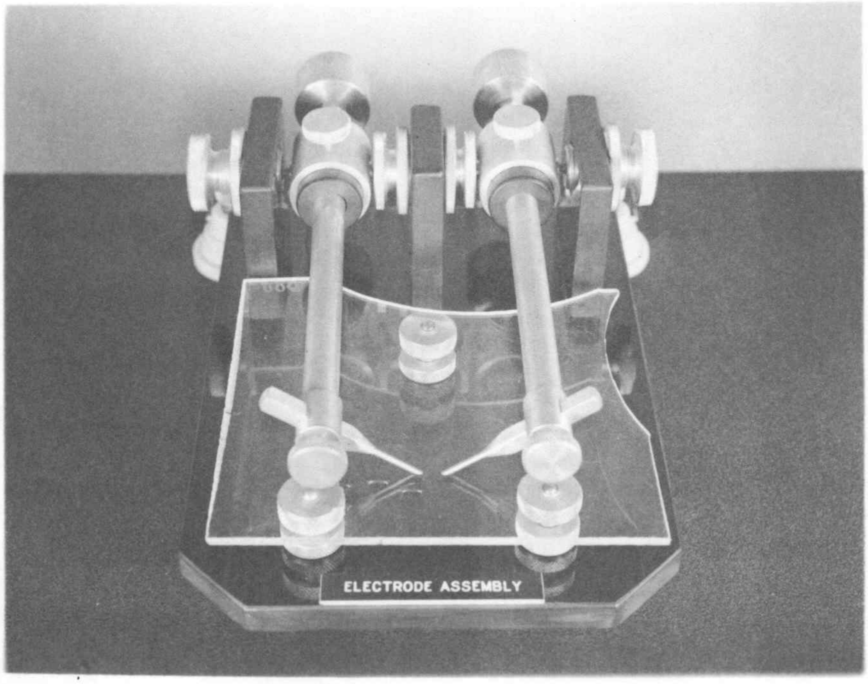

Figure 60
Electrode assembly for high voltage, low-current arc resistance testing equipment.

make possible the assembly to the prescribed tolerances. The spacing between the electrodes is 0.250 ± 0.002 inch.

A calibration was made which gave the primary voltage (measured by V_2, Figure 57) as a function of the secondary voltage (measured by V_3, Figure 57). In order to cover the entire voltage range, several electrostatic voltmeters were used on the high side. After the above data were available, it was possible to adjust the primary circuit resistors. This procedure is necessary to the establishment of a standard rate of rise of the high voltage wave for each increment of current in the primary circuit.

The conditioning of specimens and observation of atmospheric conditions for the ASTM tests conform to the methods described in the first section of this report.

As a final check after rebuilding and calibration, the equipment was operated at full voltage in a dark room to test for corona. This necessitated the re-routing of several leads to give corona-free operation.

Results of And Conclusions From ASTM Arc Tracking Tests

The arc resistance time for each specimen is shown in Table IV. The magnitude of surface arcover is increased each minute until failure of the specimen takes place. The details of the one-minute intervals in the test

TABLE IV

ASTM ARC RESISTANCE TIME FOR VARIOUS SPECIMENS
ASTM DESIGNATION: D 495-48T

Specimen	Thickness	No. of Tests	Arc Resistance Time in Min. & Sec.		
			Maximum	Minimum	Average
Isomica	0.120	5	04:05	04:03	04:04
Isomica + Dolph's Synthite	0.120	4	00:55	00:12	00:24
Isom. + D's Syn. + Glass Beads	0.120	5	00:52	00:38	00:45
Isom. + Scotch Cast	0.120	4	00:27	00:14	00:20
Isom. + Sc. Cast + Glass Beads	0.120	5	01:08	01:01	01:05
Isom. + Silicone Varnish	0.120	5	00:06	00:06	00:06
Isom. + Sil. Var. + Glass Beads	0.120	4	00:48	00:13	00:28
Isom. + Dri-Film 88	0.120	5	04:06	04:02	04:05
Isom. + D. F. 88 + Glass Beads	0.120	5	03:04	03:02	03:03
Black Bakelite	0.200	5	00:06	00:06	00:06
Blk. Bakelite + Dolph's Synthite	0.200	4	02:07	02:05	02:06
Blk. Bak. + D's Syn. + Glass Beads	0.200	5	00:60	00:33	00:42
Blk. Bak. + Scotch Cast	0.200	5	00:45	00:22	00:30
Blk. Bak. + Sc. Cast + Glass Beads	0.200	5	01:45	00:41	00:69
Blk. Bak. + Silicon Varnish	0.200	5	00:14	00:06	00:09
Blk. Bak. + Sil. Var. + Gl. Bds.	0.187	5	00:31	00:22	00:27
Blk. Bak. + Dri-Film 88	0.262	3	02:07	01:18	01:39
Blk. Bak. + D.F. 88 + Glass Beads	0.262	5	02:10	02:07	02:09
Lucite	0.125	5	01:07	01:05	01:06
Lucite + Dolph's Synthite	0.140	5	01:07	01:05	01:06
Luc. + D's Syn. + Glass Beads	0.140	5	00:37	00:35	00:36
Luc. + Scotch Cast	0.125	5	00:22	00:12	00:18
Luc. + Sc. Cast + Glass Beads	0.140	5	01:31	01:02	01:18
Luc. + Plastic Cement + Glass Bds.	0.125	5	02:05	02:03	02:04

sequence are shown in Table V.

Untreated isomica and isomica coated with Dri-Film 88 had the highest arc resistance times. The correspondence between the times for these two specimens is greater than one would expect considering ordinary experimental error. Untreated black bakelite was the poorest specimen.

The majority of the specimens treated with glass beads showed a marked improvement over the same base material coated only with the suspension medium. The exceptions may be due to the shape of the arc tracking electrodes. They are chisel-shaped with elliptical contour. The electrode shape gives rise to a very non-uniform field with a great concentration of flux at the points of the electrodes. Under these circumstances, the electrodes may find imperfection in the uniformity of the surface treatment not visible to the eye.

In general, the arc tracking tests substantiate the results obtained with the ionization tests. The suppression of ionization increases the time a specimen is able to withstand arcover.

TABLE V

SEQUENCE OF ONE-MINUTE CURRENT STEPS
ASTM DESIGNATION: (D 495-48T)

Step	Current, ma.	Time Cycle	Approximate Rate of Heat Generation, w.	Total Time in Sec.
1/8--10......	10.....	1/4 sec. on, 1 3/4 sec. off	3	60
1/4--10......	10.....	1/4 sec. on, 3/4 sec. off	6	120
1/2--10......	10.....	1/4 sec. on, 1/4 sec. off	12	180
10...........	10.....	continuous	24	240
20...........	20.....	continuous	34	300
30...........	30.....	continuous	45	360
40...........	40.....	continuous	56	420

SUMMARY AND CONCLUSIONS

The ionization experiments at atmospheric pressure proved that without exception the specimens treated with glass beads suppressed the surface ionization and corona to a very marked degree. In these experiments the usual process of ionization by collision is altered when glass beads are present on the surface. In the presence of the beads the electric field and effective resistance for the surface are altered in such a way as to restrict the formation of electron avalanches. This alteration in turn causes the reduction of the surface ionization. The decrease of surface ionization and corona reduces the ion bombardment of the dielectric which leads to the improved life of the high-voltage dielectric.

The ionization experiments performed in a gaseous atmosphere showed a further improvement in the suppression of surface ionization as the gas pressure was increased. This decrease in ionization is due to the fact that the mean free path of the ionized particles has been reduced with the increase in pressure so that for the same electrode spacing an increased voltage gradient is necessary to accelerate the particles to ionizing speeds between collisions.

The flashover tests proved that for the surfaces treated with glass beads, the flashover voltage was lower than for the base material alone or for the base material coated with the suspension medium. This is what one would expect from theory. Any surface is weaker than the gas adjacent to it. And the rougher the surface, so long as the surface length is not materially increased, the weaker the surface is electrically. This phenomenon is explained by the fact that the gas between the irregularities is subjected to a higher dielectric flux density and hence, a higher voltage gradient because the irregularities, in this case the glass beads, have a much higher dielectric constant than the air or gas between them.

In comparing the ionization experiments with the flashover tests, it must be borne in mind that surface ionization and flashover are different phenomena and hence, different parameters are involved.

The main purpose of the ASTM arc tracking tests was to serve as a standard engineering test on the specimens used in the other experiments, rather than as a research test. The electrode shape gives rise to a very non-uniform field. Furthermore, the high-voltage wave form was not nearly so good as for the other experiments. These low current ASTM tests showed that in the majority of cases, a specimen coated with a suspension medium and glass beads could withstand low-current arcover considerably longer than could a specimen coated with the suspension medium alone.

The researches accomplished have afforded an insight into future investigations. Some of these are proposed as possible experiments. For example, it would be of interest to compare the crest value of the ionization current with the rms value, because this varies greatly with the specimen involved. To accomplish this an electronic device should be constructed with balanced input and dual channels so that the positive and negative rms values of the ionization current could be measured simultaneously.

Additional precise work needs to be done on the glass beads or other materials used in their place. The dielectric constant of the particular glass beads should be determined. This may be accomplished by optical means. Measurements should be made of the bead sizes to determine their range and distribution. Irregular-shaped particles, both crystalline and amorphous should be substituted for the glass beads. The effect of roughening the surface by means other than applying glass beads should be studied. Furthermore, suspension media of an entirely different classification should be tried.

The experiments should be performed using direct current and under a known field configuration if possible. These provisions would lead to results more nearly amenable to the development of a mathematical theory.

BIBLIOGRAPHY

1. American institute of electrical engineers. Measurement of voltage in dielectric tests. New York, N.Y., September 11, 1953. 26 p. (AIEE No. 4.)

2. Camilli, G., T. W. Liao and R. E. Plump. Dielectric behavior of some fluorogases and their mixtures with nitrogen. Electrical engineering 74:580-584. July 1955.

3. Conditioning plastics and electrical insulating materials for testing. In ASTM 1954 Supplement to Book of ASTM Standards including tentatives, Part 6: Rubber, plastics, electrical insulation. Philadelphia, ASTM, 1954. pp. 308-310. (ASTM Designation: D 618-54)

4. High voltage, low-current arc resistance of solid electrical insulating materials. In ASTM 1952 Book of ASTM Standards Part 6: Rubber, plastics, electrical, insulation. Philadelphia, ASTM, 1952. pp. 1136-1147. (ASTM Designation: D 495-48T)

5. McMillan, F. O. Some characteristics of A-C conductor corona. American institute of electrical engineers transactions 54:282-291. 1935.

6. McMillan, F. O. Radio interference from insulator corona. American institute of electrical engineers transactions 51:385-391. 1932.

7. McMillan, F. O. and H. G. Barnett. A radio interference measuring instrument. Electrical engineering 54:857-862. August 1935.

8. Peek, F. W., Jr. Dielectric phenomena in high voltage engineering. 3d ed. New York, McGraw-Hill, 1929. 410 p.

APPENDIX

Due to the fact that a few questions were raised during the final examination, additional experiments have been performed. The results of these experiments are given below.

No noticeable difference was observed in the character of the ionization pulses as shown on the oscilloscope upon reversal of the exploratory electrodes provided they are kept polished and clean at all times during experiments.

In order to show that a given deflection on the oscilloscope means that the source voltage wave has a definite sense, the following experiments were made.

The connections of the cathode ray tube are as shown in Figure 5. First, when the positive terminal of a battery is connected to the upper deflector plate, the electron beam is deflected upward. Also, the insertion of a point to plane rectifier shows that the oscilloscope deflection means a definite sense which is always related to the sense of the 60 cycle wave. The polarity was checked by use of a permanent magnet moving coil instrument. In other words if the upper deflector plate is positive, the high voltage terminal of the bridge is positive and there is an upward deflection on oscilloscope.

To show that the indication on the oscilloscope denoted a discharge from only one electrode at a time, the following experiments were made.

The exploratory electrodes were observed through a rotating disc type mechanical stroboscope. Synchronization was checked with the General Radio Strobotac. The disc of the mechanical stroboscope rotates at a synchronous speed of 1800 rpm. There are two slots in the disc diametrically opposite each other. Each mechanical degree on the stroboscope represents two electrical degrees on the applied 60 cycle voltage wave. The exploratory electrodes were excited in the bridge circuit so as to show heavy ionization to the unaided eye. When viewed through the stroboscope disc, total darkness was observed at 0, 90, and 180 mechanical degrees. These are the points where the voltage wave crosses the axis as seen on the oscilloscope at 0, 180, and 360 electrical degrees. In the vicinity of the intermediate positions of 45 and 135 mechanical degrees, the ionization adjacent to both electrodes appeared at maximum brightness. This corresponds to the ionization pulses or spikes that appear near the maxima of the voltage wave at 90 and 270 electrical degrees as seen on the oscilloscope. Both electrodes appear to be bright at the same time because the time interval of observation is not short enough to show the progress of the glow across the surface of the dielectric between the electrodes. Also, the positive ionization pulses leave the positive half of the 60 cycle exciting wave in the upward direction only, rise steeply, and decay slowly as shown with the expanded sweep of the oscilloscope. The negative pulses leave the negative half of the 60 cycle wave in the downward direction only.

An explanation of the fact that there was ionization from one electrode only for a given oscilloscope deflection is shown by the following considerations.

The mobility of electrons is very very much greater than that of the oxygen and nitrogen constituents of the atmosphere, therefore, the electron flow constitutes the current and determines its sense of flow.

For any half cycle, one electrode is positive while the other is negative. During the next half cycle the polarity of both electrodes is reversed. For any half cycle the electrons are attracted by the positive electrode and repelled by the negative electrode. When a charged particle moves across the space between two electrodes, the current in the circuit will be a function of the velocity of the charged particle.